

REPORT DOCUMENTATION PAGE		READ INSTRUCTIONS BEFORE COMPLETING FORM	
1. REPORT NUMBER 4	2. GOVT ACCESSION NO.	3. RECIPIENT'S CATALOG NUMBER	
4. TITLE (and Subtitle) Intrinsic Cholinergic Mechanisms Regulating Cerebral Blood Flow as a Target for Organo-phosphate Action		5. TYPE OF REPORT & PERIOD COVERED Annual/Final 9/30/84 - 9/29/88	
7. AUTHOR(s) Donald J. Reis, Costantino Iadecola, and Stephen Arneric		6. PERFORMING ORG. REPORT NUMBER DAMD17-84-C-4185	
9. PERFORMING ORGANIZATION NAME AND ADDRESS Cornell University Medical College 1300 York Avenue New York, NY 10021		10. PROGRAM ELEMENT, PROJECT, TASK AREA & WORK UNIT NUMBERS 61102A 3M161102BS11 AA 067	
11. CONTROLLING OFFICE NAME AND ADDRESS U.S. Army Medical Research & Development Command Fort Detrick Frederick, MD 21701-5012		12. REPORT DATE October 1988	
14. MONITORING AGENCY NAME & ADDRESS (if different from Controlling Office)		13. NUMBER OF PAGES 102	
16. DISTRIBUTION STATEMENT (of this Report) Approved for public release; distribution unlimited		15. SECURITY CLASS. (of this report) Unclassified	
17. DISTRIBUTION STATEMENT (of the abstract entered in Block 20, if different from Report)		15a. DECLASSIFICATION/DOWNGRADING SCHEDULE DTIC ELECTE JUL 17 1990 S E D	
18. SUPPLEMENTARY NOTES Annual report covers period September 30, 1987 - September 29, 1988			
19. KEY WORDS (Continue on reverse side if necessary and identify by block number) acetylcholine, choline acetyltransferase, cerebral blood flow, cerebellum, fastigial nucleus, brain stimulation, muscarinic receptors, capillary endothelium, cerebral microvessels. (JCS) C			
20. ABSTRACT (Continue on reverse side if necessary and identify by block number) We investigated the possible sites of biosynthesis of that pool of acetylcholine (ACh) responsible for the global cerebrovascular vasodilation elicited by electrical stimulation of the cerebellar fastigial nucleus (FN) in anesthetized, paralyzed rats. Sites of ACh biosynthesis were identified immunocytochemically by mapping the distribution of the ACh biosynthetic enzyme choline acetyltransferase (ChAT) by light and electron microscopic immunocytochemistry. ChAT was identified for the first time in autonomic pathways presumably engaged by FN stimulation. In the cerebral cortex it was contained in afferent			

90 07 16 235

20. ABSTRACT (continued)

fibers, local neurons and in microvessels, particularly endothelium. The specific capacity of microvessels to synthesize ACh was extremely high. The FN-evoked vasodilation in the cerebral cortex was completely blocked by i.v. atropine, reduced by 60% by topically applied drug, not associated with local release of ACh, and abolished by selective destruction of cortical neurons. Locally applied physostigmine increased cortical flow. The evidence suggests that activation of an intrinsic neuronal network from cerebellum produces a potent local vasodilation throughout brain by promoting release of ACh in target tissues, probably from microvascular sites. This local cholinergic system mediating flow is not tonically active but is engaged in some states of excitation, exemplified by the FN system. Increased release of ACh by this system after exposure to agent may, by suspending cerebrovascular autoregulation, render the cerebral circulation dependent upon systemic circulation exposing brain to ischemic damage or edema in shock or stress, respectively.

REPORT #4**INTRINSIC CHOLINERGIC MECHANISMS REGULATING CEREBRAL
BLOOD FLOW AS A TARGET FOR ORGANOPHOSPHATE ACTION****Annual/Final Report**

Donald J. Reis, Costantino Iadecola and Stephen P. Arneric

October 1988

Supported by

**U.S. ARMY MEDICAL RESEARCH AND DEVELOPMENT COMMAND
Fort Detrick, Frederick, Maryland 21701-5012**

Contract No. DAMD17-84-C-4185

Cornell University Medical College
New York, New York 10021

Approved for public release; distribution unlimited

The findings in this report are not to be construed as an official Department of the Army position unless so designated by other authorized documents.

SUMMARY

1. The global increase in regional cerebral blood flow (rCBF) elicited by electrical stimulation of the cerebellar fastigial nucleus is abolished by the systemic administration of atropine indicating that the effect is mediated by the release of acetylcholine and mediated by a muscarinic cholinergic receptor.
2. Choline acetyltransferase (ChAT), the enzyme subserving the biosynthesis of acetylcholine, is distributed in specific neuronal pathways within the brain including many involved in central autonomic regulation. In the cortex, ChAT activity is found in three sites: a) in afferent fibers largely arising from basal forebrain; b) in local interneurons; and c) in cerebral microvessels including endothelial cells.
3. ChAT within the cerebral microvessels is capable of synthesizing acetylcholine. Although the contribution of microvessels to the overall biosynthesis of acetylcholine in the cerebral cortex is very small (<1%), on the basis of specific activity it is higher than that found in synaptosomes indicating that at the local microvascular level this source of acetylcholine synthesis may be important.
4. That ACh synthesized near microvessels may increase rCBF is indicated by the observations that local application of cholinergic agonists carbachol or physostigmine will increase local CBF. Local flow, however, does not appear to be tonically regulated by continuous release of ACh since atropine does not affect local flow.
5. The increase in rCBF elicited within the cerebral cortex by FN stimulation is dependent upon the release of ACh since it is blocked by topical application of atropine.
6. The increase in rCBF elicited by stimulation of the FN is abolished by destruction of neurons within the cerebral cortex indicating that the vasodilation cannot be the result of a direct neurovascular innervation by afferent cholinergic fibers arising from brainstem and, therefore, must depend upon a local interneuron. Whether the source of the acetylcholine is from a local cholinergic interneuron or from the microvessel itself is unknown.
6. Stimulation of the fastigial nucleus does not release acetylcholine from the cerebral cortex indicating that the pool of transmitter engaged in the vasodilation is small.
7. The results suggest that acetylcholine plays an important role in the vasodilation in the cerebral cortex activated by physiological stimuli. The fact that cholinergic activation, as might occur with exposure to agents, will profoundly modify cerebral blood flow with the probable arrest of autoregulation strongly suggests that under these circumstances, the cerebral circulation in critical areas will no longer be autoregulated. Hence, rCBF will become dependent upon variations in systemic arterial pressure. Thus, sharp reductions of arterial pressure, as might occur in hemorrhagic or traumatic shock, will render the cerebral circulation vulnerable to hypoxia while elevations of arterial pressure, as might be expected from stress or exercise, would permit cerebral blood flow to increase well above the autoregulated range, rendering local areas of the brain vulnerable to cerebral edema and breakdown of the blood brain barrier.

8. Cerebral blood flow following exposure to agent in non-lethal doses, therefore, may be an important target for therapeutic concern.

Accession For	
NTIS GRA&I	
DTIC TAB	
Unannounced <input type="checkbox"/>	
Justification	
DT	
Distribution/	
Availability Codes	
Health and/or	
Dist	Special
A-1	



INTRODUCTION

The objectives of the research proposal entitled "Intrinsic Cholinergic Mechanisms Regulating Cerebral Blood Flow as a Target for Organophosphate Action" submitted to the U.S. Army in 1983 was to investigate the role of acetylcholine in mediating the global vasodilation elicited by electrical stimulation of the fastigial nucleus. The background to the proposal was based on observations that first, electrical stimulation of the cerebellar fastigial nucleus (FN) could profoundly modify cerebral blood flow (CBF).

We had discovered several years earlier that electrical stimulation of the fastigial nucleus would increase regional (rCBF) or local (lCBF) cerebral blood flow (Nakai et al., 1982, 1983; see Reis and Iadecola, 1989). The maximal response, up to 300%, was within widespread regions of the cerebral cortex. Interestingly, the cerebral vasodilation was the result of activation of pathways intrinsic to the brain and not a consequence of the action upon peripheral neurons innervating the cerebral circulation. Moreover, the increase of cerebral blood flow in many regions, particularly the cerebral cortex, was unassociated with any change in local cerebral glucose utilization (LCGU) indicating, thereby, that the vasodilation was primary: i.e. unassociated with and uncoupled from proportional changes in cerebral metabolism. These findings were novel and important, for they revealed the presence of systems in the brain capable, through intrinsic networks, of profoundly modifying cerebral blood flow independently of metabolism. We have termed this role of regulation of the cerebral circulation intrinsic neurogenic control (Reis and Iadecola, 1989).

Of relevance was the fact that the vasodilation elicited by increasing cerebral blood flow through the cerebellum was associated with suspension of cerebrovascular autoregulation. Thus, under conditions of activation the cerebral circulation became much more critically dependent on systemic arterial pressure (SP).

We had recently discovered, at the time of submission of our proposals, that the increase of cerebral blood flow appeared to involve a cholinergic link: preliminary studies at that time had demonstrated that the systemic administration of atropine would abolish the increase of blood flow associated with electrical stimulation of the FN without affecting the associated profound elevations of systemic arterial pressure produced by the same stimulus, the fastigial pressor response (FPR) (Miura and Reis, 1969; Doba and Reis, 1972). Thus, this finding was of particular relevance to the issue of action of agents since it suggested that cholinergic mechanisms within the cerebral circulation could profoundly modify cerebrovascular autoregulation and activate local dilatory mechanisms with severe consequences for individuals exposed: specifically, it was conceivable that long-term facilitation of cholinergic mechanisms within the cerebrovascular bed would make the cerebral circulation much more dependent upon changes in systemic arterial pressure either in response to hemorrhagic shock or to stress. Reduction in cerebral blood flow below critical levels, in the absence of autoregulation, can lead to cerebral ischemia while elevations, in the absence of autoregulation, may lead to cerebral edema.

In our proposal, therefore, we set to establish clearly: a) whether the elevations of cerebral blood flow elicited from activation of intrinsic networks represented in the FN of the cerebellum were, in fact, cholinergically mediated; b) the possible sites at which acetylcholine was critical for the increase in blood flow, specifically within networks activated by FN or within a target area, the somatosensory cerebral cortex; and c) if the latter, to assess what possible elements in the cerebral cortex were capable of synthesizing

ACh and whether local release of the neurotransmitter was responsible for the enhanced cerebral blood flow.

Our studies, as documented below, have demonstrated that a) the increase in rCBF elicited by FN stimulation clearly depends upon the release of acetylcholine in brain; b) there is a cholinergic representation in the autonomic networks within the brain which can only account, if at all, for a relatively small contribution to the effect on the cerebral circulation and none to the effects of FN stimulation upon the systemic circulation; c) within the target area of the somatosensory cortex, acetylcholine biosynthesis may occur not only in cortical afferent fibers from neurons of the basal forebrain but also substantially from acetylcholine synthesized in capillary endothelium; d) local blockade by atropine or muscarinic receptors in the cerebral cortex can substantially attenuate the vasodilation elicited by FN stimulation; e) the source of this ACh may well be associated with capillary cholinergic synthesis and/or interneurons but not large ascending pathways.

TABLE OF CONTENTS

SUMMARY	2
INTRODUCTION	4
TABLE OF CONTENTS	6
LIST OF FIGURES	8
LIST OF TABLES	12
REPORT	13
METHODS	13
I. Animals	13
II. Physiological Studies	13
III. Neurochemical Studies	16
IV. Histology	20
V. Experimental Protocols	23
RESULTS	25
I. Effects of Atropine on Vasodilation Elicited from FN	25
II. Sources of ACh Related to Cortical Vasodilation from FN Stimulation	27
III. Microvessels as a Source of ChAT	29
IV. Role of Local Cholinergic Elements in CBF Response to FN Stimulation	31
DISCUSSION	37
I. Cholinergic Mechanisms Mediating the Vasodilation Elicited by Electrical Stimulation of FN	37
II. Central Representation of Cholinergic Systems in the Visceral Brain. A Site of Action of ACh Eliciting Global Vasodilation?	38
III. Neurovascular Sites Mediating the Cerebrovascular Vasodilation from FN	39
IV. Effect of Topical Atropine on Cortical Cerebro- vasodilation Elicited from the FN	41
V. Cortical Release of ACh Following FN-Stimulation	42
VI. Role of Intrinsic Neurons in the Local Vasodilation Elicited in the Cerebral Cortex with FN-Stimulation	43
VII. Summary, Conclusions and Relevance to Protection from Agent	44
LITERATURE CITED	46

TABLE OF CONTENTS
(continued)

FIGURES	55
TABLES	92
LIST OF PERSONNEL RECEIVING CONTRACT SUPPORT	100
BIBLIOGRAPHY OF PUBLICATIONS SUPPORTED BY CONTRACT	101
DISTRIBUTION	102

LIST OF FIGURES

<u>Figure</u>		<u>Page</u>
1A	A schematic of the device used to apply atropine to the cortical surface and collect superfusate during the release experiments.	56
1B	The region of the parietal cortex sampled during these experiments is shown following introduction of fast green dye into the superfusion device to mark the placement.	57
2	A. Release of $^3\text{H-ACh}$ from tissue slices of the targeted area of CX during steady-state spontaneous efflux and following depolarization with 55 mM K^+ . B. The effect of varying the potassium depolarization stimulus.	58
3	A. A light microscopic photomicrograph of the cortical microvessel preparation as viewed from the video screen. B. The distribution of the diameters of 690 vessels isolated from 4 separate experiments is represented.	59
4	An illustration of the later portion of a representative blood flow experiment summarizing the protocol used to measure rCBF during electrical stimulation of the fastigial nucleus (FN) of the cerebellum.	60
5	Representative tracings of the ECoG recorded from the cerebral cortex underlying the superfusion device following electrical and chemical stimulation of different brain regions.	61
6	Effect of administration of atropine sulfate (0.3 mg/kg, i.v.) on basal EEG activity and on the EEG changes produced by electrical stimulation of the cerebellar fastigial nucleus (FN) in anesthetized rat.	62
7	Effect of stimulation of the cerebellar fastigial nucleus (FN) on cortical cerebral blood flow (CBF).	63
8	Effect of systemic administration of atropine on the increase in cerebral blood flow (CBF) elicited by stimulation of the fastigial nucleus (FN) in spinal cord transected rats.	64

LIST OF FIGURES
(continued)

<u>Figure</u>		<u>Page</u>
9	Relationship between length of the stimulation period and time required for cortical blood flow to return to baseline after termination of the stimulus, in anesthetized rats after spinal cord transection.	65
10	Stimulus intensity and frequency response characteristics of the cerebrovasodilation elicited by stimulation of the fastigial nucleus in spinal cord transected rats.	66
11	Location of sites from which an elevation in cerebral blood flow (CBF) could be elicited from low intensity electrical stimulation.	67
12	Effect of administration of pentobarbital on the EEG and on the increase in cerebral blood flow (CBF) elicited by electrical stimulation of the fastigial nucleus (FN) in spinal cord transected rats.	68
13	Camera lucida drawings of transverse sections through the medulla oblongata labeled immunocytochemically for ChAT.	69
14	Darkfield photomicrograph of fine punctate varicosities (and coarser processes) in the rostral ventrolateral reticular nucleus (RVL) underlying the nucleus ambiguus (NA).	70
15	Camera lucida drawings depicting ChAT-immunoreactivity at commissural, intermediate and rostral levels of the nucleus tractus solitarius (NTS).	71
16	Darkfield photomicrographs demonstrating clusters of punctate varicosities in the dorsolateral pons.	72
17	Camera lucida drawings of ChAT-immunoreactive processes in the forebrain.	73
18	Schematic diagram summarizing the potential neuroanatomical substrates of cholinergic autonomic regulation.	74
19	Ultrastructural localization of ChAT-immunoreactive processes in layer III of the cerebral cortex.	75

LIST OF FIGURES
(continued)

<u>Figure</u>		<u>Page</u>
20	Ultrastructural localization of a ChAT-immunoreactive axon terminals and endothelial cell from layer III of cerebral cortex.	76
21	Light microscopic photomicrograph of microvessels prepared from the cortex and stained with methylene blue.	77
22	A. An electron photomicrograph of a microvessel isolated from the cerebral cortex which details many of the cellular elements commonly attached to the abluminal side of the basal lamina. B. An electron photomicrograph of the synaptosomal (P ₂ fraction) preparation of the cerebral cortex.	78
23	A. ChAT activity measured in different tissues and subcellular fractions when expressed as the absolute amount of [¹⁴ C]ACh synthesized relative to the amount synthesized from a 100-mg (wet wt.) section of the cerebral cortex. B. The same data as in A, except now it represents ChAT activity from different tissues and subcellular fractions expressed as a specific activity.	79
24	The effect of the specific inhibitor of ChAT, 4-naphthylvinylpyridine (NVP, 100 μ M), to inhibit the formation of [¹⁴ C]ACh in cortical microvessels or nerve terminals.	80
25	Representative chromatographs depicting the separation of [¹⁴ C]acetyl CoA and [¹⁴ C]ACh by the use of HPLC analysis.	81
26	A. The release of [³ H]ACh, GABA and Asp evoked by 55 mM K ⁺ in the presence of 1.2 mM Ca ²⁺ , from cerebral cortical microvessels (MV) and nerve terminals (S ₁). B. The effect of removing extracellular Ca ²⁺ on the release of [³ H]ACh evoked by 55 mM K ⁺ from cerebral cortical microvessels.	82
27	Effect of atropine sulfate (100 μ M) applied to the right parietal cortex (vehicle to left) on the increases in rCBF elicited by electrical stimulation of the FN.	83

LIST OF FIGURES
(continued)

<u>Figure</u>		<u>Page</u>
28	Effect of atropine sulfate (100 μ M) applied to the right parietal cortex on CO_2 -elicited increases in rCBF.	84
29	A representative experiment showing the effect of electrical stimulation of the fastigial nucleus or potassium depolarization on the release of [^3H]ACh from the parietal CX of anesthetized, paralyzed and artificially ventilated rats.	85
30	Grouped data demonstrating the effect of potassium depolarization (55 mM) or electrical stimulation of the FN on the release of [^3H]ACh from the parietal CX of anesthetized (chloralose), paralyzed and artificially ventilated rats.	86
31	Cardiovascular and cortical blood flow (CrtBF) responses to acetylcholine (ACh) microinjection into the parietal cortex.	87
32	Change in cortical blood flow (CrtBF) elicited by local microinjection of diisopropyl phosphofluoridate.	88
33	Cardiovascular and cortical blood flow (CrtBF) responses to diisopropyl phosphofluoridate (DFP) microinjection into the parietal cortex.	89
34	Photomicrographs illustrating effects of microinjection of excitotoxin ibotenic acid in primary sensory cortex (SmI) of rat.	90
35	Anterograde and retrograde transport of wheat germ agglutinin conjugated with horseradish peroxidase (WGA-HRP), into and from area of lesion, 5 days after microinjection of ibotenic acid in primary sensory cortex of rat.	91
36	Time course of activity of choline acetyltransferase (ChAT) and glutamic acid decarboxylase (GAD) within lesions of primary sensory cortex produced by excitotoxin ibotenic acid.	92

LIST OF TABLES

<u>Table</u>		<u>Page</u>
1	Mean arterial pressure (MAP), pH and arterial blood gases in rats examined.	93
2	pH, pCO ₂ and pO ₂ of buffer solutions applied to the parietal cortex of rats with and without FN-stimulation or with hypercarbia.	94
3	Effect of atropine sulfate on the minimal current required to elevate arterial pressure (AP) and on the elevation in AP and heart rate (HR) produced by stimulation of the fastigial nucleus (FN stim) in anesthetized rats.	95
4	Effect of stimulation of the fastigial nucleus (FN) on rCBF with and without administration of atropine.	96
5	Enrichment of γ -glutamyltranspeptidase and alkaline phosphatase activities in vascular fractions as compared to nerve terminals (S ₁) fractions.	97
6	Rank ordering of the spontaneous release of putative neurotransmitters from cerebral cortex microvessels or homogenates.	97
7	ICBF with and without restricted cortical lesions by IBO, during stimulation of FN or hypercapnia.	98
8	Effect of bilateral craniotomy and ATR on resting rCBF.	99
9	A comparison of the choline acetyltransferase (ChAT) activity measured by different authors from various fractions isolated from the cerebral cortex.	100

METHODS

I. ANIMALS

Studies were conducted on male Sprague-Dawley rats (290-380g) that were maintained in a thermally controlled (26-27°C) light-cycled (0700 on - 1900 off) environment, fed standard laboratory chow and given water ad lib.

II. PHYSIOLOGICAL STUDIES

A. Preparation of Animals

Methods for surgical preparation of rats for electrical stimulation of brain and measurement of rCBF are described in detail in publications from this laboratory (Nakai et al., 1982). In summary:

Animals were anesthetized with alpha-chloralose (40 mg/kg, s.c.) after induction with halothane (2.5% in 100% O₂) blown over the nose. Thin wall vinyl (o.d. = 0.5mm) and polyethylene (o.d. = 1.3mm) catheters were placed in each femoral artery and vein, respectively, and the trachea was cannulated.

Animals were then placed in a stereotaxic frame with the head adjusted so that the floor of the IVth ventricle was horizontal (bite bar position: -11 mm). After connecting the tracheal cannula to a small-animal respirator (Harvard Apparatus, Model 680), the animals were paralyzed with tubocurarine (0.5 mg/kg, i.m., initially; supplemented with 0.2 mg/kg hourly), and ventilated (80 cpm) with 100% O₂. Halothane was continued at a reduced rate (1%) during surgery. Continuous monitoring of arterial pressure and heart rate was done through one of the arterial catheters connected to a Statham P23Db transducer which was coupled to a chart recorder.

The lower brainstem and caudal half of the cerebellum were exposed by an occipital craniotomy. After completion of the surgery, halothane was discontinued. A small volume (about 0.2 ml) of arterial blood was sampled after surgery for measurement of pO₂, pCO₂, and pH by a blood gas analyzer (Instrument Laboratories, Model Micro 13). In control animals arterial blood gases were maintained so that pO₂ was greater than 100 mmHg, pCO₂ = 33-38 mmHg, and pH = 7.35-7.45 (see Table 1). Adjustments were made by changing the stroke volume of the ventilator.

Spinal cord transection was performed as described elsewhere (Nakai et al., 1982). In brief, the atlas was exposed and the posterior lamina removed. The dura was cut and the cord exposed at the C1-C2 junction. To prevent the elevations in AP associated with the transection procedure, 0.1-0.2 ml of 2% procaine were injected within the cord using a 1 ml syringe with a 28 G needle (Nakai et al., 1982). The cord was then severed at C1 using microscissors. To ensure a complete transection a small cord segment below C1 was removed by suction and the empty area packed with gelfoam. Just prior to the procedure, an i.v. infusion of phenylephrine (1.3-6.4 µg/min) was started so as to counteract the fall in AP which occurs after spinal cord transection. The completeness of the transection was carefully verified in all animals with a dissecting microscope at autopsy. AP was maintained by infusion of phenylephrine.

B. Electrical Stimulation of FN and Recording of Electrocorticogram

The FN was stimulated with cathodal current delivered through monopolar electrodes fabricated from Teflon-insulated stainless steel wire (150 μm , o.d.), carried in 28-gauge stainless steel tubing and exposed at the tip for 100 μm . The anode (ground) was a clip attached subcutaneously to neck muscle. Electrical pulses were generated by a square-wave stimulator (Grass, Model S88) and constant current was passed through a photoelectric stimulus-isolation unit (Grass Model PSIU6). The stimulus current was measured by continuously displaying on an oscilloscope the voltage drop across a 10 ohm resistor.

The electrode was mounted on a stereotaxic micromanipulator and lowered into the cerebellum with a posterior inclination of 10°. The area of the FN from which an increase in CBF (Nakai et al., 1982) could be elicited was identified by localization of the most active site for the fastigial pressor response (FPR; Miura and Reis, 1969). The area of the cerebellum explored extended 4.8-5.2 mm anterior to, 0.6-1.0 mm lateral to, and 2.0-0.5 mm above the calamus scriptorius, the stereotaxic zero reference point. To localize the most active area of the FN for the FPR, the electrode was moved in steps of 0.5 mm while stimulating with 8 sec trains of 0.5 msec duration pulses, at a frequency of 50 Hz and intensity of 20 μA . When the FPR was elicited, the threshold current, defined as the stimulus current which increases arterial pressure 10mmHg, was determined. For blood flow and ACh release experiments, the stimulus current was set at five times threshold.

The electrocorticogram (ECoG) was recorded between pairs of stainless steel Teflon-coated wires. The electrodes contacted the dura firmly, while ground was a metal clip placed subcutaneously in the neck. The ECoG signal was fed into an AC amplifier (Grass, Model 7P511) and displayed on a channel of the polygraph.

C. Cerebral Blood Flow Measurement

As described in detail elsewhere (Nakai et al., 1982), CBF was measured using ¹⁴C-iodoantipyrine (IAP) as indicator (Sakurada et al., 1978). Tissue concentrations of IAP were obtained by the tissue sampling technique (Ohno et al., 1979). The brain:blood partition coefficient used was 0.8 (Sakurada et al., 1978).

Arterial concentration-time curve of iodoantipyrine

4-(N-methyl-¹⁴C) iodoantipyrine in ethanol (New England Nuclear, 40-60 mCi/mmol) was dissolved in about 1 ml of normal saline after elimination of ethanol. Animals received 2000 units of heparin i.v. approximately 10 min prior to IAP infusion. The indicator was infused (5 $\mu\text{Ci}/100\text{g}$ of body weight) at a constant rate over 30-35 sec through a femoral venous catheter by an infusion pump (Harvard Apparatus, Model 940). Simultaneously, about 50 μl of arterial blood was sampled every 2-5 sec through the femoral arterial catheter in order to obtain the arterial concentration-time curve of IAP. The sampling catheter was kept short (5 cm) to more accurately reflect the arterial concentration-time curve of IAP. Aliquots (40 μl) of arterial blood were transferred to scintillation vials containing 1 ml tissue solubilizer (Protosol, New England Nuclear: ethanol, 1:1 v/v). The blood mixture was incubated at 60°C for 1 hour, decolorized with 30% hydrogen peroxide, and mixed with 15 ml of Biofluor (New England Nuclear). Radioactivity was measured by a liquid scintillation spectrophotometer (Beckman, LS 5801) and corrected to disintegrations/min (d.p.m.) using an external standard.

Measurement of tissue concentration of IAP

Approximately 30 sec following the start of the infusion of IAP, the animal was killed by a bolus injection of 1 ml of saturated KCl into the femoral vein catheter. The brain was rapidly removed, placed in liquid freon (-30°C) for 10 sec, and put on an ice-cold glass plate. Right and left samples of 5 brain regions were dissected: parietal CX (beneath, medial and lateral to the cortical superfusion device); frontal CX (2-4 mm rostral to the superfusion device); occipital CX (2-4 mm caudal to the superfusion device); caudate nucleus and hippocampus. Tissue samples were transferred to tared scintillation vials and the tissue weights determined. After solubilization of the tissue in 1 ml of Protosol, 10 ml of scintillation cocktail (Econofluor, NEN) was added and the samples counted.

Calculation of CBF

CBF (ml/100g/min) was calculated by obtaining a relationship between CBF and tissue concentration of IAP, using a computerized approximation of the equation developed by Kety (1951).

Monitoring of CBF by laser-doppler flowmetry (LDF)

CBF was monitored by LDF, a technique which allows recording of local CBF, in relative units, continuously and non-invasively, i.e. without penetrating the brain parenchyma. LDF is based on the principle that laser light is scattered from the microcirculation acquiring a Doppler shift which is related to number and velocity of circulating red blood cells within a tissue volume of about 1 mm³ (Chen et al., 1981; Tenland, 1982). In commercially available instruments laser light is carried to and from the tissue by optic fibers. The light scattered back from the tissue is analyzed by a photodetector coupled to a microprocessor to extract the fraction of the Doppler-shifted light and the frequency of the shift. The former is proportional to red blood cell volume and the latter to red blood cell velocity. Flow is computed on line from the product of volume and velocity. LDF has been recently used to monitor blood flow in the CNS where it has been validated by comparison with established methods for measuring CBF (Dirnagl et al., 1989; Haberl et al., 1989; Lindsberg et al., 1989; Tenland, 1982). These studies have shown an excellent correlation between relative changes in CBF measured by LDF and changes calculated from absolute values obtained with other techniques. Correlation with absolute flow values was shown to be poor (Dirnagl et al., 1989; Lindsberg et al., 1989).

LDF was performed using a PeriFlux PF3 (Perimed) flowmeter equipped with a 2 mW helium-neon laser with a wavelength of 632.8 nm. Flow values are expressed in relative units (perfusion units, PU). The probe (tip diameter 0.45 mm; PF 302) was mounted on a micromanipulator (Kopf). A small hole 1-1.5 mm in diameter was drilled, with the assistance of a dissecting scope, through the right parietal bone at a site approximately 2 mm lateral to the midline and 2.5 mm caudal to bregma using a 0.7 mm drill bit with a flat head. The drilling site was intermittently flushed with 0.9% NaCl at room temperature in order to remove bone debris and to avoid overheating. The bone was made very thin and then carefully removed with fine forceps. The dura was left intact. The position of the hole was chosen in preliminary experiments to expose a relatively "avascular" area of the parietal cortex corresponding to a border zone between terminal branches of second and third-order vessels (Coyle and Jokelainen, 1982). However given

the high variability in the distribution of pial vessels, it was occasionally necessary to enlarge the hole in order to reach a more suitable area. The probe was positioned approximately 0.5 mm above the dural surface. It was noticed in preliminary experiments that the presence of a translucent medium between dura and probe increases the magnitude and reactivity of the flow signal. Therefore, a drop of mineral oil was applied to the hole to fill the space between dura and probe. Alternatively, saline was applied and a small piece of cotton was rolled to form a thin thread, moistened with saline and then wrapped around the shaft of the probe as it emerged from the burr hole.

Several precautions were taken to avoid artifacts: (a) Direct light was avoided as it was found to cause a decrease in the flow signal; ambient lights were kept constant; (b) the probe was positioned away from large pial vessels as the principles on which the instrument is based are valid only for the microcirculation (Tenland, 1982). We have observed that when the probe was positioned on a large pial vessel (400-500 μ m or greater), the flow signal was unusually large (> 200 PU) and elevation of pCO_2 produced a decrease in CBF rather than the well established increase; (c) bleeding from the bone or dura was carefully avoided as red blood cells floating between the probe and the dura produce a dampening of the signal; (d) care was taken to assure maximal mechanical stability of the preparation, as the system is very sensitive to movements and vibrations (Lindsberg et al., 1989).

The analog output from the instrument was fed into a DC amplifier (Beckman) and displayed on a polygraph (Beckman). The amplifier's gain was set so that a 1 V output (100 PU) corresponded to a pen displacement of 5 cm. To avoid pulsatile variations in the flow signal, typically seen in good preparations (Haberl et al., 1989), a long time constant was used (3 sec). Baseline readings, recorded after a 5-10 min stabilization period, varied considerably depending on the position of the probe (Dirnagl et al., 1989). Placements yielding flow values less than 100 PU were chosen in this study. Probe position and reactivity of the preparation were tested at each site by determining the cerebrovascular reactivity to inhaled CO_2 (see below). Once a suitable placement was obtained, the probe was left at that site for the duration of the experiment.

III. NEUROCHEMICAL STUDIES

A. Release of Acetylcholine from Cerebral Cortex and Brain Slices

Cortical Superfusion Device

A schematic of the device used to apply atropine to the cortical surface and collect superfusate during the release experiments is shown in Fig. 1A. For the placement of this device, holes (2.5 mm, o.d.) were drilled bilaterally over the parietal CX in an area 2.0-4.5 mm lateral and +0.5 to -2.0 mm AP to bregma. Following incision of dura with a needle tip and retraction with forceps, the device was stereotactically positioned on the underlying sensory motor CX. Placement was made using microscopic examination to avoid occlusion of pial vessels. The cortical surface and superfusate temperature was clamped at $37 + 0.5^\circ C$ with the aid of a surface thermistor and overhead heating lamp coupled through a servo-mechanism (YSI Instruments, model 73A). Solutions filling the device and contacting the CX were bubbled with 95% O_2 ; 5% CO_2 immediately before each experiment to carefully control for pH (7.3-7.4), pCO_2 (30-40 mmHg) and pO_2 (300-500 mmHg) (refer to Table 2); then superfused over the pial surface at 10 μ l/min with an infusion pump (Harvard Apparatus model 940). The superfusate consisted of a modified Kreb's-bicarbonate buffer containing physostigmine to inhibit ACh degradation (in mM:

NaCl, 118; CaCl₂, 1.2; KCl, 4.8; MgSO₄, 1.2; NaH₂PO₄, 1.2; NaHCO₃, 25; D-glucose, 11; choline chloride, 0.001; physostigmine, 0.1). Fig. 1B shows the region of the CX affected by the superfusion device. The area of the cortical surface exposed was 0.018 cm².

Brain Slice Preparation

Preliminary studies were done *in vitro* to establish: (a) whether the release of ACh evoked by K⁺-depolarization could be measured from small regions of the CX, and (b) what concentration of K⁺ is required to evoke the maximal release of ACh from this restricted area of cortical tissue.

Rats were killed by decapitation. The brains were rapidly removed and placed in ice-cold Kreb's bicarbonate buffer containing 100 μ M physostigmine. Slices of CX were obtained from tissue dissected 1.5 mm rostral to and 0.5 mm caudal to the anterior commissure. Coronal sections (0.3-0.5 mm thick) were prepared with a McIlwain tissue chopper and bisected into right and left halves. Up to 8 hemi-sections of CX were prepared from each brain. To correct for possible regional variations in release, all of the samples of CX from one brain were pooled, and two slices were randomly assigned to each treatment. Average wet tissue weight for the slices was 19.9 \pm 0.8 mg (n=12).

Release of ³H-ACh was studied using modifications of the radiochemical method described by Hadhazy and Szerb (1977). Briefly, two slices were incubated for 20 min at 37°C in Kreb's bicarbonate buffer gassed with 95% O₂: 5% CO₂, which also contained 20 μ Ci/ml of (³H)-methylcholine (New England Nuclear, 80 Ci/nmol). The slices were then transferred at 5-min intervals, through a series of 1.5 ml micro centrifuge tubes (Eppendorf) containing 1.0 ml of gassed Kreb's bicarbonate buffer. Neurotransmitter release was evoked by exposing the tissue to potassium (5-55 mM) for 5 min. Increased potassium concentrations were compensated by an equiosmolar decrease in sodium concentration. Immediately following exposure to the brain slices, the buffer was stored at -20°C for later analysis of ³H-ACh.

In vitro studies showed that spontaneous efflux reached a steady-state by 10-15 min (Fig. 2A). Depolarization with 55 mM K⁺ in the presence of Ca²⁺ elicited a marked stimulus-locked release of ³H-ACh. In preliminary experiments we established that this K⁺-evoked release of ³H-ACh is abolished when extracellular Ca²⁺ is removed. The evoked efflux of ³H-ACh was dependent upon the concentration of potassium (5-55 mM) and was supramaximal at 55 mM K⁺ (Fig. 2B). These experiments established that release of ³H-ACh can be accurately measured from small tissue samples of the CX and that the depolarization stimulus required to evoke the maximal release of ³H-ACh is 55 mM K⁺.

B. Preparation of Microvessels and Synaptosomes

Intraparenchymal vessels were separated from brain. These ranged from the largest penetrating arterioles (50 μ m) to the small capillaries (5 μ m) (Nakai et al., 1981). Others have shown preparations enriched in rat cortical capillaries (i.e. 90% of the vessels have diameters <10 μ m) contain very little of the ChAT activity found in whole homogenates (2-5%, see Goldstein et al., 1975; Santos-Benito and Gonzalez, 1985). In order to include other vascular segments which may be more densely innervated by cholinergic neurons, the method described by Reinhard and co-workers (1979) was used. This procedure was shown previously to result in a pellet that contained MVs ranging from 5-50 μ m, o.d.

Rats were stunned and killed by decapitation. The brains and livers were rapidly removed and placed in ice-cold modified Kreb's bicarbonate buffer containing (in mM): NaCl, 118; KCl, 5; MgSO₄, 1.2; NaHCO₃, 25; D-glucose, 11; NaH₂PO₄, 1.2; CaCl₂, 1.2; choline chloride, 0.001; and physostigmine, 0.1. All subsequent procedures were performed at 4°C. The pia-arachnoid membranes were carefully removed from the brain. Portions of the parietal cortex (CX), caudate nucleus (CN), cerebellum (CRB) and liver (LIV) were removed and homogenized (10 strokes) in 10 vols of 0.32 M sucrose using a Potter-Elvehjem tissue grinder. The homogenate was centrifuged at 900 x g for 10 min. After decanting, the supernatant (S1) was centrifuged at 27,000 x g for 20 min to obtain a crude synaptosomal pellet (P2). Fractions S1 and P2 are enriched in resealed nerve terminals, i.e. synaptosomes (Gray and Whittaker, 1962; Whittaker, 1969). The P1 pellet was resuspended in 0.25 M sucrose (0.75 ml) and layered over a discontinuous sucrose gradient consisting of 1.25 ml of 1.0 M sucrose (middle layer) and 3.0 ml of 1.5 M sucrose (bottom layer) and centrifuged at 65,000 x g for 45 min in a Beckman SW-55 rotor. The resultant pellet containing the microvessels (MV) or the synaptosomes (P2) were reconstituted to their original volume using gassed (95% O₂; 5% CO₂) buffer, pH = 7.4. These fractions were either assayed the same day or frozen at -20°C for future analysis.

C. Biochemical Assays

Measurement of Radiolabeled ACh

Release of ³H-ACh was measured using modification of the radiochemical method of Hadhazy and Szerb (1977).

³H-choline and ¹⁴C-acetylCoA were used as precursors for the synthesis of radiolabeled ACh after prelabeling of cortex *in vivo*, brain slices, or preparations of synaptosomes and/or microvessels. It was necessary to verify that the radioactivity released from the tissue was authentic ACh. This was established by two methods: an enzymatic liquid-cation exchange method modified from Briggs and Cooper (1981) and HPLC separation of ³H- or ¹⁴C-ACh by the methods of Potter et al. (1984).

Radiolabeled ACh was routinely separated after incubation using the enzymatic liquid-cation exchange method. 200 µl of the superfusate was incubated for 30 min at 37°C in a final volume of 400 µl containing (in mM): NaH₂PO₄, 100 (pH = 8.5); ATP, 0.36; MgCl₂, 6.0; and 50 µg/ml choline kinase. The reaction was stopped by placing the sample on ice, adding 0.5 ml of tetraphenylboron in 2-heptanone and the microcentrifuge tube shaken vigorously. The samples were centrifuged, the organic layer containing radioactive ACh removed and the extraction repeated with an additional 0.5 ml of tetraphenylboron in 2-heptanone. The radioactivity in the organic and aqueous layers was measured by liquid scintillation counting methods (LS-5801, Beckman Instruments). Preliminary studies have shown that greater than 99% of the radioactivity in the organic phase corresponds to radiolabeled ACh (Arneric and Reis, 1986).

Further confirmation of the identity of the radioactivity was accomplished by using HPLC analysis. Samples were injected with a Model U6K injector (Waters Associates) onto a 10 µm ODS column (4.6 x 100 mm). The mobile phase was 96% 0.01 M sodium acetate (pH = 5.0) containing 30 mg/liter 1-octanesulfonic acid, sodium salt (SOS), and 4% acetonitrile. The flow rate was 0.8 ml/min produced by a single-stage miniPump (Laboratory Data Control) operating at pressure of 250- 350 psi. The identity of unknown metabolites was determined by matching the retention times to radioactive standards.

Before injection of the biological samples, each sample was evaporated and reconstituted in 30 μ l of mobile phase. As for the standards, 20 μ l aliquots were analyzed. Fractions were collected at 0.25 min intervals to resolve the peaks of radioactivity; retention times of 2.75 min for ^{14}C -acetylCoA, 4.5 min for ^3H -choline and 6.75 min for ^{14}C -ACh were observed.

Synaptosomes or microvessel fractions were incubated for 20 min at 37°C in Kreb's bicarbonate buffer gassed with 95% O₂:5% CO₂, containing 100 μ Ci/ml (^3H)-methylcholine (New England Nuclear, 80 Ci/mmol). Using a vacuum manifold, aliquots of synaptosomal (200 μ l) or MV (500 μ l) suspensions (approximately 0.2 - 0.5 mg protein) were deposited on Metrical Membrane Filters (25 mm o.d.; 0.45 μ m; Gelman Sciences, Inc.). The filters were then washed three times with Kreb's bicarbonate buffer to remove the excess ^3H -choline. The filters containing the tissue were transferred to glass scintillation vials containing Kreb's bicarbonate buffer (1 ml) warmed to 37°C. Neurotransmitter release was measured after exposing the tissue to K⁺ (5 - 55 mM) for 10 min. Increased K⁺ concentrations were compensated by equimolar reductions in Na⁺ concentration. To determine the Ca²⁺-dependency of neurotransmitter release, the Kreb's bicarbonate solution was modified by replacing Ca²⁺ with Mg²⁺ (1.2 mM) during the K⁺-depolarization. To stop the release process, the scintillation vials were placed on ice and the incubation media was filtered through disposable syringe filter assemblies (13 mm o.d.; 0.45 μ m; Gelman Sciences) into microcentrifuge tubes containing 100 μ l of 1 N perchloric acid. Samples were then stored at -20°C for later analysis of ^3H -ACh and AA.

Measurement of Endogenous Amino Acids

Endogenous gamma-aminobutyric acid (GABA), aspartate (Asp) and glycine (Gly) were measured by HPLC (Meeley et al., 1989). This technique involves precolumn derivation of the amino acids with O-phthalaldehyde, separation by reverse-phase chromatography and fluorescence detection of the AA derivatives. The details of this technique have been reported previously (Meeley et al., 1989) demonstrating a limit of detection of 50 fmol/10 μ l of injectate.

Measurement of Choline Acetyltransferase (ChAT) Activity

ChAT activity was measured by modification of the method of Fonnum (1975). Suspensions (25 μ l aliquots) of whole homogenate (HOM), MVs, or synaptosomes were sonicated for 5 sec in 5 mM KH₂PO₄ (pH = 7.0) containing 0.2% triton X-100 and 5 mM EDTA (2:1, suspension/buffer) just prior to use. The production of ^{14}C -ACh from ^{14}C -acetyl-CoA (58.6 mCi/mmol, New England Nuclear) was determined following a 40 min incubation at 37°C. This method has been shown to selectively extract ^{14}C -ACh, but not ^{14}C -acetyl carnitine (Tucek et al., 1978) which is the product of another acetyltransferase, carnitine acetyltransferase (EC. 2.3.1.7) (Bresolin et al., 1982).

In some experiments the selective inhibitor of ChAT, 4-naphthylvinylpyridine (NVP), was used to confirm that the activity measured was the result of ChAT and not some other enzyme. For these experiments, it was necessary to prepare a soluble form of the enzyme. To do so, fractions were sonicated in buffer as before, then centrifuged at 109,000 \times g for 1 hr (SW-55 rotor, Beckman). An aliquot of the supernatant was incubated in the presence and absence of 100 μ M NVP for the determination of ChAT activity.

Other Enzyme Activities

Alkaline phosphatase and gamma-glutamyl transpeptidase (γ -GTP) activity was measured in samples of MV and synaptosomes. Tissue samples were sonicated in 5 mM KH₂PO₄ (pH = 7.0) for 5 sec and aliquoted for each assay. Alkaline phosphatase was measured by modification of the method of Williams et al. (1980). Tissue samples (100 μ l) were incubated at 37°C for 20 min with 5 mM CaCl₂, 100 mM KCl, 50 mM MgCl₂ and 100 mM Tris HCl (pH = 9.0), in a total volume of 0.2 ml. The reaction was stopped by adding 0.4 ml of 1 N NaOH; then 0.6 ml of distilled H₂O (4°C). Samples were centrifuged for 2 min in a microcentrifuge; the absorbance of the supernatant was measured at 410 nm and compared with nitrophenol standards. γ -GTP activity was measured by the method of Orlowski and Meister (1965) using 5 mM L- γ -glutamyl-p-nitroanilide (Sigma) as substrate. Glutamic acid decarboxylase was measured by the method of Fonnum et al. (1977).

The protein content of samples were measured by the Coomassie Blue dye-binding method (Bradford, 1976), with bovine serum albumin as standard.

IV. HISTOLOGY

A. Electrode Placement

Localization of electrode placements were analyzed in sections stained by thionin.

B. Immunocytochemical Localization of Cholinergic Pathways

Experiments were conducted in 25 adult male Sprague-Dawley rats (250 - 400 g). To enhance cell staining ten animals (anesthetized with halothane (2% in 100% O₂) were injected stereotactically into the right lateral ventricle with colchicine (Sigma; 150 μ g in 10 μ l distilled water) over 50-60 minutes and allowed to survive for 24 hours.

Animals were anesthetized with Nembutal (50 mg/kg, i.p.) and perfused transcardially with normal saline for 30 seconds followed by 500 ml of 4% (w/v) paraformaldehyde in 0.1 M phosphate buffer (pH 7.3). Frozen 30 μ m sections were cut transversely or sagittally on a sliding microtome; alternate sections through the medulla or entire brainstem were processed immunocytochemically for ChAT by a modification of the peroxidase-antiperoxidase technique of Sternberger (1979). Monoclonal antibodies specific to ChAT of porcine brain origin and produced in rat-mouse hybridomas were obtained from Boehringer-Mannheim. In control studies, immunocytochemical specificity was tested by omitting the primary antibody. In several animals adjacent sections were incubated with primary antisera to ChAT, TH or PNMT. Antibodies to TH and PNMT were produced in rabbits against enzymes of bovine adrenal origin and localized immunocytochemically based on procedures described previously (Park et al., 1982; Joh and Ross, 1983; Ruggiero et al., 1985).

Sections were mounted on gelatin-coated slides, dehydrated through graded alcohols, cleared in xylene and coverslipped with Histoclad. Section outlines and gross nuclear borders were drawn from adjacent Nissl-stained sections using an overhead Bausch and Lomb projector. The total number of immunoreactive perikarya on each section was mapped under brightfield illumination with the aid of a camera lucida attached to a Leitz microscope. Labeled processes (dendrites, axons and bouton-like varicosities) were drawn under darkfield illumination. The distributions of cholinergic

perikarya and fine punctate varicosities were compared to the locations of (a) catecholaminergic neurons immunostained on alternate sections, and (b) perikarya labeled with wheat germ agglutinin-horseradish peroxidase conjugate (WGA-HRP) or fluorescent tracers (e.g., fluorogold) injected into thoraco-lumbar or cervical segments of spinal cord (most axoplasmic transport material was available from previous or concomitant (Cravo et al., 1988) studies). Methods used to demonstrate WGA-HRP reaction product were identical to those described previously (Ruggiero et al., 1987).

C. Axonal Transport Studies

Neural pathways were traced using WGA-HRP as retrograde-anterograde tracer. Five days after microinjection of IBO or vehicle into the primary sensory cortex, rats were anesthetized with halothane, as described above, and placed in the stereotaxic frame. The pipette was lowered into the cerebral cortex through the holes in the skull made 5 days earlier, and WGA-HRP (Sigma, 30-60 nl of a 2% solution in H₂O) was microinjected at the same site in which IBO or vehicle were previously microinjected. Thirty-six to forty-eight hours after injections of WGA-HRP, rats were deeply anesthetized with pentobarbital sodium (100 mg/kg) and perfused through the heart with saline followed by fixative containing 1% formaldehyde solution and 1% glutaraldehyde in 0.1 M phosphate buffer (pH 7.2). Following cryoprotection in 30% sucrose the brain was sectioned at 40 μ m using a freezing microtome, and the sections were mounted on slides and processed using tetramethylbenzidine as substrate. Alternate sections were stained with thionine, using conventional histological procedures. WGA-HRP material was examined using dark and bright field illumination. Sections were first projected on paper, using a vertical projector (Bausch and Lomb), and the major anatomical structures were identified and outlined. The location of the label was then plotted on the drawings using a microscope equipped with a camera lucida attachment.

D. Morphological Analysis of Microvessels

Light Microscopy

The MV and synaptosomal fractions were routinely examined by light microscopy for composition and purity. Twenty-five μ l aliquots of MV or synaptosomes were spread onto gelatin (0.5%) or poly-D-lysine (1%; MW = 150,000 - 300,000) coated slides and allowed to dry at room temperature. The tissue was post-fixed with 10% buffered formalin or 4% paraformaldehyde in 0.1 M phosphate buffer (pH = 7.4), dehydrated, rehydrated and stained with 0.75% methylene blue. Ten random fields were examined qualitatively for each preparation at a final magnification of 200x.

For quantitative analysis of the distribution of the diameters of the vascular elements a computerized image analysis system was used (Spatial Data System, Eyecon II; PDP 11/45). The slides were viewed with a Leitz microscope (at 40x) coupled to a Vidicon scanner. With a joystick-controlled cursor the diameters of the vessels were calculated at the branching points of the vascular tree (see Fig. 3).

Electron Microscopy

Aliquots (0.2 - 1.0 ml) of MVs or synaptosomes were post-fixed for 10 min with 2% glutaraldehyde in 0.1 M phosphate buffer (pH = 7.4) contained in 1.5 ml microcentrifuge tubes. All steps of the tissue processing were completed in the microcentrifuge tubes by gently centrifuging the tissue (500 x g for 1 min), drawing off

the supernatant, and adding the next reactant. The fixed tissue was washed with 0.1 M phosphate buffer (pH = 7.4), dehydrated with alcohols, placed in propylene oxide and treated with 2% osmium tetroxide for 2 hours. Pellets of the fixed tissue were embedded in Epon-812 and sections (500 Å) cut through selected portions of the pellet on a LKB microtome. Sections were collected on grids and counterstained with uranyl acetate (20 min) and Reynold's lead citrate (5 min) for examination with a Philips 201 electron microscope.

E. Morphological Analysis of ChAT-Immunoreactive Cellular Processes Using Light and Electron Microscopy

Light microscopic methods were used to analyze the laminar distributions of cholinergic processes and somata throughout the brainstem and cerebellum. Electron microscopic analysis was carried out to determine the types of associations formed with cholinergic neurons. These may be cholinergic somata, dendrites or axons forming synaptic or non-synaptic associations with unlabeled or labeled somata, dendrites, spines, axons, endothelial cells around blood vessels or glial processes.

Male Sprague-Dawley rats (200-250 gm) were deeply anesthetized with Nembutal (50 mg/kg, i.p.) and perfused through the heart with 0.2% glutaraldehyde and 4% paraformaldehyde in 0.1 M phosphate buffer (pH=7.4). At the termination of the procedure, the brains were removed from the skulls, cut into 4 mm wide blocks and placed in the above fixative for 30 min. The blocks were then placed in 0.1 M phosphate. The region of the cerebral cortex at the level of the caudate nucleus was coronally sectioned (30 μ m) on a Vibrotome (vibrating microtome).

A monoclonal antiserum to ChAT was produced from rat-mouse hybridomas and tested for specificity by Boehringer-Mannheim Biochemicals (Eckenstein and Thoenen, 1983). The antiserum was localized in the tissue by a modification (Pickel et al., 1975; Pickel, 1981) of the peroxidase anti-peroxidase (PAP) method of Sternberger (1979). Briefly, this procedure consisted of a sequential incubation of the sections with: (1) a 1:40 dilution of the ChAT antiserum; (2) a 1:50 dilution of rabbit anti-rat immunoglobulin (IgG); (3) a 1:100 dilution of a rat PAP complex. The diluent and washes were prepared with 1% rabbit serum in 0.1 M Tris-Saline (pH=7.6). Tissues were incubated with primary antiserum for 18-24 hours at 4°C and with IgG or PAP for 1 hour at room temperature. All reactions were carried out with continuous agitation. The PAP reaction product was demonstrated by incubation with 3,3'-diaminobenzidine (DAB) and hydrogen peroxide.

For light microscopy, the immunoreacted sections were mounted on gelatin-coated slides, dehydrated, coverslipped and viewed by differential interference contrast optics. For electron microscopy, the labeled sections were postfixed for 10 min with 2% glutaraldehyde in 0.1M phosphate buffer, then for 1 hour in 2% osmium tetroxide in 0.1M phosphate buffer, dehydrated in a graded series of ethanol and embedded between two plastic coverslips in Epon 812. Regions of the cerebral cortex containing ChAT-labeled processes were selected and embedded in Beem capsules. Ultrathin sections were collected on grids from the surface of the plastic embedded tissues, counterstained with 5% uranyl acetate and Reynolds lead citrate, and examined with a Philips 201 electron microscope.

V. EXPERIMENTAL PROTOCOLS

Stimulation of Fastigial Nucleus for Measurement of rCBF and ACh Release

One hour after completion of surgery, a stimulating electrode was lowered through the cerebellum and positioned in the most "active" portion of the FN, as described above. Care was taken during exploration to avoid large abrupt changes in AP and to maintain AP within the autoregulated range of CBF for the rat (80-150 mmHg) (Hernandez et al., 1978). The electrode was left in place at the active site and blood gases were carefully adjusted. At this point in the protocol the animal was either prepared for cortical application of drugs and measurement of rCBF, or prepared for measuring the release of $^3\text{H-ACh}$.

Cortical Application of Atropine for rCBF Measurement

In these experiments the cortical superfusion device was carefully placed on the pial surface 30 min prior to rCBF measurement. Either vehicle (Kreb's-bicarbonate buffer) or atropine sulfate (100 μM) was superfused for 10 min prior to electrical stimulation of FN. For rCBF measurement the FN was stimulated with an intermittent stimulus train (1 sec on/1 sec off; pulse duration, 0.5 msec; frequency, 50 Hz). During the first 2-4 min of stimulation the intensity of the stimulus was gradually increased to reach 5x the threshold current while the evoked rise in AP was concurrently reduced by slow, controlled withdrawal of blood (4-6 ml) to maintain the AP in the autoregulated range. FN stimulation continued for 7-10 min during which the AP remained stable and the blood gases were adjusted (Fig. 4). At the end of this phase $^{14}\text{C-IAP}$ was infused for 30 sec, the animals killed, and the amount of radioactivity in the arterial blood and brain tissue determined.

Release of $^3\text{H-ACh}$ From Cortical Surface

For these studies, a stimulating electrode was positioned in the FN and the cortical superfusion device placed shortly following the completion of the surgery. Just prior to the placement of the superfusion device, nerve terminal stores of the cholinergic innervation to the primary motor CX were prelabeled with $^3\text{H-methylcholine}$ (1.5 $\mu\text{Ci}/1 \mu\text{l}$; specific activity 80 $\mu\text{Ci}/\text{nmol}$, New England Nuclear). The $^3\text{H-methylcholine}$ was microinjected at a depth of 1.5 mm below dura through a 70 μm (o.d.) glass pipette at a rate of 200 nl/min with the aid of a micromanipulator and an air-driven mechanical valve system (Amaral and Price, 1983). When the cortical superfusion device was put in place, the pial surface was superfused with modified Kreb's-bicarbonate buffer (100 μM physostigmine) at a rate of 10 $\mu\text{l}/\text{min}$. Superfusate was collected in 8 min epochs for 2 hours into microcentrifuge tubes containing 8 μl 1.0 N perchloric acid. Immediately following the experiment the samples were frozen (-20°C) for later analysis of $^3\text{H-ACh}$.

Release of $^3\text{H-ACh}$ was quantified during: (a) resting conditions (i.e., spontaneous release); (b) during electrical stimulation of FN; and (c) during depolarization of the cortical surface with 55 mM K⁺. Increased potassium concentrations were compensated by an equiosmolar decrease in sodium concentration.

Preliminary experiments (n=5) demonstrated that one hour following microinjection of $^3\text{H-methylcholine}$ greater than 99% of the tritium was restricted to the right parietal cortex (data not presented). This suggested that the release of $^3\text{H-ACh}$ measured during the experiments was from the target area of the CX and not from adjacent structures.

Moreover, to discount the possibility that the procedure of microinjecting ^3H -choline into the parietal CX caused a paralysis of the vasculature, we concurrently measured the release of ^3H -ACh and rCBF in the targeted area. In five rats, FN stimulation elevated rCBF in the parietal CX to 179 ± 16 ml/100g/min, which was not significantly different from operated control animals (188 ± 21 ml/100g/min). Finally, we verified the viability of the underlying cortical area to generate a normal ECoG that was responsive to electrical stimulation of distant brain regions. As previously demonstrated (Underwood et al., 1983), electrical stimulation of the FN was characterized by a stimulus-locked, regular, slow-wave activity, without a substantial change in amplitude (Fig. 5A). Also, electrical stimulation of the pontine reticular formation (4.0 mm ventral to FN) elicited the classical stimulus-locked low amplitude fast activity (Fig. 5B) identical to the desynchronization response first described by Moruzzi and Magoun (1949). Lastly, application of K^+ did not result in spreading depression since the ECoG shifted to a lower amplitude pattern of similar frequency (Fig. 5C) and not to the flat or desynchronous pattern which is typical of spreading depression.

RESULTS

I. EFFECTS OF ATROPINE ON VASODILATION ELICITED FROM FN

A. Measured by IAP

Electrical stimulation of the FN elicited the well-established elevation in AP and HR (Miura and Reis, 1969) (Table 3). It also elicited EEG changes characterized by stimulus-locked, regular, slow-wave activity (2-3 Hz) which on occasion persisted for 2-4 s after termination of the stimulus (Fig. 6). In untreated rats (n=5), FN stimulation elicited a global increase in rCBF (Table 4). The increases ranged from $121 \pm 7\%$ of control in hypothalamus to $246 \pm 50\%$ in frontal cortex ($p < 0.05$; Table 4), and were similar in magnitude and regional pattern to those previously reported from our laboratory (Iadecola et al., 1983; Nakai et al., 1982; Nakai et al., 1983). In the inferior colliculus, the 122% of control increase did not reach statistical significance ($p < 0.05$). Atropine (0.3 mg/kg, i.v.) did not significantly change the minimal current required for elevation of AP (i.e. threshold current) nor the magnitude of AP elevations elicited from FN at 5 times threshold (Table 3). Basal HR rose by 75 ± 11 bpm (mean \pm S.E.M.) ($p < 0.001$) after atropine, while the increase in HR elicited by FN stimulation was significantly reduced (Table 3).

Atropine did not affect basal EEG nor the evoked change in EEG activity described above (Fig. 6). Resting rCBF in unstimulated rats was not affected by atropine ($p > 0.05$; n=5). However, the drug virtually abolished the increase in rCBF, but not AP, elicited by FN stimulation (Table 4; n=5).

B. Measured by Laser-Doppler

Stimulation of the FN with intermittent trains of stimuli (1 sec on/1 sec off) produced large increases in CBF (Fig. 7). At $75-100 \mu\text{A}$ and 50 Hz the increases averaged 20.2 ± 1.6 PU (n=12) and were accompanied by only slight (< 10%) fluctuations in AP (Figs. 7,8), probably reflecting release of vasopressin (Del Bo et al., 1983). In order to compare the magnitude of the CBF response as measured by LDF with that determined by the IAP technique, we used the relationship between CBF measured by laser-Doppler (CBF_{LD}) and CBF measured by IAP (CBF_{IAP}) developed above. By this equation it appears that FN stimulation produces an increase in CBF of $124 \text{ ml}/100 \text{ g} \times \text{min}$, a figure comparable to the flow increases reported during FN stimulation in the rat cerebral cortex using the IAP technique (Iadecola et al., 1986b; Iadecola et al., 1987a; Nakai et al., 1982; Nakai et al., 1983).

The increase in CBF elicited from the FN ($50-100 \mu\text{A}$; 50-70 Hz) usually began after a small and transient decrease, reached 50% of maximum after 24 ± 1 sec, and reached a plateau after 49 ± 2 sec (n=17). The elevations persisted steadily during stimulation and declined upon its termination. The rate of decline however was slower than the rate of rise (Fig. 7). Thus, CBF reached its baseline in a period of time ranging from 84 to 540 sec after termination of the stimulation. There was a positive and significant correlation between the duration of the stimulation and the time of recovery of CBF (time to baseline = $1.14 \times \text{stim. time} + 15.8$; $r = 0.93$; $p < 0.001$; n=15). This relationship is illustrated in Fig. 9.

We then sought to establish whether the characteristics of the response as determined by LDF were comparable to those previously described with respect to dependence on stimulus parameters, anatomical localization of active sites, and sensitivity to cholinergic blockade or barbiturates.

The increase in CBF were dependent upon the intensity and frequency of the stimulus (McKee et al., 1976; Mraovitch et al., 1986) (Fig. 10). When the current intensity was varied, while the stimulation frequency was kept constant at 50 Hz, the response appeared between 10 and 20 μ A, its magnitude increased linearly with the increase in current intensity and reached a plateau at 100 μ A (Fig. 10). Similarly, when the stimulation frequency was varied while the intensity was kept at 75-100 μ A, the response appeared between 5 and 15 Hz, peaked at 70-100 Hz and decreased at stimulation frequency of 200 and 300 Hz (Fig. 10).

The increases in CBF evoked from the FN were best elicited from the rostral ventromedial portion of the nucleus (Doba and Reis, 1972; McKee et al., 1976; Mraovitch et al., 1986; Nakai et al., 1982) (Fig. 11). However, stimulation of the VPRF at a site located 4 mm ventral to the FN also produced large, stimulus-locked, increases in CBF (Fig. 11).

In three rats the increases in CBF elicited by stimulation of the FN were abolished by administration of atropine (1 mg/kg, i.v.) (Fig. 8). Interestingly, the effect of atropine was not immediate. Two to 10 min after administration, the response was still present although reduced to 50 and 27% of control respectively. Fifteen min after administration the flow increase evoked from the FN was abolished while that elicited from the VPRF was still present (Fig. 8), indicating that the effect of atropine was not due to a loss of reactivity of the preparation. The delayed effect of atropine may reflect its poor CNS penetration (Witter et al., 1973) and may suggest that this drug does not exert its action by blocking cerebrovascular muscarinic receptors (Estrada et al., 1983).

In three other rats the effect of pentobarbital on the response was examined. This agent abolishes the elevations in AP and HR elicited from FN stimulation (Miura and Reis, 1970). Five min after 20 mg/kg of pentobarbital were given, the increase in CBF elicited from the FN was markedly reduced (Fig. 12). Administration of additional pentobarbital (10 mg/kg, i.v., cumulative dose 30 mg/kg) abolished the increase in CBF evoked from the FN without abolishing cortical electrical activity (Fig. 12).

C. Summary

These studies, therefore, indicate that the release of acetylcholine somewhere in the brain is required for the expression of the cerebrovascular vasodilation elicited by electrical stimulation of the FN. Moreover, the effect of the cholinergic link is relatively selective for the cerebrovascular effect since it does not modify the elevations of AP evoked by electrical stimulation of the nucleus. Hence, the cholinergic link does not lie in the pathway between FN and the area of the rostral ventrolateral medulla containing reticulospinal projections (Chida et al., 1989).

II. SOURCES OF ACH RELATED TO CORTICAL VASODILATION FROM FN STIMULATION

A. Autonomic-Cholinergic Pathways

The site at which ACh release is critical for the expression of the cerebrovascular vasodilation from FN along the pathway from FN to the target region. Since cholinergic elements contributing to these critical pathways have not been well established, a study was undertaken to identify the origins of cholinergic autonomic neurons and cholinergic projection fields within the autonomic core of the brainstem. Cholinergic pathways were identified by using monoclonal antisera against choline acetyltransferase (ChAT), the ACh synthesizing enzyme to map the distribution of central cholinergic autonomic loci.

Perikarya and punctate varicosities immunoreactive for ChAT were discovered in several brainstem autonomic substructures including several known to play a role in the regulation of arterial blood pressure and cerebral blood flow. ChAT positive perikarya were identified in the nucleus of Koelliker-Fuse (KF) of the parabrachial complex, medial, intermediate and commissural divisions of the NTS, medullary periventricular grey (PVG) lining of the floor of the fourth ventricle, nucleus raphe obscurus (a bilaterally symmetrical vertical array of cells bordering the medial longitudinal fasciculus), nucleus raphe magnus and the medial aspect of the rostral ventrolateral medulla (RVL). Cells in the RVL lay in close proximity to the ventral medullary surface and were medial to the adrenergic perikarya of the C1 area. The weak and inconsistent staining of cells in KF and NTS suggest that these neurons contain relatively low levels of the enzyme.

The camera lucida drawings in Fig. 13 illustrate ChAT-immunoreactive cell bodies in autonomic nuclei of the medulla oblongata.

New terminal fields were identified throughout the brainstem and cerebellum. In the medulla, immunoreactive fibers were admixed with labeled perikarya as described above. Within an area of the RVL identified by PNMT-positive adrenergic cell bodies were labeled varicosities of unknown origin, as well as dendrites derived from the overlying compact division of nucleus ambiguus. Labeled fibers were also seen along the ventral subpial surface of the RVL (Figs. 13,14). The presence of cholinergic terminals in the ventrolateral medulla was, moreover, supported by our electron microscopic data, which demonstrate symmetric synapses between ChAT immunoreactive terminals and proximal dendrites in the RVL (Drs. T. Milner and V. Pickel, unpublished data). Punctate varicosities were also seen in areas of the NTS innervated by primary cardiopulmonary afferents, the dorsal motor nucleus of the vagus, raphe, and in the PVG along the floor of the fourth ventricle (Fig. 15).

In the pons, terminals were concentrated in the periventricular gray, raphe and parabrachial nuclei (PBN). In the PBN, new fields distinguished the superior, internal and dorsal divisions of the lateral PBN, the nucleus of KF and an area of medial PBN underlying the superior cerebellar peduncle. In contrast to evidence suggesting a cholinergic input to the LC (Palkovits and Jacobowitz, 1974), we found that terminals surrounded, but did not overlap the LC (Fig. 16). As observed under darkfield optics, presumptive terminals in the PBC formed clusters restricted to specific subnuclei as defined by the Nissl and connectional studies of Fulwiler and Saper (1984) as prethalamic or precortical. Axons of cholinergic fields in the PBC were traced to cholinergic pontine cell groups (Ch6 and Ch5) projecting to nuclei of the medial forebrain bundle or to non-specific thalamic nuclei of the midline and intralaminar complex and the basal forebrain.

The locus ceruleus, although not receiving direct axosomatic innervation from cholinoreceptive fields (labeled for ChAT), nevertheless gives rise to dendrites extending into neighboring cholinergic fields: within the nucleus subceruleus ventrally, periventricular gray dorsally and the parabrachial complex laterally. Ceruleal dendrites within these cholinergic "presumptively terminal" fields originate from neurons of the LC which, like the PBC, project to the intrathalamic complex and widespread areas of the cerebral cortex. Cholinergic varicosities were concentrated surrounding deep cerebellar neurons in the rostral aspect of the fastigial nucleus and neighboring folia of the anterior cerebellar vermis (lobules I-IV). The close appositions between medial cerebellar perikarya and punctate varicosities immunoreactive for ChAT, resembling terminal boutons, is suggestive of axosomatic contacts (not illustrated).

In basal forebrain, terminals were labeled in the nucleus of the stria terminalis (NST). In anterior and tuberal regions of hypothalamus, immunoreactive processes occurred in the zona incerta, perifornical and dorsal subnuclei and in an area of the lateral hypothalamus, transitional with the amygdala and overlying the supraoptic nucleus (SON). Few if any terminals were labeled in the supraoptic or paraventricular hypothalamic nuclei (PVN). In the caudal hypothalamus terminals conformed to the cytoarchitectonic borders of the subparafascicular nucleus adjacent to the fasciculus retroflexus, posterior hypothalamic nucleus, and portions of the medial and lateral mammillary nuclei.

In the amygdala, terminals were localized to subnuclei surrounding the central nucleus; in contrast to previous reports, terminals were not detected in the main body of the central nucleus (a principal subcortical relay of visceral afferents from NTS). The camera lucida drawings in Fig. 17 illustrate ChAT-immunoreactive cell bodies in cutonomic nuclei of the diencephalon and basal forebrain.

Anatomical substrates are summarized in Figs. 17 and 18.

1) Several new groups of perikarya with the ability to synthesize acetylcholine were discovered in regions that are interconnected to the fastigial nucleus: the solitary nucleus, parabrachial complex, the periventricular gray and the nucleus RVL. Functional and structural studies suggest that these nuclei receive input from peripheral autonomic afferents as well as the fastigial nucleus (FN) (Batton et al., 1977; Ross et al., 1981) and, in turn, project directly to the intermediolateral cell column in thoracic cord. Cholinergic nuclei also project rostrally to midline and intralaminar thalamic relay nuclei known to project to widespread areas of the cerebral cortex by terminals concentrated in supragranular associative layers.

2) New terminal fields were also found in the above areas and in other autonomic substructures throughout brain, including sites which are known to elicit site specific changes in arterial blood pressure and regional alterations in cerebral blood flow (e.g. lateral tegmental field and fastigial nucleus).

3) The absence of cholinergic terminals in the LC, paraventricular or supraoptic nuclei was unexpected, and suggests that cholinergic processing attributed to these structures may be mediated by adjacent neurons or by synapses on dendrites (or axons) lying outside their nuclear borders.

4) The functions of cholinergic and adrenergic cells in the RVL are unclear, although the evidence strongly suggests that: a) the C1 area contains a significant density of muscarinic receptors, b) neurons within the C1 area release ACh, and c) the integrity

of neurons in the C1 area is essential for the maintenance of normal levels of AP, the fastigial pressor response and the primary cerebrovasodilation to hypoxia but not hypercarbia.

B. Cholinergic Markers in the Cerebral Cortex: Ultrastructural Studies

We also sought to determine the distribution of cholinergic elements in a target field, the cerebral cortex, in order to test the possibility that local release of ACh was responsible for the vasodilation.

By light microscopy, perikarya with bipolar morphology were evident in rat cortex, as has been reported by others (Houser et al., 1985; Eckenstein and Baughman, 1984; Kimura et al., 1981; Stichel and Singer, 1985). ChAT-containing axons were also in abundance.

By EM, ChAT was immunocytochemically localized to axons and axon terminals in the neuropil of layers I, II, III and V of the CX (Fig. 19A), as previously described (Houser et al., 1985; Lysakowski et al., 1986). These axon terminals contained numerous small clear vesicles (0.1-0.2 μm) surrounded by the peroxidase product. Within layer III, ChAT-labeled axons (0.2 μm in diameter) were found in close apposition to the basal lamina of unlabeled endothelial cells (Fig. 19B). These elements did not form any classical synaptic or junctional specializations.

In less than 5% of the cases ChAT immunoreactivity was found in the cytoplasm of capillary endothelial cells (Figs. 19C and 20). These ChAT-labeled endothelial cells usually were associated with small blood vessels (4-8 μm) and most frequently observed in layer III of the CX. Their unlabeled nucleus was elongated and contained dense clumps of heterochromatin. The presence of ChAT-labeled endothelial cells has also been reported to occur in other regions of the brain such as the medulla (Milner et al., 1987). Rarely, a ChAT-immunoreactive terminal was observed in close proximity to a ChAT-labeled endothelial cell (Fig. 20A). In this type of situation thin astrocytic processes separated the two labeled elements by approximately 0.1 μm . It is unlikely that endogenous peroxidase activity localized to the endothelium accounted for the presence of ChAT-labeled endothelial cells, since substitution of the monoclonal antibody with non-immuno rat IgG abolished the detection of the relationship.

III. MICROVESSELS AS SOURCES OF CHAT

The localization of ChAT and microvessels is a most intriguing observation and confirms one other report by Parnavelas et al. (1985). However, it is essential, if one is to propose that capillaries are a source of acetylcholine, to demonstrate that they have the capacity to synthesize and release the agent. We, therefore, undertook studies to establish whether microvessels have the capacity to synthesize acetylcholine.

A. Characterization of Microvessels

The MV and nerve terminal fractions were routinely examined by light microscopy to assess their purity and composition. As shown in Fig. 21 the preparation contained vessels ranging from 4 to 40 μm in diameter, with minimal contamination by non-vascular elements such as dendrites and glia. The MV fraction was heterogeneous in that it

contained capillaries (10 μm), endothelial and, presumably, smooth muscle cells from terminal arterioles and venules (10-40 μm).

In 4 separate experiments, the distribution of the diameters of the vascular segments isolated was quantified with a computerized image analysis system. With a joystick-controlled cursor the diameters of the vessels were calculated at the branching points of the vascular tree (Fig. 3A). After counting a total of 690 vessels, 67.7% were less than 10 μm (Fig. 3B), which corresponds to a capillary fraction (Nakai et al., 1981). About one third (32.3%) were, therefore, small arterioles and venules ranging from 11 to 40 μm (Fig. 3B).

γ -GTP and AP, two marker enzymes which have been localized to intraparenchymal brain vessels (Goldstein et al., 1975; Orlowski et al., 1974; Rowan and Maxwell, 1981; Williams et al., 1980), were enriched in the microvesel fractions both from the CX and CN (Table 5). When compared to the nerve terminal (S_1) fraction, γ -GTP and AP were enriched by 6- to 29-fold and 3- to 22-fold, respectively, which is consistent with the values reported by others for fractions containing MVs and capillaries (Estrada et al., 1983; Goldstein et al., 1975).

Further characterization of the MV preparation at the ultrastructural level demonstrated that many vessels of the CX are surrounded by a basal lamina, which usually encapsulates an intact endothelium. The smaller blood vessels (4-10 μm in diameter) were identified as having endothelial cells with a heterochromatic cell nucleus surrounded by a basal lamina and a few astrocytic processes with no association with smooth muscle, suggesting that they were capillaries. Although a majority of vessels had an intact endothelium with morphological characteristics representative of that seen *in situ*, sometimes the larger isolated vessels ($>10 \mu\text{m}$) shared a perivascular basal lamina, pericytes, occasional smooth muscle cells and a once-present endothelium (Fig. 22A). Erythrocytes were sometimes found within the lumen of the vessels. Other non-vascular debris such as neuronal perikarya was infrequently observed, although material resembling astrocytic end processes and nerve terminals was frequently found attached to the basal lamina.

In contrast, the nerve terminal fractions (S_1 and P_2) did not contain any vascular elements. In the P_2 fraction (Fig. 22B), nerve terminals and attached postsynaptic elements were found to make both symmetric and asymmetric synapses as previously reported (Gray and Whittaker, 1962; Whittaker, 1969).

B. ChAT Activity in Microvessels

ChAT activity was measured in different fractions isolated from the CX, CN, CRB and LIV. When the data are expressed as the absolute amount of ACh synthesized (pmol [^{14}C]ACh) from each respective fraction and tissue, relative to the amount synthesized from a 100 mg (wet wt.) section of the CX, 2.4% of the total cortical activity was associated with MVs and 94% was associated with nerve terminals (Fig. 23A). No significant differences were observed across the MV fractions from each tissue (Fig. 23A). In contrast, ChAT activity varied 10-fold among the nerve terminals containing fractions (S_1) from the CX, CN, CRB and LIV (Fig. 23A), and in a manner consistent with the known cholinergic innervation to these areas (Kuhar, 1976; Mesulam et al., 1983b). However, when the data were calculated as a specific activity (i.e. nmol [^{14}C]ACh formed/mg protein/40 min), it was discovered that MVs isolated from the 3 brain structures, but not LIV, synthesized [^{14}C]ACh at rates significantly greater than the nerve

terminal fraction (Fig. 23B). The percent increase above the corresponding homogenate was +95%, +268% and +313% for the CX, CN and CRB, respectively.

The ability of cortical MVs to synthesize ACh was confirmed by two additional methods, since [¹⁴C]acetyl CoA, which serves as substrate in the assay of ChAT activity, may also serve as substrate for other acetyltransferases present in the brain. First, the specific inhibitor of ChAT (Smith et al., 1967), NVP, inhibited ChAT activity in cortical MVs by 95% (Fig. 24). Second, the product formed by incubation of [¹⁴C]acetyl CoA with cortical MVs was extracted by the enzymatic liquid-cation exchange method and co-chromatographed with [¹⁴C]ACh standards separated by HPLC (Fig. 25). These findings established that elements associated with cortical MVs have the capacity to synthesize authentic ACh.

C. Release of [³H]ACh from Cortical Microvessels

The release of [³H]ACh and, for comparison, endogenous AAs neurotransmitters, GABA, Gly and Asp were measured from cortical MVs and nerve terminals (S₁). The pattern of spontaneous release in the presence of 1.2 mM Ca²⁺ is shown in Table 6. For MVs, Gly had the highest and ACh the lowest spontaneous release. In contrast, in the nerve terminal homogenate, GABA had the highest rate of release, which was 10-fold higher than that observed in the MVs. Also, Gly release was one third less in the nerve terminal homogenate, while release of ACh was 3-fold higher. Asp release was only slightly higher in the nerve terminal homogenate compared to the MVs. The marked differences in the pattern of release suggests that two distinct fractions were isolated and that the release of neurotransmitters from the MV fraction was not the result of a simple contamination from the nerve terminal homogenate.

Cortical MVs depolarized with 55 mM K⁺, in the presence of Ca²⁺, released a substantial amount of [³H]ACh (Fig. 26A). This effect was graded, since depolarization with 25 mM K⁺ resulted in smaller, but significant, release of [³H]ACh (149 ± 19% of the spontaneous release; p<0.05; n=5). Importantly, the K⁺-evoked release of [³H]ACh from MVs was entirely dependent on extracellular Ca²⁺ concentrations (Fig. 26B), suggesting a possible neurotransmitter function of the ACh to affect the microvasculature.

Release of GABA, Gly and Asp from MVs by 55 mM K⁺ was small and not statistically significant (Fig. 26A). In contrast, release of ACh, GABA and Asp, but not Gly, was evoked from the homogenate by 55 mM K⁺ (Fig. 26A). Thus, cortical MVs may be selectively innervated by cholinergic, but not GABAergic, glycinergic or aspartergic nerves.

IV. ROLE OF LOCAL CHOLINERGIC ELEMENTS IN CBF RESPONSE TO FN STIMULATION

The following studies were undertaken to assess the relative contribution of efferent cholinergic fibers to the cortex largely arising from the basal forebrain, of local cholinergic neurons, and possibly of vascular cholinergic elements in the vasodilation elicited by electrical stimulation of the FN. The strategy of this study was basically to establish whether local neurons were responsible for the vasodilation or, if they were not, whether the response could be attributed to ascending cholinergic axons from basal forebrain.

A. Effect of Topical Application of Atropine on the Cortical Vasodilation Elicited by Stimulation of the FN

In animals in which the cranium was intact (n=6), rCBF ranged from 70 ± 5 in hippocampus to 95 ± 7 in parietal CX (Table 8). Values did not differ between right and left side ($p>0.05$) and were similar to those obtained in the anesthetized rat from this (Nakai et al., 1982) and other (Sakurada et al., 1978) laboratories. After a bilateral craniotomy, application of vehicle or atropine (100 μ M) to the cortical surface did not affect resting rCBF in the underlying parietal CX nor in other regions (Table 8).

Electrical stimulation of the FN in untreated rats increased rCBF bilaterally and symmetrically in all regions sampled (Fig. 4), with the greatest increases occurring in the parietal CX. Topical application of atropine (100 μ M) to the right parietal cortex significantly reduced the elevation in rCBF by 55% in the ipsilateral parietal CX and by 62% in the ipsilateral frontal CX (Fig. 27). However, in the remainder of the brain the elevations in rCBF were not significantly reduced by atropine (Fig. 27).

Effect of Topical Application of ATR on the Cerebrovasodilation Elicited by Hypercarbia

Arterial pCO_2 elevated to 59.0 ± 1.4 mm Hg (n=5) with 5% CO_2 , increased rCBF in all areas of brain to a level comparable to that obtained with FN stimulation (Fig. 28). ATR (100 μ M) applied to the right parietal CX (n=5) had no effect on the magnitude of the cerebrovasodilation either locally or elsewhere in brain (Fig. 28). Thus, the reduction of the cortical vasodilation evoked from the FN by ATR is not a consequence of a non-specific action of the drug on cerebral vessels, and the cortical vasodilation elicited by hypercarbia does not involve a cholinergic link.

Effect of Stimulation of the Fastigial Nucleus on the Release of ACh from CX

The observation that topical cortical application of atropine attenuates the cortical vasodilation elicited from the FN strongly suggests that ACh released locally is involved in the cortical vasodilation. We therefore sought to establish whether stimulation of the FN releases ACh from the CX.

Release of [3 H]ACh from the cortical surface was measured following microinjection of [3 H]choline into the parenchyma of the parietal CX, which initiates the local biosynthesis of [3 H]ACh. After the microinjection, the superfusion device was stereotactically positioned on the dura and superfusion was begun. The effect of electrically stimulating the FN or depolarizing the cortical surface with 55 mM K $^+$ is illustrated in a representative experiment (Fig. 29). Within 30 min of superfusion the rapid efflux of [3 H]ACh began to stabilize. When FN was stimulated for 16 min there was no apparent effect on the efflux of [3 H]ACh. In contrast, local depolarization with K $^+$ increased [3 H]ACh release over 2.5-fold. This K $^+$ -evoked release of [3 H]ACh indicated that we could reliably measure the release of [3 H]ACh with the experimental conditions used. The grouped data of 9 similar experiments demonstrated that FN-stimulation significantly reduced the release of [3 H]ACh (Figs. 27,30). The validity of this finding was supported by establishing that during these experiments cortical rCBF was elevated (n=5), and release of [3 H]ACh evoked by K $^+$ was increased up to 251% of control (Figs. 27,30).

These data indicate that the release of cortical [³H]ACh is, in general, reduced by FN stimulation. Thus, an FN-elicited release of [³H]ACh, if small in magnitude, would not be detectable.

B. Effect of Cholinergic Agonists

As reported previously (1st quarter, year 03), using Laser-Doppler flowmetry the microinjection of saline (100 nl) into the cortex elicited a small transient increase in local cortical blood flow (CrtBF). Subsequent microinjections had no effect, hence the testing of drugs always followed microinjections of saline which elicited no effect.

Microinjection of ACh (0.36-3.6 nmol/100 nl) elicited increases in CrtBF which appeared within the first 10 sec following the onset of the infusion (Fig. 31) and lasted as long as 9 min before returning to baseline values. Low dose (0.36 nmol/100 nl) microinjection of ACh elicited a 19-46% increase in CrtBF, while the highest dose (3.6 nmol/100 nl) gave rise to an increase in CrtBF from 23% to 38% and lasted 7 ± 2 min (n=5). Arterial blood pressure (AP), heart rate (HR) and blood gases were unaffected by the microinjections.

Microinjection of 0.1-0.9 ng diisopropyl phosphofluoridate (DFP) (n=4) elicited increases in CrtBF from 26% to 54% lasting up to 10 min. The increases were dose-dependent (Fig. 32) with the exception of the highest dose (0.9 ng) where only a 33% increase in CrtBF was observed. The increase in CrtBF began within 10 sec of the onset of the infusion (Fig. 33) and reached maximum at 50 ± 10 sec. The largest increases were observed at a dose of 0.5 ng and were unassociated with any change in AP, HR or arterial blood gases. These findings are consistent with the view that local accumulation of ACh increases CBF, an effect blocked by atropine.

C. Role of Local Neurons

The previous studies demonstrate that local release of ACh mediates, in large measure, the vasodilation from electrical stimulation of FN. Whether the effect depends upon a cholinergic neurovascular input from basal forebrain or interposition of local neurons was investigated.

Effect of Local Cortical Microinjection of Ibotenic Acid on Local Neurons and Fibers

First, we sought to establish by histological, biochemical, and axonal transport studies, whether in cerebral cortex, as in other brain regions (Schwarcz et al., 1979), microinjection of IBO destroys only local neurons, sparing axons and terminals within the area.

Histology. IBO was microinjected (10 µg in 1 µl) in a region of the parietal cortex corresponding to the primary sensory cortex in five rats. Animals were allowed to recover and were returned to their cages. Five days later animals were deeply anesthetized with halothane (5%), decapitated, and the brain removed, sectioned at 20 µm, and stained by the Nissl method for histological analysis.

Five days after treatment the site of IBO microinjection was well demarcated, consisting of an area measuring 5.8 ± 0.3 mm² (n=5; mean ± SE) in the coronal plane. At low magnification (x24) the area was characterized by disruption of the cortical laminar

pattern and increased cellular density (compare Fig. 34, A and B). At higher magnification ($\times 450$), no neurons were detected in Nissl-stained sections (compare Fig. 34, C and D) and the area contained an increased number of nonneuronal cells, including astrocytes, macrophages, and endothelia (Iadecola et al., 1986a). The area of neuronal loss and cellular proliferation were well demarcated in the dorsoventral and dorsolateral planes. Thus the underlying corpus callosum and the cortical areas adjacent to the lesion were undamaged (Fig. 34B). In the contralateral hemisphere the homotopic area of the cerebral cortex appeared normal (Fig. 34A).

Retrograde and anterograde axonal transport studies. To determine whether axons and terminals within the lesioned area were still intact, we examined the anterograde and retrograde transport of WGA-HRP from and into the lesion.

WGA-HRP was microinjected into the area of an IBO lesion placed 5 days earlier in five rats. Thirty-six to forty-eight hours later brains were processed as described in METHODS. Analysis of retrograde transport was restricted to the ventromedial globus pallidus and the ventral nucleus of the thalamus, regions that send substantial projections to the primary sensory cortex in rats (Jones, 1981; Saper, 1984). In two animals the injections of WGA-HRP were confined to the area of the lesion (Fig. 33A). In two other cases injections also involved the corpus callosum and the dorsal aspect of the caudate nucleus, whereas in a third case the injection caused a large hemorrhage into the lesion. These latter three animals were excluded from the study. In the two cases with injections restricted to the lesion, many neurons were retrogradely labeled with reaction product within the dorsolateral aspect of the ventrobasal thalamus and in the medial border of the globus pallidus (Fig. 35, B and D).

The anterograde transport of the tracer into the lesion was studied in two other rats in which WGA-HRP was microinjected into the area of the contralateral cerebral cortex homotopic to that treated with IBO. This area projects directly to the site of the lesion through the fibers of the corpus callosum (Isseroff et al., 1984). In both cases WGA-HRP, restricted to the primary sensory cortex, resulted in dense labeling of fibers projecting ventrally into the underlying corpus callosum. Labeled fibers could also be traced into the commissural portion of the corpus callosum. These crossed the midline and projected dorsally into the lesion, giving rise to a dense terminal field within the dorsolateral part of the lesion (Fig. 35C).

Biochemistry. To independently assess the integrity of afferent fibers and terminals in the lesion, we measured the activity of two neurotransmitter biosynthetic enzymes: ChAT, as marker primarily of the extrinsic cholinergic innervation of the cerebral cortex (Johnston et al., 1979), and GAD, an enzyme contained in local α -aminobutyric acid-(GABA)-ergic neurons (Schwarz et al., 1979). Enzyme activity was determined in the lesion site and in the contralateral cortical area in rats killed 3 ($n=7$), 5 ($n=7$), 7 ($n=7$), and 14 ($n=4$) days after IBO treatment (Fig. 36) and compared with the enzyme activity of the homotopic cortex of sham-lesioned rats ($n=15$).

Within the lesion, ChAT activity transiently declined by 19% at day 3 ($p<0.01$), reflecting, presumably, the loss of intrinsic cholinergic neurons (Johnston et al., 1979), and recovered by day 5 ($p>0.05$) (Fig. 36). In contrast the activity of GAD decreased by 79% ($p<0.01$) by day 3 and remained significantly reduced up to 14 days after lesion. In the contralateral cortex, ChAT activity declined slightly 3 days after lesion ($p<0.01$), recovering by day 5 ($p>0.05$), whereas GAD activity did not change ($p>0.05$) (Fig. 36).

These anatomical and biochemical data together suggest that the dose of IBO utilized in this study destroys local neurons but preserves afferent fibers, a finding in agreement with results of others (Schwarz et al., 1979).

Effect of Ibotenic Acid Lesion of Cerebral Cortex on Local Cerebral Blood Flow

Resting ICBF. Resting ICBF was measured 5 days after the microinjection of IBO or vehicle into the cerebral cortex, at a time when local neurons were destroyed but input fibers were intact.

In sham-lesioned rats (n=6) (Table 7) resting ICBF ranged from 55 ± 7 in corpus callosum to 188 ± 6 ($\text{ml} \cdot 100 \text{ g}^{-1} \text{ min}^{-1}$) in the vestibular complex. Values were similar to those reported previously in the anesthetized rat (Iadecola et al., 1983; Nakai et al., 1983) and did not differ between right and left side, except for a small asymmetry in frontal cortex and amygdala ($p<0.02-0.01$; paired t-test) (Table 7).

At 5 days after IBO (n=7), ICBF within the lesion did not differ from that within the contralateral cortex nor from that measured in the homotopic cortex in sham-lesioned rats (Table 7). However, the variance of ICBF was increased within the lesion (Table 7). In the remainder of the brain ICBF was similar to that of sham-lesioned controls ($p<0.05$; analysis of variance and Newman-Keuls test) (Table 7) and, with the exception of the parabrachial complex and globus pallidus, values did not differ between sides (Table 7).

Vasodilation elicited from FN. In sham-lesioned controls (n=6) (Table 7), in agreement with previous findings (Iadecola et al., 1983; Iadecola et al., 1986b; Nakai et al., 1982; Nakai et al., 1983), FN stimulation increased ICBF significantly ($p<0.01$; analysis of variance and Newman-Keuls test) in 26 of the 28 regions studied. The increases were bilateral and symmetrical ($p>0.05$; paired t-test) and were greatest in cerebral cortex (up to 203% of control in the right sham-lesioned cortex), thalamus (up to 207% in the right anterior thalamic nucleus), right hippocampus (196%), and in the reticular formation of the medulla pons (up to 202% in the left nucleus reticularis parvocellularis). Substantial increases also occurred in caudate putamen (175%), parabrachial complex (176%), and in the white matter of the corpus callosum (177%), whereas in the inferior colliculus and cerebellar hemispheres, differences were not significant ($p>0.05$).

Five days after microinjection of IBO (n=6), stimulation of the FN did not increase ICBF significantly within the lesion (Table 7), whereas in the contralateral homotopic cortical area ICBF rose to 171% of control ($p<0.01$), an increase lower than that of the corresponding cortical region of sham-lesioned controls ($p<0.05$; analysis of variance on percent of controls). In the remainder of the brain the magnitude of the elevations in ICBF was, in general, not different from that of sham-lesioned rats (Table 7). However, in the left ventrobasal thalamus the increases were 42% lower, and in the dentate nucleus and vestibular complex ICBF did not increase significantly ($p>0.05$). In contrast, in hypothalamus and substantia nigra, the elevations in ICBF after IBO lesion were greater than those observed in sham-lesioned rats ($p<0.05$).

Thus 5 days after IBO the vasodilation elicited by stimulation of the FN is abolished within the lesion.

Vasodilation by hypercapnia. To exclude the possibility that the failure of the lesioned cortex to vasodilate was due to local vasoparalysis resulting from tissue injury

(Paulson et al., 1972), we investigated whether the cerebrovasodilation elicited by hypercapnia was also impaired.

Five days after IBO lesion, hypercapnia $Pa_{CO_2}=62.7 \pm 3$; $n=5$) increased ICBF in brain globally and symmetrically (Table 7). Within the lesion, ICBF rose to 330% of control and the elevation was not different from that occurring in the contralateral cortex ($p>0.05$; paired t-test). Thus 5 days after IBO the vasodilation elicited by CO_2 was preserved within the area of the lesion.

Partition coefficient of IAP. To establish whether, within the lesion, neuronal necrosis and cellular proliferation altered the PC, thereby affecting the accuracy of the measurement of ICBF, we determined the PC both in the lesion and in the contralateral homotopic cortex. In three rats, 5 days after IBO treatment, the value of PC within the lesion (0.90 ± 0.1) was virtually identical to that of the contralateral intact cortical area (0.92 ± 0.15) ($p>0.05$; paired t-test).

Summary

These studies, therefore, demonstrate that the vasodilation elicited from FN depends upon the integrity of local neurons and, hence, cannot reflect direct neurovascular innervation by ascending projections.

DISCUSSION

I. CHOLINERGIC MECHANISMS MEDIATING THE VASODILATION ELICITED BY ELECTRICAL STIMULATION OF FN

This study has demonstrated that blockade of muscarinic cholinergic receptors by atropine abolishes the increase in rCBF elicited by electrical stimulation of the FN. The action of atropine on rCBF cannot be attributed to effects of the drug upon blood gases or AP, since these parameters did not differ among experimental groups. Nor is it likely to be a consequence of a non-specific effect of the drug upon cerebral circulation: atropine had no effect on resting rCBF and the vasodilation elicited by stimulation of the dorsal medullary reticular formation in rat is not affected by the drug (Iadecola et al., 1982, 1983; Reis and Iadecola, 1989).

It is also unlikely that atropine's effect upon the cerebrovascular response is mediated by blockade of muscarinic receptors located outside the CNS since the vasodilation elicited by FN-stimulation occurs through neural pathways entirely contained within brain (Nakai et al., 1982; Nakai et al., 1983). In particular, its action cannot be attributed to blockade of the purported cholinergic pathway innervating the cerebral vasculature through the facial and greater superficial petrosal nerves (Bevan et al., 1982; Vasquez and Purves, 1979), since, in rabbit, transection of this nerve does not affect the vasodilation elicited from FN (Reis et al., 1982). Since atropine did not modify the associated elevation in AP or EEG, the cholinergic blockade is relatively selective for the actions of the FN upon rCBF. It is, therefore, likely that the global abolition of the vasodilation elicited from FN is due to blockade of central cholinergic receptors of the muscarinic class.

Since it appears that central cholinergic stimulation initiates the vasodilation evoked by FN stimulation it is evident that an understanding of the site at which atropine acts to block the effects will cast light upon the mechanism of the cerebrovascular vasodilation elicited from FN. Receptor autoradiography has demonstrated that neuronal muscarinic receptors have a heterogeneous distribution throughout the brain, with highest concentrations in cerebral cortices (mostly laminae I, III, VI), caudate-putamen, hippocampus, and cranial nerve nuclei (Kuhar and Yamamura, 1976; Wamsley et al., 1984). In addition, these receptors are also located on cerebral vessels and/or upon neurons situated near cerebral vessels. In vessels, muscarinic receptors are localized to all segments of cerebral vasculature, including large cerebral arteries (Lee et al., 1978), small pial arteries (Kuschinsky et al., 1974) and capillaries (Estrada and Krause, 1982), wherein the receptors are associated with endothelial and/or smooth muscle cells (Estrada et al., 1983). It is of interest that ACh dilates through muscarinic receptors cerebral arteries *in vitro* (Lee et al., 1978), or *in vivo* (Heistad et al., 1980). Moreover, CBF is increased, also via muscarinic receptors, by intracarotid infusion (Heistad et al., 1980) or topical application of ACh (Kuschinsky et al., 1974).

However, since the effects of FN stimulation produce their effects through the release of locally synthesized ACh and receptors may occur at sites distant from sites of synaptic interaction [the concept of transmitter/receptor mismatch (Herkenham, 1987), efforts were directed towards defining the potential sources of ACh responsible for the vasodilation.

ACh elicited by FN stimulation could arise from two broadly defined sources: the first is at synapses within the central pathway from FN to those regions in which

stimulation of FN increases flow and encompassing, in the main, the central autonomic core of brain (Reis and Iadecola, 1989). The second would be at the neurovascular interface, i.e. in the "target" tissue in which rCBF is increased.

II. CENTRAL REPRESENTATION OF CHOLINERGIC SYSTEMS IN THE VISCERAL BRAIN. A SITE OF ACTION OF ACH ELICITING GLOBAL VASODILATION?

In previous studies, the cholinergic representation within brain has been examined either by mapping the distribution of cholinesterase (e.g. Shute and Lewis, 1967) or by mapping the distribution of ChAT, the enzyme synthesizing ACh (Sofroniew et al., 1982, 1985; Mesulam et al., 1983a,b, 1984). In these studies the focus was on the so-called cholinergic subgroups Ch1-Ch6 of the basal forebrain and extrapyramidal system. Little attention was given to areas of visceral representation. Thus, despite ample physiological, pharmacologic and biochemical evidence for circuits involving cholinergic autonomic neurotransmission in the rostral ventrolateral medulla (RVL), nucleus tractus solitarius (NTS) and hypothalamus, the presence of cholinergic or cholinoreceptive elements in these areas was either unknown, not studied in detail or complicated by conflicting data.

By carefully examining the expression of ChAT in those areas of brain underlying visceral control a number of new observations were made. Our principal findings are: 1) newly identified cholinergic cell groups in the RVL, NTS, and subjacent areas of reticular formation (e.g. nucleus reticularis dorsalis), raphe, periventricular gray and the parabrachial complex, and 2) putative terminal fields in the above areas and other substructures known to be involved in autonomic responses, in particular, AP and HR.

The presence of ChAT in cell bodies of central autonomic nuclei, such as the NTS--the first order relay of primary visceral afferents--implies that its end product, ACh, may act as a neurotransmitter in the neurogenic control of autonomic function. ChAT is synthesized by cholinergic perikarya and transported to presynaptic nerve endings (Tucek, 1985). The significance of different intensities of immunoreaction product in individual neurons is unknown. Low or inconsistent levels, as for example, in some neurons of the solitary complex or hypothalamus, suggest that their detection depends on the specific antiserum or that the levels of enzyme in these neurons lie near or below the sensitivity of our technique (see Benno et al., 1982). It is also conceivable that variations in labeling reflect differences in cell function intraventricularly prior to processing for immunocytochemistry.

Overall, a broader and more complexly organized distribution of bouton-like punctata was labeled for ChAT in central autonomic subnuclei than has been reported previously. Putative terminal fields generally conformed to normal cytoarchitecture and were organized topographically or in some areas (e.g. NTS), viscerotopically. Immunocytochemical data provided anatomical substrates for previous functional observations, and also confirmed and extended findings from biochemical assay and receptor binding studies. They also provided greater resolution differentiating cholinoreceptive from cholinergic elements. The use of darkfield optics to view tissues processed with the peroxidase-antiperoxidase technique aided greatly in the recognition of labeled processes. This was probably the single major advantage over studies employing brightfield optics to view cholinoreceptive fields.

The possibility that ACh released in any of these structures is responsible for the cerebrovascular vasodilation elicited by FN stimulation, however, does not seem likely for

two reasons. First, the persistence of the elevations of AP and HR evoked by FN stimulation after administration of atropine demonstrates that ACh release is not required for the expression of the entire constellation of autonomic events elicited by FN stimulation: it is only critical for the expression of the vasodilation. Second, since the topical application of atropine to the cortical surface of the cerebral cortex substantially reduces the vasodilation at that site suggests that elements in the target are important for the expression of the elevation of rCBF. It is more likely that the principal site resides within neural networks close to the dilating vessels, i.e. at the neurovascular junction.

III. NEUROVASCULAR SITES MEDIATING THE CEREBROVASCULAR VASODILATION FROM FN

Since it seemed unlikely that the source of ACh responsible for the FN-elicited vasodilation was within the central pathways mediating the effect, we therefore investigated the possibility that ACh released from a source(s) close to the vascular target might be responsible. For this purpose we investigated the representation of elements in the cerebral cortex capable of synthesizing ACh. This was accomplished anatomically by mapping the distribution of ChAT by LM and EM and biochemically by measuring ACh biosynthesis.

By LM we established that, in cortex, elements stained for ChAT were contained within axon terminals, many of which are in contact with the cerebral microvasculature, but also in the endothelium of cerebral capillaries. Moreover, by biochemical analysis we have found that the cholinergic elements associated with small ($<40 \mu\text{m}$) intraparenchymal blood vessels in the rat cerebral cortex, including cholinergic nerve terminals closely apposed to the basal lamina and endothelial cells, have the capacity to synthesize, store and release ACh following depolarization with K^+ . While earlier physiological and pharmacological experiments have demonstrated that with appropriate stimuli ACh may be released from large cerebral vessels surrounding brain (Duckles, 1981) and that these vessels dilate in response to ACh (Duckles, 1981; Florence and Bevan, 1979; Lee et al., 1978), this study provides evidence for the first time that the microvascular innervation and/or endothelium have the capacity to synthesize, store, and release ACh.

Cholinergic Innervation of Cerebral Microvessels

Although the present study confirms earlier reports that microvessels isolated from rat and bovine cerebral cortex contain ChAT activity (Estrada et al., 1983; Goldstein et al., 1975; Santos-Benito and Gonzales, 1985), it differs from those reports in the quantity (i.e. activity) of ChAT found there. Previous reports indicated that intraparenchymal vessels from the rat cortex have 2-5% of the specific activity associated with cortical grey matter (Table 9) (Goldstein et al., 1975; Santos-Benito and Gonzales, 1985). Our study also indicates cortical microvessels constitute a small fraction (2.3%) of the total ACh biosynthetic capacity of the cortex. However, it has demonstrated that based upon specific activities, microvessels isolated from the cortex, caudate, and cerebellum have the ability to synthesize ^{14}C -ACh at rates 100-300% greater than the nerve terminal fraction. This observation raises the possibility that the concentrations of ACh synthesized at the cortical neurovascular junction may be as great, or greater than at the transneuronal site.

There are two reasons that could explain the differences between the ChAT activities measured in this and previous studies. First and foremost, the distribution of the size of the vessel diameters isolated were different, which could result in a differential sampling of those vessels innervated by cholinergic nerves. Earlier reports (Goldstein et

al., 1975; Santos-Benito and Gonzales, 1985) indicate that 90-95% of the vessels were $<10 \mu\text{m}$ in diameter and, therefore, capillaries. This study demonstrates that only two thirds of the vessels sampled were capillaries, while the remaining one third consisted of vessels $11-40 \mu\text{m}$ in diameter. Second, the isolation procedure used in the earlier reports are lengthier and may have resulted in a deterioration in the viability of the ChAT activity, although this is less likely because the values for the other marker enzymes were similar between the studies. Together, these data suggest that unlike capillaries in the cortex, small precapillary arterioles, or perhaps postcapillary venules, have a substantial capacity to synthesize ACh.

Additional data indicate that the ChAT activity measured in the microvessel fraction is in direct association with the microvasculature and not the result of contamination from cortical gray matter. First, ultrastructural examination of sections of cortex immunocytochemically stained for ChAT revealed that capillary endothelial cells and nerve terminals that directly contact the basal lamina of microvessels actually contain ChAT. Second, light and electron microscopic level examination of the microvessel fractions suggest that perikaryal contamination was minimal. Third, the enriched activities of γ -GTP and AP suggest that distinct fractions were isolated. Fourth, the cerebellum, which is known to contain relatively low levels of gray matter ChAT activity (Estrada, et al., 1983), had in the microvessel fraction an equivalent capacity to the cortex to synthesize ACh. Also, the cerebellar microvessels have a higher specific activity of ChAT than the tissue of origin. If contamination had occurred, it would be expected to be similar for all regions since the isolation procedure used was the same. The enhanced specific activities associated with the microvessel fraction and the unpredicted ratios of microvessels to gray matter activities of ChAT argue against contamination as a significant factor in determining the activities measured. Finally, preliminary studies indicate that even when the whole S₁ fraction (which contains 95% of the total cortical ChAT activity) is deliberately layered over the discontinuous sucrose gradient to contaminate the preparation, less than 50% of the activity normally observed from the P₁ fraction is measured. Therefore, in the worst possible case, the activity measured is approximately 2-fold greater than the actual value. This lower value for the specific activity of ChAT for cortical microvessels is still at least 10-fold greater than any previous report.

The concept of an innervation of capillaries and other segments of the microvasculature is not new (Rennels et al., 1977). However, this study is the first to demonstrate that depolarization of isolated intraparenchymal blood vessels results in the Ca²⁺-dependent release of a putative neurotransmitter such as ACh. As shown by the ultrastructural studies, there are two possible sources of the released ACh found in association with the microvessels. Both endothelial cells and nerve terminals that closely appose pericytes or the basement membrane contain ChAT. Further experimentation is required to determine which of these cellular source(s) of ChAT contributed to the synthesis and K⁺-evoked release of ³H-ACh.

Functional Implications of Microvessel Innervation

The function of neurotransmitters that innervate cortical intraparenchymal vessels is unclear, since this level of the microvasculature (i.e. $<50 \mu\text{m}$) is relatively devoid of smooth muscle cells with which transmitters could interact with to cause vasodilation. Despite this paradox, there is now good evidence that cholinergic neurotransmission exists at this level of the vasculature, since ChAT activity, acetylcholinesterase activity, ACh release and muscarinic receptors are all found in association with capillaries and

endothelial cells (Edvinsson et al., 1972, 1977; Estrada and Krause, 1982; Estrada et al., 1983; Goldstein et al., 1975; Parnavelas et al., 1985; present study). Moreover, ChAT, generally considered a specific marker of cholinergic neurons (Mesulam et al., 1983b), is found both in nerve terminals that closely appose the basement membrane and in non-neuronal endothelial cells (Parnavelas et al., 1985; present study). This type of innervation appears non-classical in that synaptic specializations are absent. This has, perhaps, led others to suggest that cholinergic transmission may be important in modulating less anatomically restricted functions such as amino acid transport (Duckles, 1982), or capillary permeability (Parnavelas et al., 1985).

There are, however, two other possible mechanisms by which release of ACh could still regulate local tissue perfusion. Although not yet confirmed, cholinergic nerve terminals may innervate precapillary sphincters that divert local cerebral blood flow (Nakai et al., 1981). Alternatively, endothelial cells and adjoining pericytes could modulate the diameter of the microvessels directly since these cells contain contractile proteins such as actin. This possibility seems plausible, since decreasing ACh synthesis in sperm, another non-neuronal cell that contains ChAT (Sastry and Sadavongvivad, 1979), results in decreased cell motility.

IV. EFFECT OF TOPICAL ATROPINE ON CORTICAL CEREBROVASCODILATION ELICITED FROM THE FN

Having established the anatomical substrate for cholinergic involvement at the neurovascular unit we next sought to establish whether the cerebrovascular vasodilation elicited in the cerebral cortex by electrical stimulation of the FN was mediated by the local release of ACh. To do this we examined the effects of topical application of atropine on the response.

We have demonstrated that atropine applied unilaterally over the parietal cortex attenuates, by 59%, the vasodilation elicited by FN stimulation locally without affecting the responses in flow within adjacent or remote brain areas.

The action of atropine in attenuating the FN-elicited response is not the result of vasoparalysis since atropine does not modify the vasodilation elicited by hypercarbia. Nor is it possible that the effect of atropine is a consequence of differences in pCO_2 or pO_2 of arterial blood and superfusate, nor to changes in AP, since these parameters were carefully controlled and did not differ among experimental groups. The specificity of atropine is further supported by the inability of the drug to alter resting rCBF or affect the cerebrovasodilation elicited by stimulation of the dorsal medullary reticular formation (Iadecola et al., 1987b).

The finding that atropine applied locally to cortex does not affect resting rCBF indicates it is unlikely that there is any continuous (i.e. tonic) cholinergic regulation of cortical rCBF. It is also unlikely that the effect of atropine upon the cerebrovascular response to FN stimulation is mediated by muscarinic receptors located outside the CNS, since this vasodilation occurs through neuronal pathways contained entirely within brain (Nakai et al., 1982; Reis et al., 1985).

The finding that the topical application of atropine only prevented 59% of the cortical vasodilation contrasts with the fact that systemically, atropine reduces the vasodilation by 92% (Iadecola et al., 1986b). The most likely explanation for the discrepancy between the effects of topical and systemic administration of the drug is that

in the study on topical application the area of cortex in which atropine effectively diffused was smaller than the area removed for analysis. Thus, the effect of atropine in blocking flow within a small region was diluted by the flow changes in a larger brain area.

Another possibility is that FN stimulation not only results in release of ACh but also a co-transmitter which contributes to the vasodilation. This possibility would be consistent with the recent report that ACh and vasoactive intestinal polypeptide, another potent vasodilator of cerebral vessels (Heistad et al., 1980), coexist in a subpopulation of local cortical neurons (Eckenstein and Baughman, 1984). However, it is difficult to reconcile the fact that atropine blocks virtually all cortical vasodilation when administered systemically with this explanation. Additional experiments using local cortical microinjection of atropine and autoradiographic techniques to measure local cortical blood flow will be required to establish understand the differing effects of topical and systemic atropine on the vasodilation evoked by electrical stimulation of the FN.

The finding that the topical application of atropine will attenuate most of the FN-elicited increase in cortical rCBF suggests that a substantial component of the cholinergic link resides locally in the target, in this case the cortex, and that release of ACh in the target, presumably in close apposition to cerebral vessels mediates the effect.

V. CORTICAL RELEASE OF ACH FOLLOWING FN-STIMULATION

The ability of topically applied atropine to block a substantial portion of the local vasodilation in the underlying cortex elicited by FN stimulation is further evidence strongly suggesting that ACh, locally synthesized and released, is essential for the expression of the vascular response. It would be expected, therefore, that it would be possible, as others have noted with electrical or chemical stimulation of the basal forebrain (Kurosawa et al., 1989), to detect release of ACh over the cortex. However, we were unable to detect any stimulus-locked release of ACh during FN-stimulation.

The failure to detect any release of ACh from the cortex during stimulation cannot be attributed to a failure to detect release of ACh from the cerebral cortex: depolarization with potassium resulted in a stimulus-locked release of the transmitter. In our experiments potassium depolarization elevated ACh by 151%, a magnitude comparable to the maximal release reported by others for rats and cats (50-200%) (Pepeu, 1973; Yaksh and Yamamura, 1975). Likewise the failure to detect ACh can not be attributed to local vasoparalysis or an impaired reactivity of the tissue as a result of the microinjection [³H]choline: In 5 of 5 experiments in which rCBF and release of ACh was measured concurrently, cortical rCBF was elevated to the expected levels by FN stimulation.

It also seems unlikely, for two reasons, that endogenous ACh is contained in a different releasable pool than is the pool labeled by microinjection of [³H]choline. First, Yaksh and Yamamura (1975) have shown in cats that neuronal pools containing endogenous ACh and those containing ACh newly synthesized from radiolabeled choline, if not identical, are released in the same manner following depolarization of the nerve terminals. Second, in 3 additional experiments that were performed to avoid the possible problems associated with using radiolabeled choline, we could not detect an increase in the release of endogenous ACh following FN-stimulation as measured by gas chromatographic/mass spectrophotometric techniques (unpublished observation, Armeric et al.). Taken together, we interpret these results to suggest that during FN stimulation the amount of ACh released by the subpopulation of cholinergic neurons producing local vasodilation is too small to be detected by currently available methods.

The failure to detect release of ACh from the cerebral cortex with FN stimulation stands in contrast with the more substantial release of ACh which has been reported to follow electrical or chemical stimulation of the basal forebrain (Kurosawa et al., 1989). These observations, therefore, suggest that source of ACh released in the vicinity of cortical vessels by FN stimulation is not from the bulk of the cholinergic cortical afferents arising from or passing through basal forebrain. Rather, it arises either from a small population of the cortical afferents, from cholinergic interneurons, or from vascular endothelium. It is possible that the small but significant decrease in the release of ACh during FN stimulation is related to a more generalized decrease in cholinergic activity not directly involved with cerebrovascular regulation.

Note: Others have demonstrated that there may be a direct relationship between the amount of ACh released from the cortical surface and the level of generalized brain activity as indicated by the cortical EEG (Jasper and Tessier, 1971; Pepeu, 1973; Szerb, 1967). In addition, stimulation of the FN does not substantially alter cortical cerebral glucose utilization (Nakai et al., 1983) and, in fact, slightly decreases the frequency of the cortical EEG (Underwood et al., 1983 and present study). Thus, in addition to the presumed evoked release of ACh involved with the cortical cerebrovasodilation, FN stimulation may act through other, perhaps parallel, neuronal pathways to modify release of ACh not related to CBF regulation.

VI. ROLE OF INTRINSIC NEURONS IN THE LOCAL VASODILATION ELICITED IN THE CEREBRAL CORTEX WITH FN-STIMULATION

We discovered that the vasodilation was abolished within a discrete area of the cerebral cortex in which local neurons were selectively eliminated using the excitotoxin IBO. That IBO destroyed local neuronal perikarya but preserved afferent fibers was established by the demonstration that after treatment: 1) local neurons were lost; 2) WGA-HRP was transported from or into the lesion; and 3) the activity of ChAT, largely a marker of extrinsic cholinergic terminals (Johnston et al., 1979), was preserved, whereas the activity of GAD, a marker of local GABA-ergic neurons (Schwarcz et al., 1979), was markedly reduced.

The failure of FN stimulation to increase ICBF within the lesioned cortex appears specifically related to the loss of neurons within the area of the lesion. Thus, the lack of vasodilation cannot be attributed to differences in AP or blood gases between sham-lesioned and lesioned animals, since these variables did not substantially differ among groups. Moreover, effects on ICBF attributable to differences in AP or blood gases should affect the entire cerebral cortex and not just the area of the lesion, nor can the effects of IBO be due to changes in the PC of IAP since, within the lesion, PC was unaffected. Finally, the abolition of the vasodilation evoked from the FN cannot be the consequence of loss of vascular reactivity (vasoparalysis) resulting from local tissue injury (Paulson et al., 1972), since hypercapnia elicited elevations in ICBF within the lesion comparable to those of undamaged cortex.

These results suggest that the afferent projections to the cerebral cortex, originating from or passing through the basal forebrain and mediating the cortical vasodilation elicited from the FN, do not directly contact cortical blood vessels. Rather, these pathways must engage local cortical neurons which, in turn, initiate the local vascular response.

The identity of the local neurons and the mechanism whereby they act on the local vasculature remains unknown. One possibility is that these neurons are of the nonpyramidal type whose axons, for the most part, do not leave the cortical area in which they lie (Jones, 1984). In support of this contention is the observation that, in cortex as in other brain areas, the soma or processes of some local neurons may contact local blood vessels, principally small arterioles, venules, or capillaries (Eckenstein and Baughman, 1984; Hendry et al., 1983). These neurons are mostly bipolar and have been described as containing peptides, including cholecystokinin (Hendry et al., 1983) or vasoactive intestinal polypeptide, and/or classical neurotransmitters, such as acetylcholine (ACh) (Eckenstein and Baughman, 1984). Alternatively, the neurons mediating the vasodilation may project to distant cortical or subcortical relay areas but engage vessels via collateral branches or by local release of vasoactive substances.

Another question concerns the segment of the local microvasculature on which these local neurons exert their influence to determine the increases in rCBF evoked from the FN. The arterial blood supply of the cerebral cortex derives, almost exclusively, from the pial arteries, which are also an important site of regulation of cerebrovascular resistance (Heistad and Kontos, 1983). However, within the cortical parenchyma, perfusion may also be regulated by fine adjustments of the local microcirculation, resulting in changes in the number of perfused capillaries, i.e. capillary recruitment (Weiss et al., 1982). Whether the increased tissue perfusion elicited by stimulation of the FN reflects pial arterial dilation or capillary recruitment, is unknown. It is, however, conceivable that, given the magnitude and the ubiquity of the increases in cortical blood flow, both pial and intraparenchymal vessels are involved. If this is the case, then the neural and/or humoral signals originating from local neurons and mediating the cortical vasodilation, must interact in a highly coordinated fashion both with the surrounding local microvasculature and with the more distant pial vessels.

VII. SUMMARY, CONCLUSIONS AND RELEVANCE TO PROTECTION FROM AGENT

The present study, therefore, has established that an important cholinergic mechanism is present within the CNS which functions to activate the local cerebral circulation in response to stimulation from the cerebellar FN since the systemic administration of atropine will completely block the response. The evidence, moreover, suggests that the cholinergic link mediating the vasodilation is largely, contained within target areas since local application of atropine to the cerebral cortex will reduce, by approximately 60%, the response to FN stimulation. Whether the remaining 40% of the effect not abolished by topical atropine represents a pool in cortex not affected by the spread of the drug or reflects interruption of a cholinergic synapse in the ascending pathway is not known.

The central cholinergic vasodilation system is not tonically active since atropine will not modify resting rCBF. However, some local release probably occurs since physostigmine locally applied as shown here, or administered systemically as demonstrated by Scrimin and associates (Hudson et al., 1985; Scrimin et al., 1983, 1988), also increases cortical rCBF independently of metabolism.

The findings that the vasodilation in the cerebral cortex elicited by FN stimulation is not associated with local release of ACh suggests that the transmitter is released from a very small local pool. Since the vasodilation depends upon the integrity of local neurons, it is unlikely to represent a direct cholinergic neurovascular connection from a small

group of cortical afferents arising from either basal forebrain or from the small cholinergic projection to cortex from the pedunculopontine tract (Saper and Loewy, 1982). The vasodilation, therefore, depends upon release of ACh from local interneurons excited by ascending projections from the brainstem or by neuronal activation of endothelial release of ACh. The vasodilation, in turn, is mediated by an interaction of ACh with, in part, a local muscarinic cholinergic receptor either within the vessel or in a local neuron.

The finding that topical physostigmine increases rCBF extends the observations of Scremrin et al. (1988) and indicates that continuous biosynthesis and release of ACh is occurring at the site of vasodilation. It also raises the possibility that this system may be driven reflexively by other drives through the brainstem including those involving noxiousception and possibly hypercarbia (Hudson et al., 1985).

It therefore appears that an important cholinergic vasodilation system within brain is capable of eliciting large increases in blood flow independently of metabolism. This study has demonstrated, unequivocally, the preponderant role of the local neurovascular network in mediating the effect and its capacity to be activated by inputs from the brainstem. The fact that electrical stimulation of the FN can activate and coordinate the effects on regional flow throughout the brain and spinal cord with increases of flow up to 300% of resting values demonstrates the potency of the system. The fact that the system may respond to hypercarbia and to noxious stimulation places it within a relevant biomedical framework.

The relevance of the study to an understanding of protection from exposure to chemical agents of the cholinomimetic class relates, therefore, to the possibility that exposure to low levels of agent may interfere, through activation of the cholinergic neurovascular network, with cerebrovascular autoregulation. Under these conditions, cerebral blood flow becomes dependent upon the systemic circulation. Loss of cerebrovascular autoregulation conceivably could present hazards to personnel in which extreme changes in blood pressure might be a consequence of exposure to combat conditions. Thus, reduction of AP in hemorrhagic shock would lead to hypoperfusion much earlier than under conditions in which autoregulation is intact and amplifying, thereby, the risks of cerebral hypoxemia and infarction. Conversely, severe elevations of AP with stress or strenuous exertion might make the cerebral circulation vulnerable to cerebral edema. Direct tests of these possibilities in the framework of the cholinergic primary vasodilation system would be in order.

LITERATURE CITED

Amaral, D.G. and Price, J.L. (1983) An air pressure system for the injection of tracer substances into the brain. *J. Neurochem.* 19: 35-44.

Arneric, S.P. and Reis, D.J. (1986) Somatostatin and cholecystokinin octapeptide differentially modulate the release of ³H-acetylcholine from caudate nucleus but not cerebral cortex: role of dopamine receptor activation, *Brain Res.* 374: 153- 161.

Batton, R.R., Jayaraman, A., Ruggiero, D. and Carpenter, M.B. (1977) Fastigial efferent projections in the monkey: an autoradiographic study. *J. Comp. Neurol.* 174: 281-306.

Benno, R.H., Tucker, L.W., Joh, T.H. and Reis, D.J. (1982) Quantitative immunocytochemistry of tyrosine hydroxylase in the rat brain. II. Variations in the amount of tyrosine hydroxylase among individual neurons of the locus ceruleus in relationship to neuronal morphology and topography. *Brain Res.* 246:237-247.

Bevan, J.A., Buga, G.M., Jope, C.A., Jope, R.S. and Moritoki, H. (1982) Further evidence for a muscarinic component to the neural vasodilator innervation of cerebral and cranial extracerebral arteries of the cat. *Circ. Res.* 51: 421-429.

Bradford, M. (1976). A rapid and sensitive method for the quantitation of microgram quantities of protein utilizing the principle of protein-dye binding. *Anal. Biochem.* 72: 248-254.

Bresolin, N., Freddo, L., Vergani, L. and Angelini, C. (1982) Carnitine, carnitine acyltransferases, and rat brain function. *Exp. Neurol.* 78: 285-292.

Briggs, C.A. and Cooper, J.A. (1981) A synaptosomal preparation from the guinea pig ileum myenteric plexus. *J. Neurochem.* 36: 1097-1108.

Chen, S.H., Chu, B. and Nossal, R. (Eds.) (1981) *Scattering Techniques Applied to Supramolecular and Non-equilibrium Systems*. New York, Plenum Press.

Chida, K., Iadecola, C. and Reis, D.J. (1989) Lesions of rostral ventrolateral medulla abolish some cardio- and cerebrovascular components of the cerebellar fastigial pressor and depressor responses. *Brain Res.*, in press.

Coyle, P. and Jokelainen, P.T. (1982) Dorsal cerebral arterial collaterals of the rat. *Anat. Rec.* 203: 397-404.

Cravo, S.L., Ruggiero, D.A., Anwar, M. and Reis, D.J. (1988) Quantitative- topographic analysis of adrenergic and non-adrenergic spinal projections of cardiovascular area of RVL. *Soc. Neurosci. Abstr.* 14(1):328.

Del Bo, A., Sved, A.F. and Reis, D.J. (1983) Fastigial stimulation releases vasopressin in amounts which elevate arterial pressure. *Am. J. Physiol. (Heart Circ. Physiol.)* 244: H687-H694.

Dirnagl, U., Kaplan, B., Jacewicz, M. and Pulsinelli, W. (1989) Laser-Doppler-Flowmetry for the estimation of CBF changes: A validation using autoradiography in a rat stroke model. *J. Cereb. Blood Flow Metab.* 9, Suppl. 1: S128.

Doba, N. and Reis, D.J. (1972) Changes in regional blood flow and cardiodynamics evoked by electrical stimulation of the fastigial nucleus in cat and their similarity to orthostatic reflexes. *J. Physiol. (Lond.)* 227: 729-747.

Duckles, S.P. (1981) Evidence for a functional cholinergic innervation for cerebral arteries. *J. Pharmacol. Exp. Therap.* 217: 544-548.

Duckles, S.P. (1982) Choline acetyltransferase in cerebral arteries: modulator of amino acid uptake? *J. Pharmacol. Exp. Therap.* 223: 716-720.

Eckenstein, F. and Thoenen, H. (1983) Cholinergic neurons in the rat cerebral cortex demonstrated by immunocytochemical localization of choline acetyltransferase. *Neurosci. Lett.* 36: 211-215.

Eckenstein, F. and Baughman, R.W. (1984) Two types of cholinergic innervation in cortex, one co-localized with vasoactive intestinal polypeptide. *Nature* 309: 153-155.

Edvinsson, L., Nielsen, K.C., Owman, C. and Sporrong, B. (1972) Cholinergic mechanisms in pial vessels. Histochemistry, electron microscopy and pharmacology. *Z. Zellforsch.* 134: 311-325.

Edvinsson, L., Falck, B. and Owman, C. (1977) Possibilities for a cholinergic action on smooth musculature and on sympathetic axons in brain vessels mediated by muscarinic and nicotinic receptors. *J. Pharmacol. Exp. Ther.* 200: 117-126.

Estrada, C. and Krause, D. (1982) Muscarinic cholinergic receptor sites in cerebral blood vessels. *J. Pharmacol. Exp. Ther.* 221: 85-90.

Estrada, C., Hamel, E. and Krause, D.N. (1983) Biochemical evidence for cholinergic innervation of intracerebral blood vessels. *Brain Res.* 266: 261-270.

Florence, V.M. and Bevan, J. (1979) Biochemical determination of cholinergic innervation of cerebral arteries. *Circ. Res.* 45: 212-218.

Fonnum, F. (1975) A rapid radiochemical method for the determination of choline acetyltransferase. *J. Neurochem.* 24: 407-409.

Fonnum, F., Walaas, I. and Iversen, E. (1977) Localization of GABA-ergic, cholinergic and aminergic structures in the mesolimbic system. *J. Neurochem.* 29: 221-230.

Fulwiler, C.E. and Saper, C.B. (1984) Subnuclear organization of the efferent connections of the parabrachial nucleus in the rat. *Brain Res. Rev.* 7: 229-259.

Goldstein, G.W., Wolinsky, J.S., Csejtey, J. and Diamond, I. (1975) Isolation of metabolically active capillaries from rat brain. *J. Neurochem.* 25: 715-717.

Gray, E.G. and Whittaker, V.P. (1962) The isolation of nerve endings from brain: an electron microscopic study of cell fragments derived from homogenization and centrifugation. *J. Anatomy* 96: 79-88.

Haberl, R.L., Heizer, M.L., Marmarou, A. and Ellis, E.F. (1989) Laser-Doppler assessment of brain microcirculation: effect of systemic alterations. *Am. J. Physiol.* 256 (Heart Circ. Physiol. 25): H1247-H1254.

Hadhazy, P. and Szerb, J.C. (1977) The effect of cholinergic drugs on ^3H -acetylcholine release from slices of rat hippocampus, striatum and cortex. *Brain Res.* 123: 311-322.

Heistad, D.D., Marcus, M.L., Said, S.I. and Gross, P.M. (1980) Effect of acetylcholine and vasoactive intestinal polypeptide on cerebral blood flow. *Am. J. Physiol.* 239: H73-H80.

Heistad, D.D. and Kontos, H.A. (1983) Cerebral circulation. In: *Handbook of Physiology. The Cardiovascular System*, Sect. 2, Vol. III, Bethesda: American Physiological Society, pp. 137-182.

Hendry, S.H.C., Jones, E.G. and Beinfeld, M.C. (1983) Cholecystokinin-immunoreactive neurons in rat and monkey cerebral cortex make symmetric synapses and have intimate association with blood vessels. *Proc. Natl. Acad. Sci. USA* 80: 2400-2404.

Herkenham, M. (1987) Mismatches between neurotransmitter and receptor localizations in brain: observations and implications. *Neuroscience* 23: 1-38.

Hernandez, M.J., Brennan, R.W. and Bowman, G.S. (1978) Cerebral blood flow autoregulation in the rat. *Stroke* 9, 150-155.

Houser, C.R., Crawford, G.D., Salvaterra, P.M. and Vaughn, J.E. (1985) Immunocytochemical localization of choline acetyltransferase in rat cerebral cortex: a study of cholinergic neurons and synapses. *J. Comp. Neurol.* 23: 17-34.

Hudson, D.M., Jenden, D.J., Scremin, O.U. and Sonnenschein, R.R. (1985) Cortical acetylcholine efflux with hypercapnia and nociceptive stimulation. *Brain Res.* 338: 267-272.

Iadecola, C., Nakai, M., Mraovitch, S., Tucker, L. and Reis, D.J. (1982) Global increase in cerebral metabolism and blood flow during stimulation of a subnucleus of the medullary reticular formation. *Neurology* 32(2): A111.

Iadecola, C., Nakai, M., Arbit, E. and Reis, D.J. (1983) Global cerebral vasodilation elicited by focal electrical stimulation of the dorsal medullary reticular formation in anesthetized rat. *J. Cereb. Blood Flow Metab.* 3: 270-279.

Iadecola, C., Arneric, S.P., Baker, H.D., Callaway, J.L. and Reis, D.J. (1986a) Nonneuronal cells contribute to local cerebral blood flow regulation after acute neuronal injury. *Neurology* 36(Suppl. 1): 228.

Iadecola, C., Underwood, M.D. and Reis, D.J. (1986b) Muscarinic cholinergic receptors mediate the cerebrovasodilation elicited by stimulation of the cerebellar fastigial nucleus in rat. *Brain Res.* 368: 375-379.

Iadecola, C., Arneric, S.P., Baker, H., Tucker, L.W. and Reis, D.J. (1987a) Role of local neurons in the cerebrocortical vasodilation elicited from cerebellum. *Am. J. Physiol.* 252 (Regulatory Integrative Comp. Physiol. 21) R1082-R1091.

Iadecola, C., Lacombe, P.M., Underwood, M.D., Ishitsuka, T. and Reis, D.J. (1987b) Role of adrenal catecholamines in cerebrovasodilation evoked from brainstem. *Am. J. Physiol.* 252: H1183-H1191.

Isseroff, A., Schwartz, M.L., Dekker, D.J. and Goldman-Rakic, P.S. (1984) Columnar organization of callosal and associational projections from rat frontal cortex. *Brain Res.* 293: 213-223.

Jasper, H.H. and Tessier, J. (1971) Acetylcholine liberation from cerebral cortex during paradoxical (REM) sleep. *Science* 172: 601-602.

Joh, T.H. and Ross, M.E. (1983) Preparation of catecholamine-synthesizing enzymes as immunogens for immunocytochemistry. In: A.C. Cuello (Ed.), *Immunocytochemistry*. IBRO Handbook Series: Methods in the Neurosciences, John Wiley and Sons, New York, Vol. 3, pp. 121- 138.

Johnston, M.V., McKinney, M. and Coyle, J.T. (1979) Evidence for a cholinergic projection to neocortex from neurons in basal forebrain. *Proc. Natl. Acad. Sci. USA* 76: 5392-5396.

Jones, E.G. (1981) Functional subdivision and synaptic organization of the mammalian thalamus. In: R. Porter (Ed.) *Neurophysiology IV*, Baltimore: University Park, pp. 173-245.

Jones, E.G. (1984) Laminar distribution of cortical efferent cells. In: A. Peters and E.G. Jones (Eds.) *Cerebral Cortex*, Vol. 1, New York: Plenum Press, pp. 521-533.

Kety, S.S. (1951) The theory and applications of the exchange of inert gas in the lungs and tissues. *Pharmacol. Rev.* 3: 1-41.

Kimura, H., McGeer, P.L., Peng, J.H. and McGeer, E.G. (1981) The central cholinergic system studied by choline acetyltransferase-immunohistochemistry in the cat. *J. Comp. Neurol.* 200: 151-201.

Kuhar, M.J. (1976) The anatomy of cholinergic neurons. In: A.M. Goldberg and I. Hanin (Eds.) *Biology of Cholinergic Function*, New York: Raven Press, pp. 3-27.

Kuhar, M.J. and Yamamura, H.I. (1976) Localization of cholinergic muscarinic receptors in rat brain by light microscopic radioautography. *Brain Res.* 110: 229-243.

Kurosawa, M., Sato, A., Sato, Y. (1989) Stimulation of the nucleus basalis of Meynert increases acetylcholine release in the cerebral cortex in rats. *Neurosci. Lett.* 98: 45-50.

Kuschinsky, W., Wahl, M. and Neiss, A. (1974) Evidence for cholinergic dilatory receptors in pial arteries of cats. *Pflugers Arch.* 347: 199-208.

Lee, T.J.F., Hume, W.R., Su, C. and Bevan, J.A. (1978) Neurogenic vasodilation of cat cerebral arteries. *Circ. Res.* 42: 535-542.

Lindsberg, P.J., O'Neill, J.T., Paakkari, I.A., Hallembeck, J.M. and Feuerstein, G. (1989) Validation of laser-Doppler flowmetry in measurement of spinal cord blood flow. *Am. J. Physiol.* 257 (Heart Circ. Physiol. 26): H674-H680.

Lysakowski, A., Wainer, B.H., Rye, D.B., Bruce G. and Hersh, L.B. (1986) Cholinergic innervation displays strikingly different laminar preferences in several cortical areas. *Neurosci. Lett.* 64: 102-107.

McKee, J.C., Denn, M.J. and Stone, H.L. (1976) Neurogenic cerebral vasodilation from electrical stimulation of the cerebellum in the monkey. *Stroke* 7: 179-186.

Meeley, M.P., Underwood, M.D., Talman, W.T. and Reis, D.J. (1989) Content and *in vitro* release of endogenous amino acids in the area of the nucleus of the solitary tract of the rat. *J. Neurochem.* 53: 1807-1817.

Mesulam, M.M., Mufson, E.J., Levey, A.I. and Wainer, B.H. (1983a) Cholinergic innervation of cortex by the basal forebrain: cytochemistry and cortical connections of the septal area, diagonal band nuclei, nucleus basalis (substantia innominata) and hypothalamus in the rhesus monkey. *J. Comp. Neurol.* 214:170- 197.

Mesulam, M.M., Mufson, E.J., Wainer, B.H. and Levey, A.I. (1983b) Central cholinergic pathways in the rat: an overview based on an alternative nomenclature (Ch.1 - Ch.6), *Neuroscience* 10: 1185-1201.

Mesulam, M.M., Mufson, E.J., Levey, A.I. and Wainer, B.H. (1984) Atlas of cholinergic neurons in the forebrain and upper brainstem of the macaque based on monoclonal choline acetyltransferase immunohistochemistry and acetylcholinesterase histochemistry. *Neuroscience* 12:669-686.

Milner, T.A., Pickel, V.M., Abate, C. and Reis, D.J. (1987) Choline acetyltransferase in the rat rostral ventrolateral medulla: ultrastructural localization and synaptic interactions with neurons containing catecholamine synthesizing enzymes. *Soc. Neurosci. Abstr.* 13: 227.

Miura, M. and Reis, D.J. (1969) Cerebellum: A pressor response elicited from the fastigial nucleus and its efferent pathway in brainstem. *Brain Res.* 13: 595-599.

Miura, M. and Reis, D.J. (1970) A blood pressure response from the fastigial nucleus and its relay pathways in brainstem. *Am. J. Physiol.* 219: 1330-1336.

Moruzzi, G. and Magoun, H.W. (1949) Brainstem reticular formation and activation of the EEG. *Electroenceph. clin. Neurophysiol.* 1: 455-473.

Mraovitch, S., Pinard, E. and Seylaz, J. (1986) Two neural mechanisms in rat fastigial nucleus regulating systemic and cerebral circulation. *Am. J. Physiol.* 251 (Heart Circ. Physiol 20): H153-H163.

Nakai, K., Imai, H., Kamei, I., Itakura, T., Komari, N., Kimura, H., Nagai, T. and Maeda, T. (1981) Microangioarchitecture of rat parietal cortex wth special reference to vascular "sphincters". *Stroke* 12(5): 653-659.

Nakai, M., Iadecola, C. and Reis, D.J. (1982) Global cerebral vasodilation by stimulation of rat fastigial cerebellar nucleus. *Am. J. Physiol.* 243 (Heart Circ. Physiol. 12): H226-H235.

Nakai, M., Iadecola, C., Ruggiero, D.A., Tucker, L.W. and Reis, D.J. (1983) Electrical stimulation of cerebellar fastigial nucleus increases cerebral cortical blood flow without change in local metabolism: Evidence for an intrinsic system in brain for primary vasodilation. *Brain Res.* 260: 35-49.

Ohno, K., Pettigrew, K.D. and Rappoport, S.I. (1979) Local cerebral blood flow in the conscious rat as measured with ¹⁴C-iodoantipyrine and ³H-nicotine. *Stroke* 10: 62-67.

Orlowski, M. and Meister, A. (1965) Isolation of γ -glutamyl transpeptidase from hog kidney. *J. Biol. Chem.* 240: 338-347.

Orlowski, M., Sessa, G. and Green, J.P. (1974) Gamma-glutamyltranspeptidase in brain capillaries: possible site of a blood-brain barrier for amino acids. *Science* 184: 66-68.

Palkovits, M. and Jacobowitz, D.M. (1974) Topographic atlas of catecholamine and acetylcholinesterase-containing neurons in the rat brain. II. Hindbrain (mesencephalon, rhombencephalon). *J. Comp. Neurol.* 157:29-42.

Park, D.H., Baetge, E.E., Kaplan, B., Albert, V.R., Reis, D.J. and Joh, T.H. (1982) Different forms of adrenal phenylethanolamine N-methyltransferase: species- specific posttranslational modification. *J. Neurochem.* 38:410-414.

Parnavelas, J.C., Kelly, W. and Burnstock, G. (1985) Ultrastructural localization of choline acetyltransferase in vascular endothelial cells in rat brain. *Nature* 316: 724-725.

Paulson, O.B., Olesen, J. and Christensen, M.S. (1972) Restoration of autoregulation of cerebral blood flow by hypocapnia. *Neurology* 22: 286-293.

Pepeu, G. (1973) The release of acetylcholine from the brain: an approach to the study of the central cholinergic mechanisms. *Prog. Neurobiol.* 3: 259-288.

Pickel, V.M., Joh, T.H. and Reis, D.J. (1975) Ultrastructural localization of tyrosine hydroxylase in brain by light and electron microscopy. *Brain Res.* 85: 295-300.

Pickel, V.M. (1981) Immunocytochemical methods. In: L. Heimer and M.J. Robards (Eds.) *Neuroanatomical Tract-tracing Methods*, New York: Plenum Press, pp. 483-509.

Potter, P.E., Hadjiconstantinou, M., Meek, M.L. and Neff, N.H. (1984) Measurement of acetylcholine turnover rate in brain: an adjunct to a simple HPLC method for choline and acetylcholine. *J. Neurochem.* 43: 88-90.

Reinhard, J.F., Liebmann, J.E., Schlossberg, A.J. and Moskowitz, M.A. (1979) Serotonin neurons project to small blood vessels in brain. *Science* 106: 85-87.

Reis, D.J., Iadecola, C., MacKenzie, E., Mori, M., Nakai, M. and Tucker, L. (1982) Primary and metabolically coupled cerebrovascular dilation elicited by stimulation of two intrinsic systems in brain. In: D. Heistad and M. Marcus (Eds.) *Cerebral Blood Flow: Effects of Nerves and Neurotransmitters*, New York: Elsevier/North Holland, pp. 475-484.

Reis, D.J., Iadecola, C. and Nakai, M. (1985) Control of cerebral blood flow and metabolism by intrinsic neural systems in brain. In: F. Plum and W. Pulsinelli (Eds.) *Cerebrovascular Diseases*, New York: Raven Press, pp. 1-25.

Reis, D.J. and Iadecola, C. (1989) Central neurogenic regulation of cerebral blood flow. In: J. Seylaz and R. Sercombe (Eds.) *Neurotransmission and Cerebrovascular Function Vol. II*, Amsterdam: Elsevier, pp. 369-390.

Rennels, M.L., Forbes, M.S., Anders, J.J. and Nelson, E. (1977) Innervation of the microcirculation in the central nervous system and other tissues. In: C. Owman and L. Edvinsson, (Eds.), *Neurogenic Control of Brain Circulation*, Oxford: Pergamon Press, pp. 91-104.

Ross, C.A., Ruggiero, D.A. and Reis, D.J. (1981) Afferent projections to cardiovascular portions of the nucleus of the tractus solitarius in the rat. *Brain Res.* 223: 402-408.

Rowan, R.A. and Maxwell, D.S. (1981) An ultrastructural study of vascular proliferation and vascular alkaline phosphatase activity in the developing cerebral cortex of the rat. *Am. J. Anat.* 160: 257-265.

Ruggiero, D.A., Ross, C.A., Anwar, M., Park, D.H., Joh, T.H. and Reis, D.J. (1985) Distribution of neurons containing phenylethanolamine N-methyltransferase in medulla and hypothalamus of rat. *J. Comp. Neurol.* 239:127-154.

Ruggiero, D.A., Mraovitch, S., Granata, A.R., Anwar, M. and Reis, D.J. (1987) A role of insular cortex in autonomic function. *J. Comp. Neurol.* 257: 189-207.

Sakurada, O., Kennedy, C., Jehle, J., Brown, J.D., Carbin, G.L. and Sokoloff, L. (1978) Measurement of local cerebral blood flow with iodo (14C) antipyrine. *Am. J. Physiol.* 234 (Heart and Circ. Physiol.): H59-H66.

Santos-Benito, F.F. and Gonzales, J.L. (1985) Decrease of choline acetyltransferase activity of rat cortex capillaries with aging. *J. Neurochem.* 45: 633-636.

Saper, C.B. and Loewy, A.D. (1982) Projections of the pedunculopontine tegmental nucleus in the rat: evidence for additional extrapyramidal circuitry. *Brain Res.* 252: 367-372.

Saper, C.B. (1984) Organization of cerebral cortical afferent systems in the rat. II. Magnocellular basal nucleus. *J. Comp. Neurol.* 222: 313-342.

Sastray, B.V.R. and Sadavongvivad, C. (1979) Cholinergic systems in nonnervous tissues. *Pharmacol. Rev.* 30: 65-132.

Schwarz, R., Hokfelt, T., Fuxe, K., Jonsson, G., Goldstein, M. and Terenius, L. (1979) Ibotenic acid-induced neuronal degeneration: a morphological and neurochemical study. *Exp. Brain Res.* 37: 199-216.

Scremin, O.U., Sonnenschein, R.R. and Rubinstein, E.H. (1983) Cholinergic cerebral vasodilation: lack of involvement of cranial parasympathetic nerves. *J. Cereb. Blood Flow Metab.* 3: 362-368.

Scremin, O.U., Allen, K., Torres, C. and Scremin, A.M. (1988) Physostigmine enhances blood flow-metabolism ratio in neocortex. *Neuropsychopharmacol.* 1: 297-303.

Shute, C.C.D. and Lewis, P.R. (1967) The ascending cholinergic reticular system: neocortical, olfactory and subcortical projections. *Brain* 90: 497-520.

Smith, J.C., Cavallito, C.J. and Foldes, F.F. (1967) Choline acetyltransferase inhibitors: a group of styryl-pyridine analogs. *Biochem. Pharmacol.* 16: 2438-2441.

Sofroniew, M.V., Eckenstein, F., Thoenen, H. and Cuello, A.C. (1982) Topography of choline acetyltransferase-containing neurons in the forebrain of the rat. *Neurosci. Lett.* 33:7-12.

Sofroniew, M.V., Campbell, P.E., Cuello, A.C. and Eckenstein, F. (1985) Central cholinergic neurons visualized by immunohistochemical detection of choline acetyltransferase. In: G. Paxinos (Ed.), *The Rat Nervous System, Vol. 1: Forebrain and Midbrain*. New York: Academic Press, pp. 471-485.

Sternberger, L.A. (1979) *Immunocytochemistry*, New York: Wiley, 524 pp.

Stichel, C.C. and Singer, W. (1985) Organization and morphological characteristics of ChAT-containing fibers in the visual thalamus and striate cortex of the cat. *Neurosci. Lett.* 53: 155-160.

Szerb, J.C. (1967) Cortical acetylcholine release and electroencephalographic arousal. *J. Physiol. (Lond.)* 192: 329-343.

Tenland, T. (1982) *On Laser Doppler Flowmetry. Methods and Microvascular Applications*. Linkoping University Medical Dissertations No. 136, Linkoping.

Tucek, S., Havranek, M. and Ge, I. (1978) Synthesis of (acetyl-14C)carnitine and the use of tetraphenylboron for differential extraction of (acetyl-14C)choline and (acetyl-14C)carnitine. *Anal. Biochem.* 84: 589-593.

Tucek, S. (1985) Regulation of acetylcholine synthesis in the brain. *J. Neurochem.* 44:11-24.

Underwood, M.D., Iadecola, C. and Reis, D.J. (1983) Stimulation of brain areas increasing cerebral cortical blood flow and/or metabolism does not activate the electroencephalogram. *J. Cereb. Blood Flow Metab.* 3(Suppl. 1): S218-219.

Vasquez, J. and Purves, M.J. (1979) The cholinergic pathways to cerebral blood vessels. I. Morphological studies. *Pflugers Arch.* 379: 157-163.

Wamsley, J.K., Zarbin, M.A. and Kuhar, M.J. (1984) Distribution of muscarinic cholinergic high and low affinity against binding sites: A light microscopic autoradiographic study. *Brain Res. Bull.* 12: 233-243.

Weiss, H.R., Buchweitz, H., Murtha, T.J. and Auletta, M. (1982) Quantitative regional determination of morphometric indices of the total and perfused capillary network in rat brain. *Circ. Res.* 51: 494-503.

Whittaker, V.P. (1969) The synaptosome. In: A. Lajtha (Ed.) *Handbook of Neurochemistry*, Vol. 2, New York: Plenum Press, pp. 327-364.

Williams, S.K., Gillis, J.F., Matthews, M.A., Waschner, R.C. and Bitensky, M.W. (1980) Isolation and characterization of brain endothelial cells: morphology and enzyme activity. *J. Neurochem.* 35: 374-381.

Witter, A., Slanger, J.L. and Terpstra, G.K. (1973) Distribution of ³H-methylatropine in rat brain. *Neuropharmacology* 12: 835-841.

Yaksh, T.L. and Yamamura, H.I. (1975) The release *in vivo* of [³H]-acetylcholine from cat caudate nucleus and cerebral cortex by atropine, pentylenetetrazol, K⁺-depolarization and electrical stimulation. *J. Neurochem.* 25: 123-130.

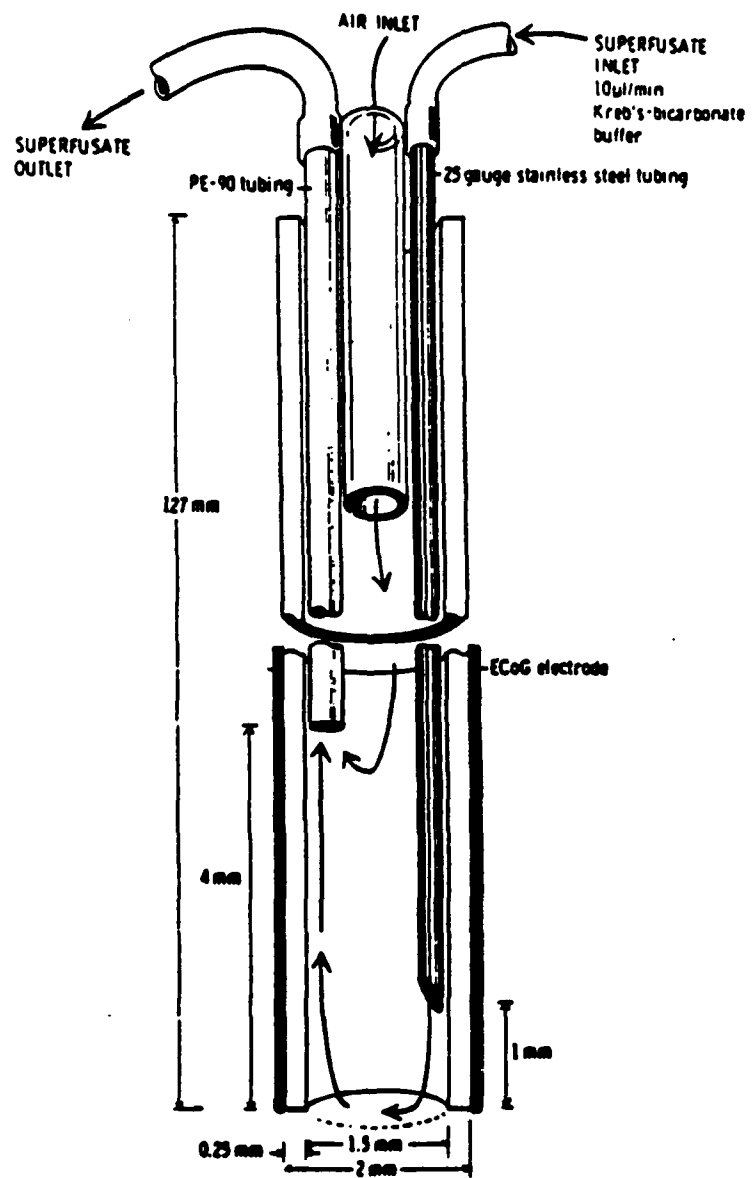


Fig. 1A. A schematic of the device used to apply atropine to the cortical surface and collect superfusate during the release experiments.



Fig. 1B. The region of the parietal cortex sampled during these experiments is shown following introduction of fast green dye into the superfusion device to mark the placement.

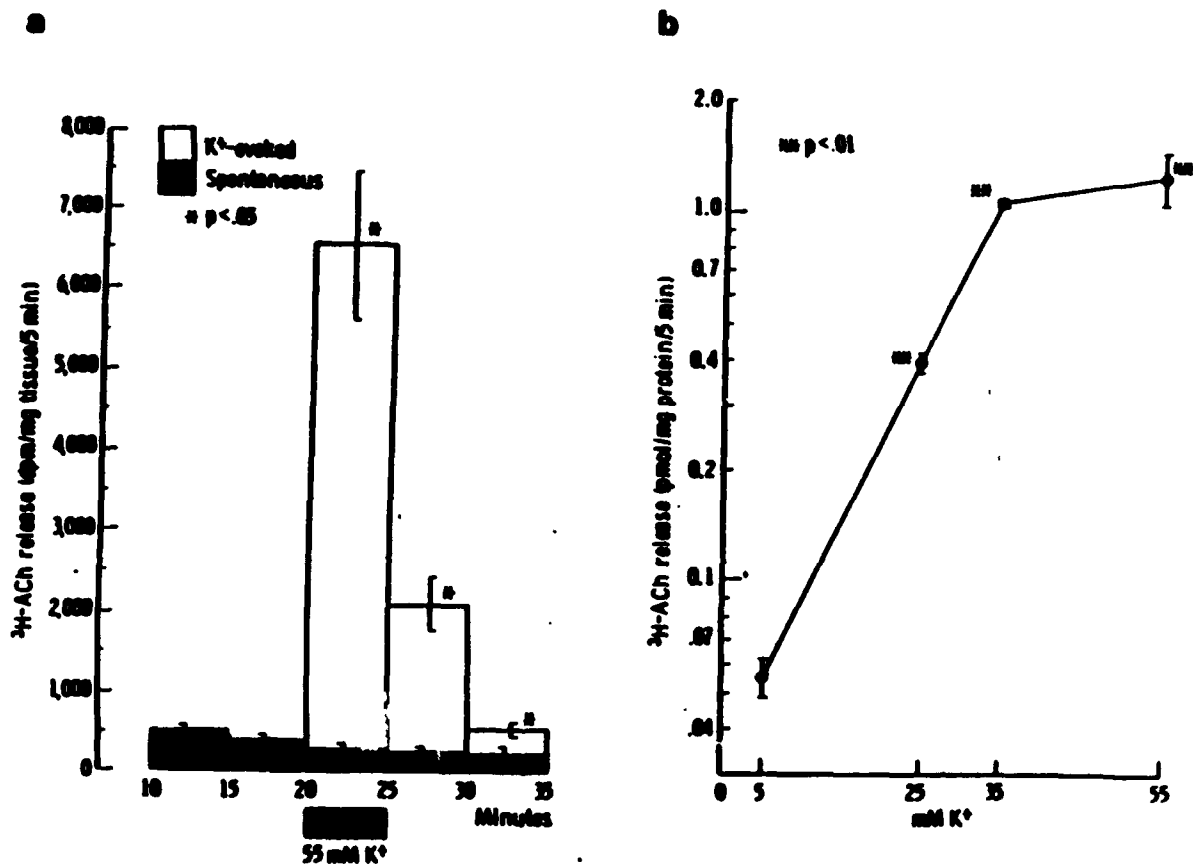


Fig. 2. A. Release of $^3\text{H-ACh}$ from tissue slices of the targeted area of CX during steady-state spontaneous efflux and following depolarization with 55 mM K⁺. **B.** The effect of varying the potassium depolarization stimulus. Values are means \pm SEM (n = 3).

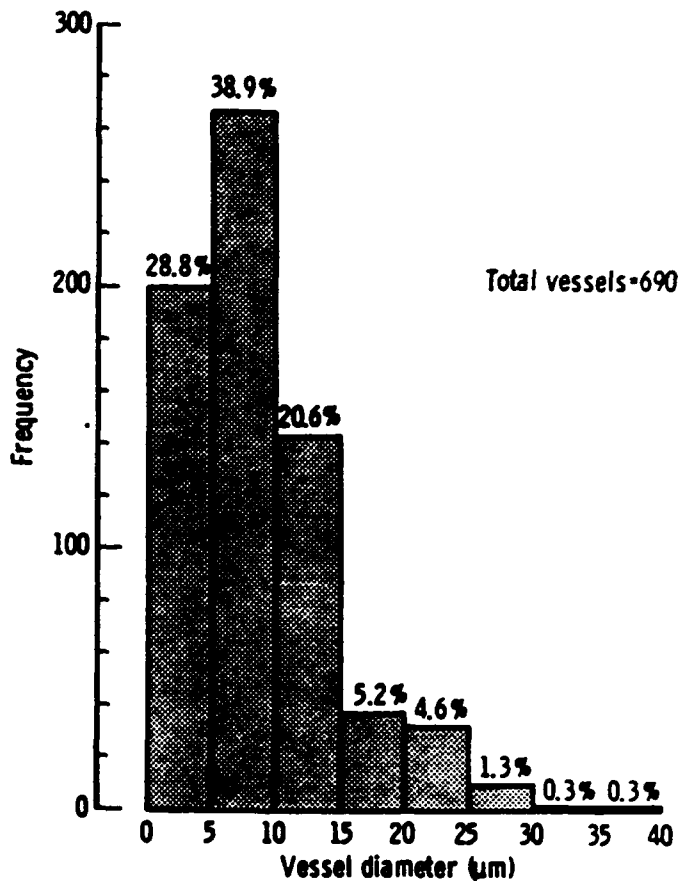
A**B**

Fig. 3. A. A light microscopic photomicrograph of the cortical microvessel preparation as viewed from the video screen. With the aid of a joystick-controlled cursor, and a computerized image analysis system, the diameters of the vessels were calculated at the branching points of the vascular tree. The placement of the cursor is indicated by the white bar positioned perpendicular to the longitudinal axis of each vessel. B. The distribution of the diameters of 690 vessels isolated from 4 separate experiments is represented.

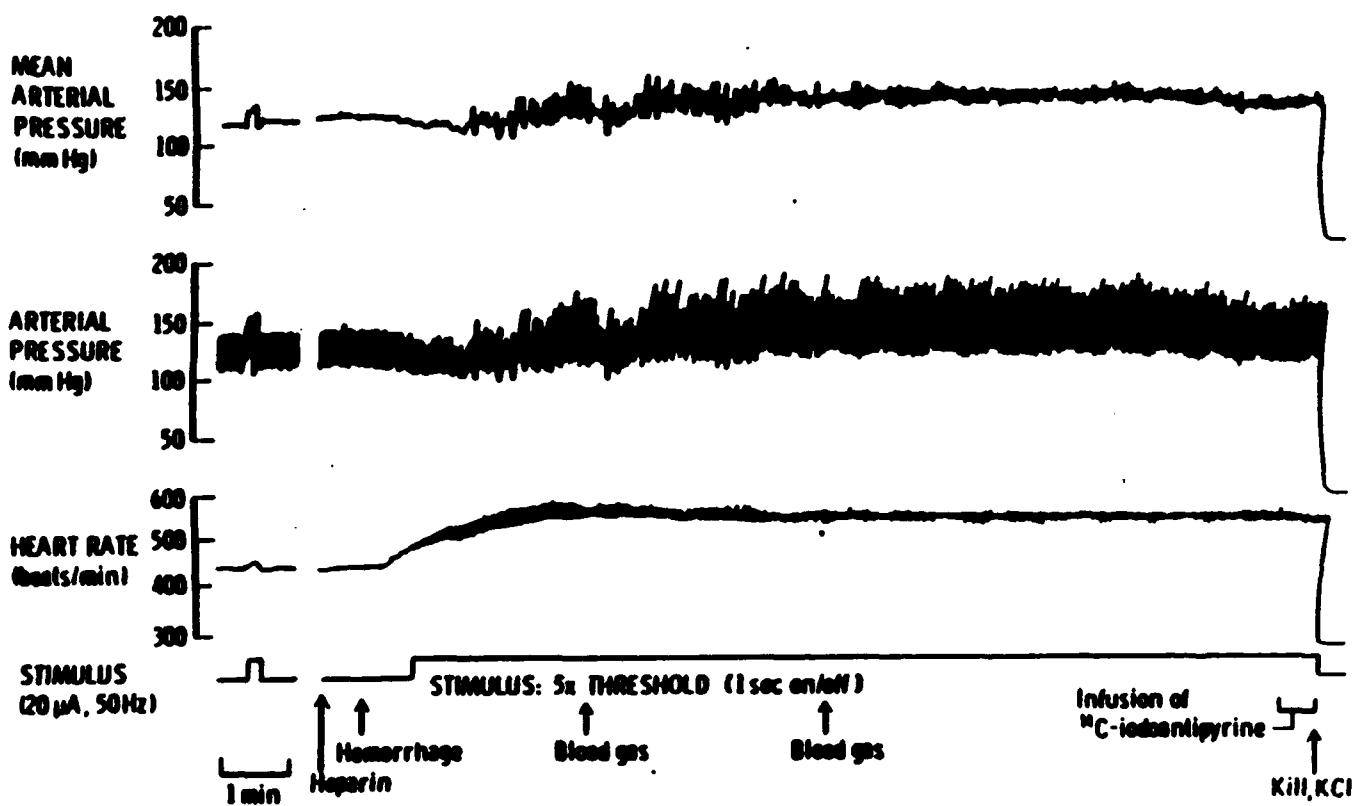


Fig. 4. An illustration of the later portion of a representative blood flow experiment summarizing the protocol used to measure rCBF during electrical stimulation of the fastigial nucleus (FN) of the cerebellum. Three hours prior the animal was anesthetized with chloralose, paralyzed with d-tubocurarine and ventilated with 100% O₂. Note that during FN stimulation mean AP is maintained within the autoregulated range (80-150 mmHg) and that arterial blood gases are monitored and adjusted.

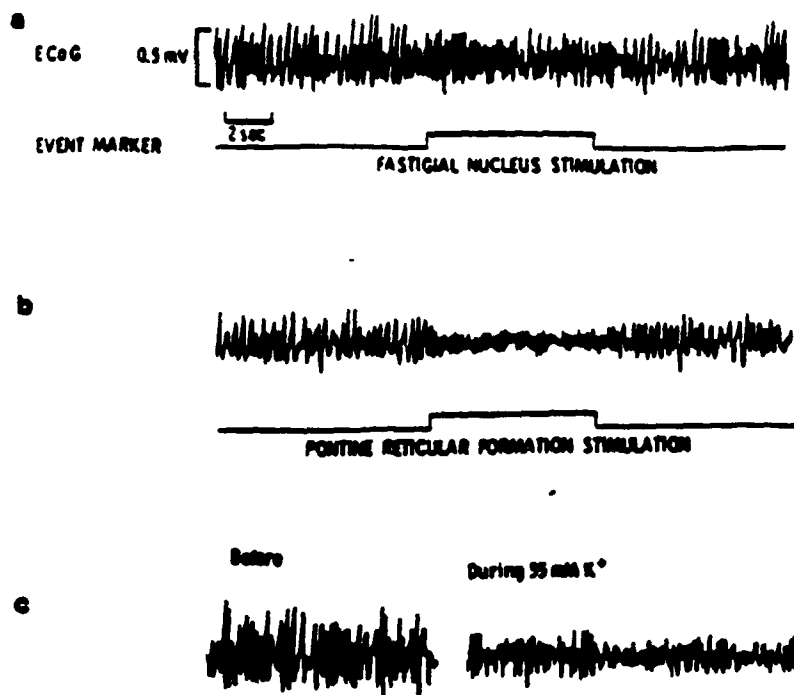


Fig. 5. Representative tracings of the ECoG recorded from the cerebral cortex underlying the superfusion device following electrical and chemical stimulation of different brain regions. Note the difference in the ECoG following electrical stimulation (100 μ A; 50 Hz; 0.5 msec) of the fastigial nucleus (A) or the pontine reticular formation (B). Importantly, the classical cortical "arousal response" described by Moruzzi and Magoun (1949) can be elicited while the superfusion device is in place on the cortical surface. C shows the electrocorticogram (ECoG) immediately before and two minutes after initiating depolarization of the parietal Cx with local application of K⁺ (55 mM).

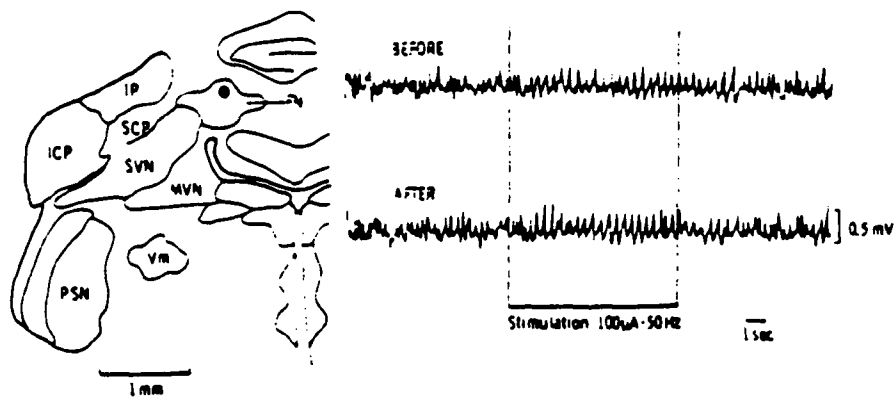
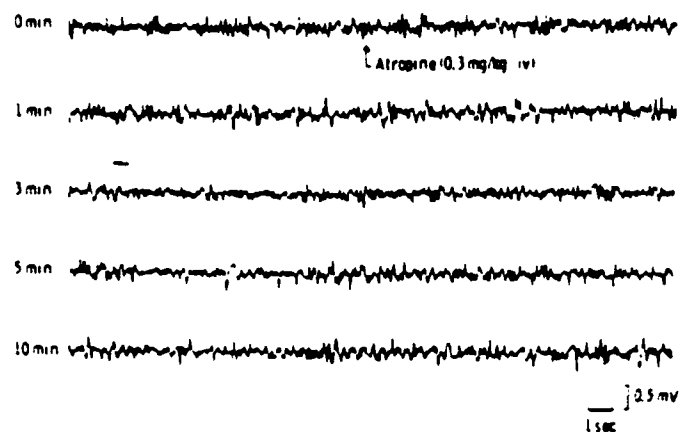


Fig. 6. Effect of administration of atropine sulfate (0.3 mg/kg, i.v.) on basal EEG activity and on the EEG changes produced by electrical stimulation of the cerebellar fastigial nucleus (FN) in anesthetized rat. Atropine did not affect basal EEG (upper panel) nor the slow-wave activity elicited by FN stimulation (lower panel).

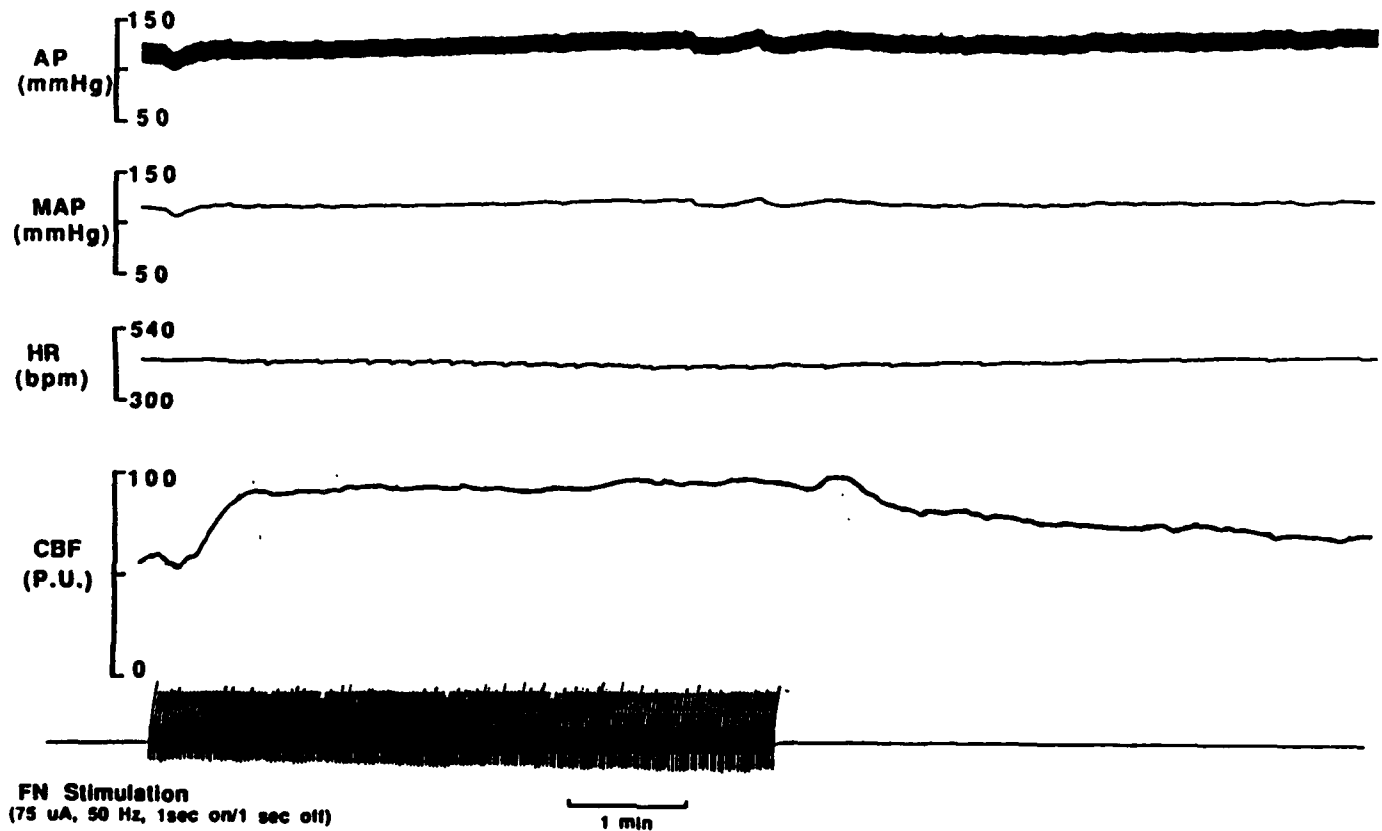


Fig. 7. Effect of stimulation of the cerebellar fastigial nucleus (FN) on cortical cerebral blood flow (CBF). CBF, expressed in arbitrary units (perfusion units, PU), was continuously monitored in the rat parietal cortex by laser doppler flowmetry. The increase in arterial pressure (AP) elicited by FN stimulation was prevented by spinal cord transection. After cord transection AP was maintained by i.v. infusion of phenylephrine. FN stimulation produced a large and sustained increase in CBF which was independent of AP. Notice that the increase reached a plateau after about 1 min of stimulation (75 μ A, 50 Hz, 1 sec on/1 sec off) and that it persisted after termination of the stimulus.

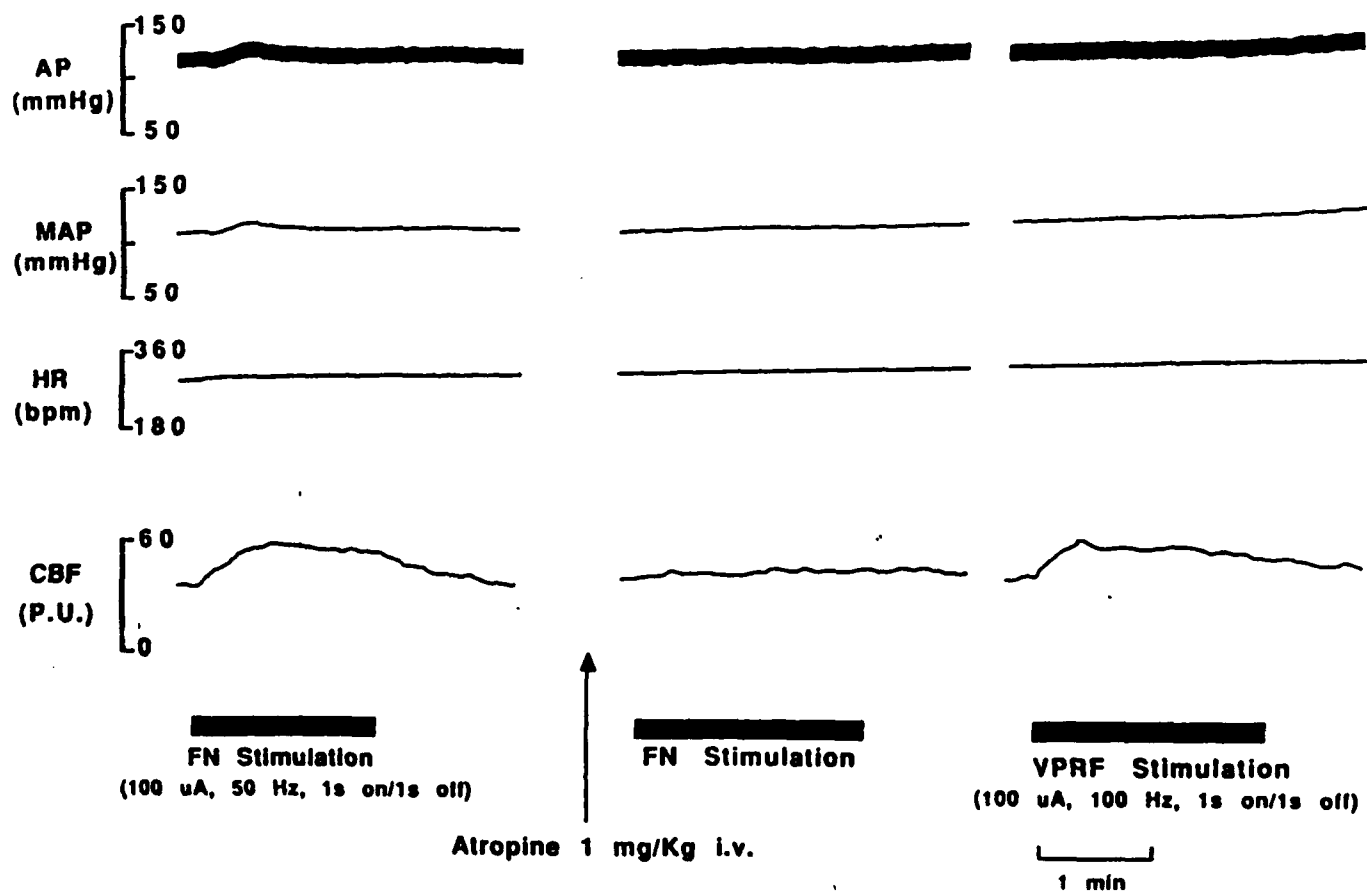


Fig. 8. Effect of systemic administration of atropine (1 mg/kg, i.v.) on the increase in cerebral blood flow (CBF) elicited by stimulation of the fastigial nucleus (FN) in spinal cord transected rats. CBF was measured by laser doppler flowmetry and expressed in relative units (perfusion units, PU). Prior to administration of atropine, stimulation of the FN increases CBF (left panel). Two to 10 min after administration the response was still present although markedly reduced (not shown). Fifteen min after administration of atropine the flow increase evoked from the FN was abolished (middle panel), while that elicited from the VPRF was still present (right panel).

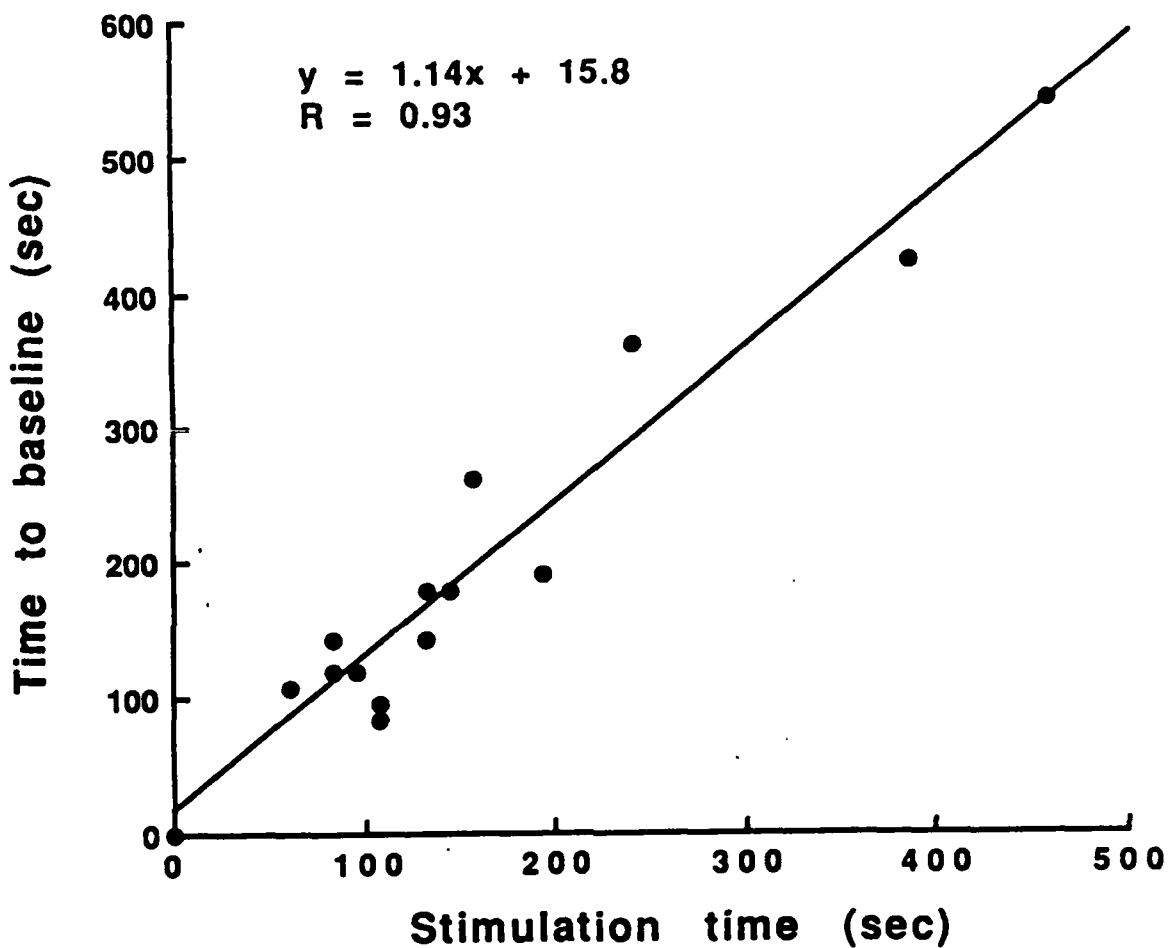


Fig. 9. Relationship between length of the stimulation period and time required for cortical blood flow to return to baseline after termination of the stimulus, in anesthetized rats after spinal cord transection. The fastigial nucleus (FN) was stimulated with intermittent trains of pulses at 50-70 Hz and with a current intensity of 50-100 μ A and cortical flow was continuously monitored by laser-Doppler flowmetry. Notice that there is a positive linear relationship between length of the stimulation and time required for flow to return to baseline after termination of the stimulation ($r = 0.93$, $n = 15$, $p < 0.001$).

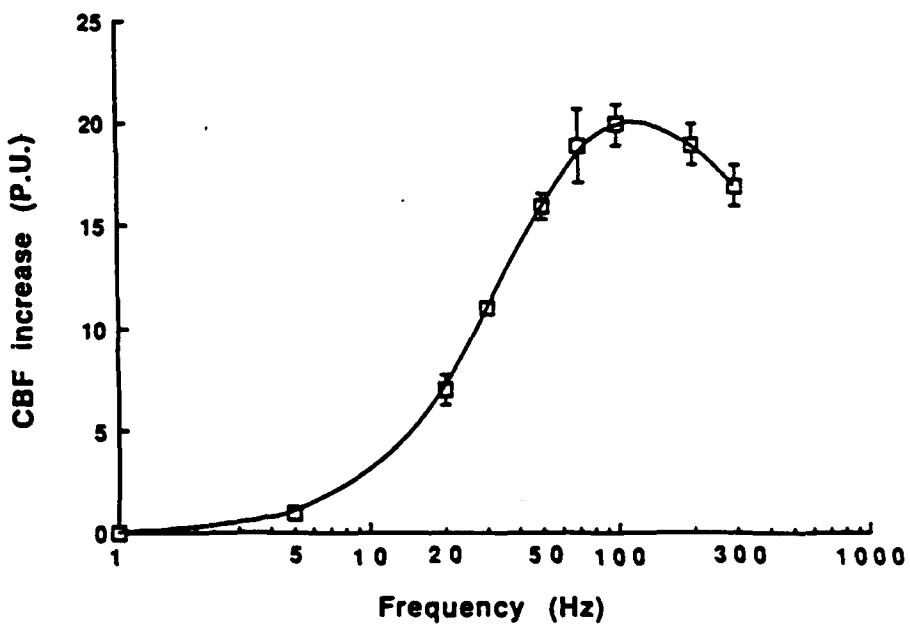
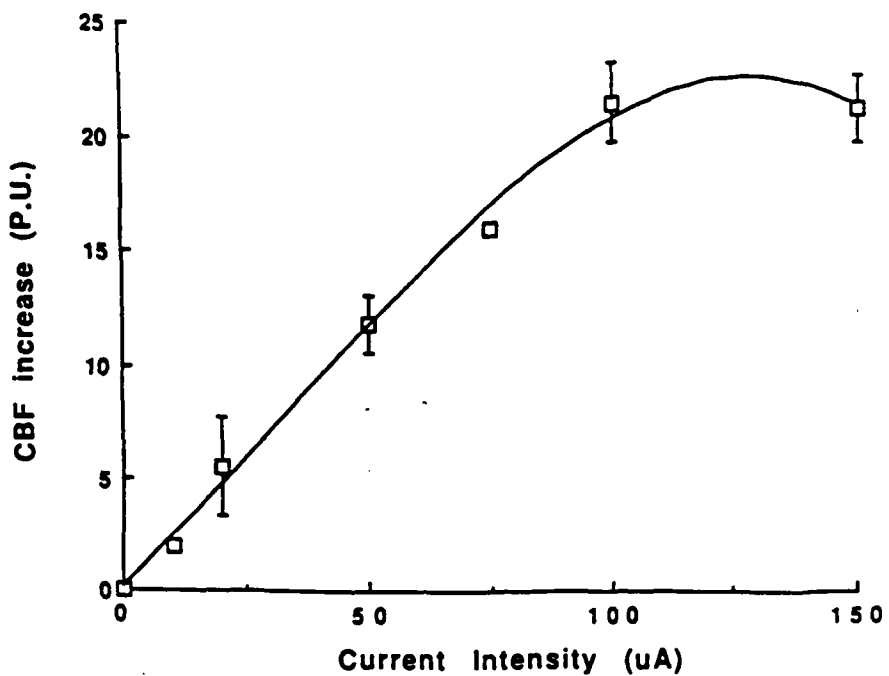


Fig. 10. Stimulus intensity and frequency response characteristics of the cerebrovasodilation elicited by stimulation of the fastigial nucleus in spinal cord transected rats (see legend to Fig. 7 and methods for details). Cortical blood flow (perfusion units, PU) was measured by laser doppler flowmetry. When the stimulus intensity was varied ($n = 2-4$) (upper panel) while the frequency was kept constant at 50 Hz, the response appeared between 10 and 20 μ A, its magnitude increased linearly with the increase in current intensity and reached a plateau at 100 μ A. Similarly, when the stimulation frequency was varied ($n = 2-5$) (lower panel) while the intensity was kept constant at 75-100 μ A, the response appeared between 5 and 15 Hz, reached a maximum at 70-100 Hz and then decreased at stimulation frequency of 200 and 300 Hz.

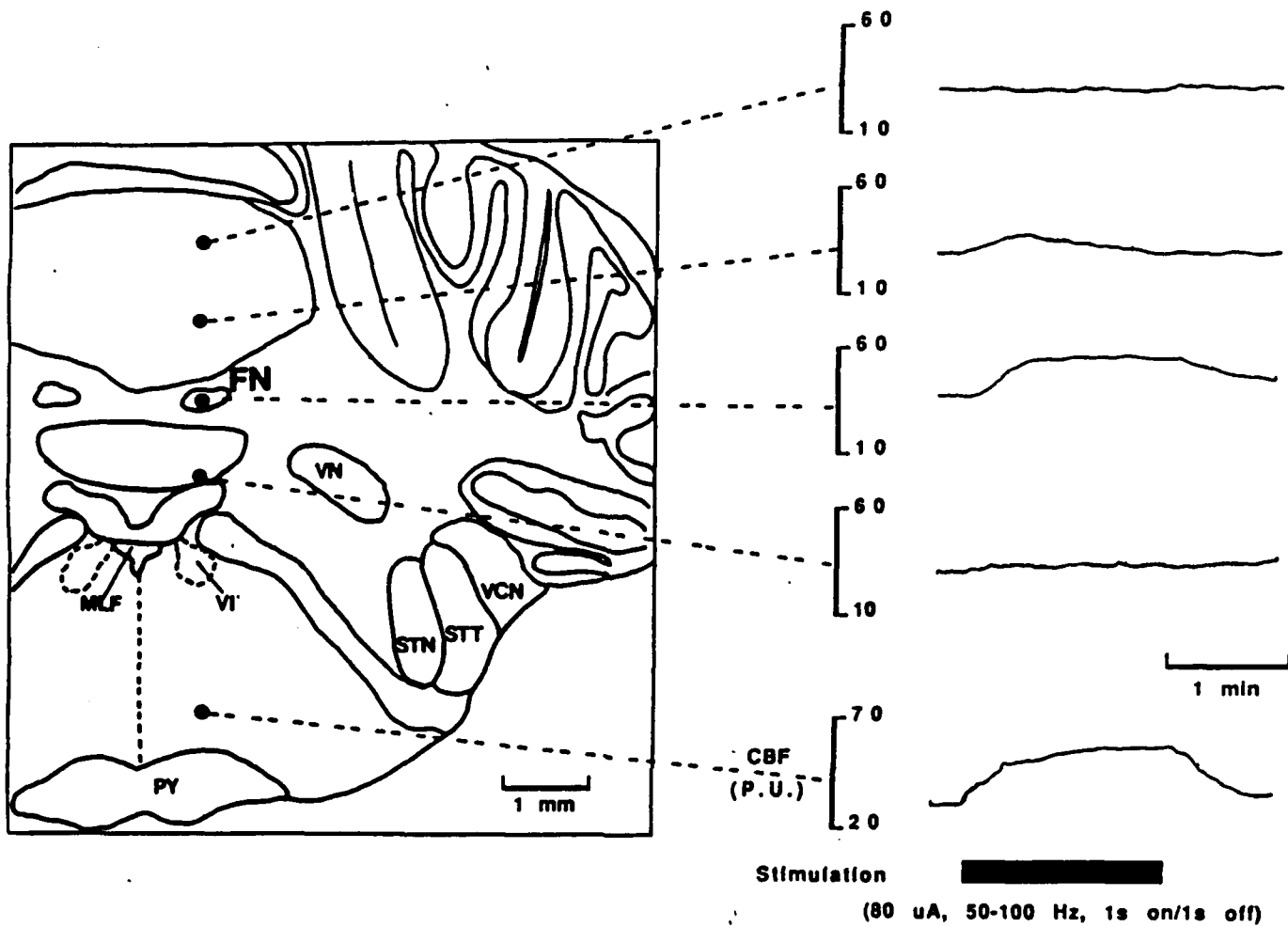


Fig. 11. Location of sites from which an elevation in cerebral blood flow (CBF) could be elicited from low intensity electrical stimulation. CBF, in arbitrary units (perfusion units, PU), was continuously recorded from the parietal cortex by using laser-doppler flowmetry. The increases in CBF were anatomically confined to the FN and they were best elicited from the rostral ventromedial portion of the nucleus. The small and non-sustained increase elicited from the vermis overlying the FN probably reflects stimulus spread. However, stimulation of the ventral pontine reticular formation (VPRF) at a site located 4 mm ventral to the FN also produced large, stimulus-locked, increases in CBF.

Abbreviations: MLF, medial longitudinal fasciculus; PY, pyramidal tract; STN, spinal trigeminal nucleus; STT, spinal trigeminal tract; VCN, ventral cochlear nucleus; VN, superior vestibular nuclei; VI, sixth cranial nerve nucleus.

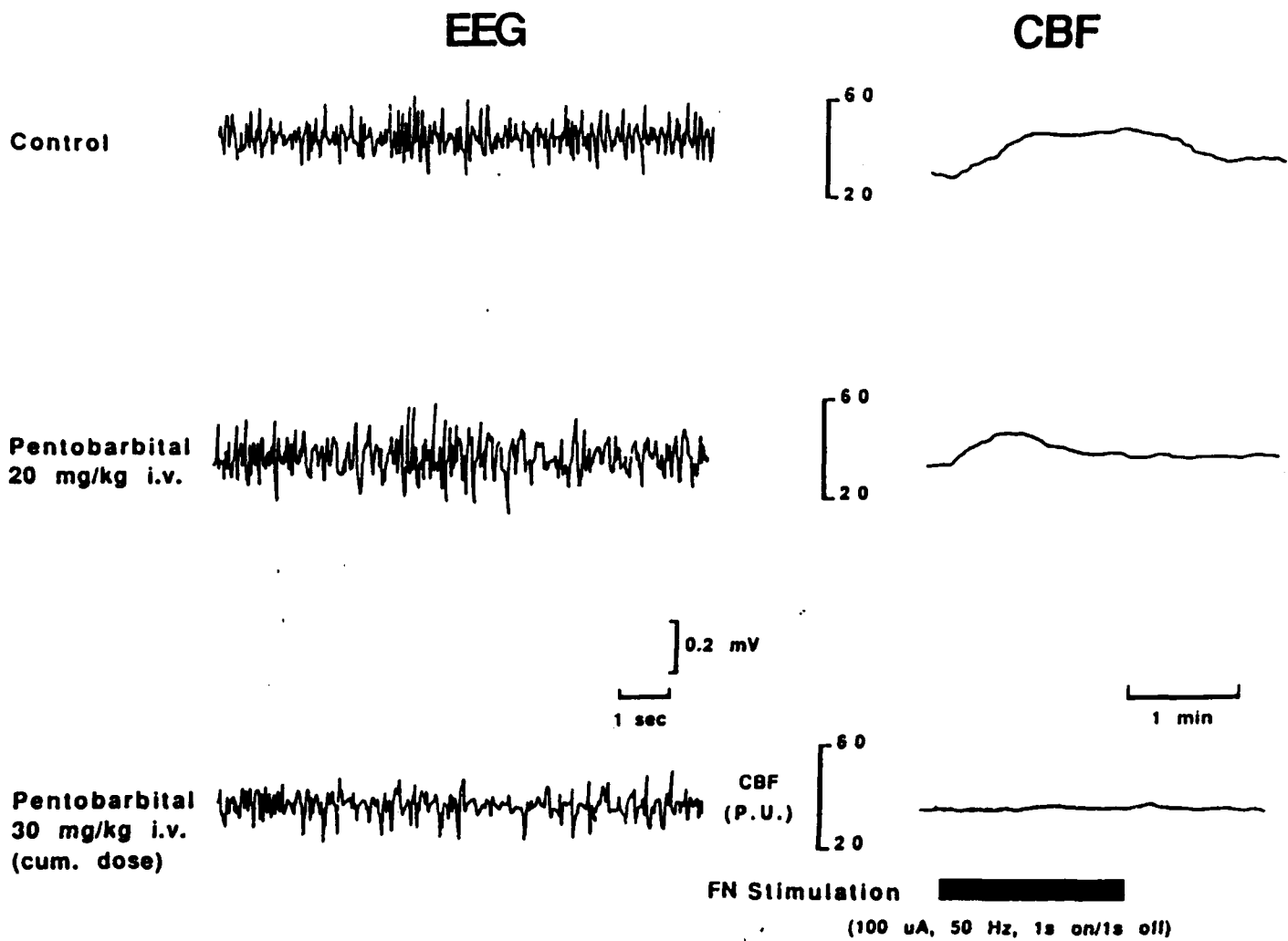


Fig. 12. Effect of administration of pentobarbital on the EEG and on the increase in cerebral blood flow (CBF) elicited by electrical stimulation of the fastigial nucleus (FN) in spinal cord transected rats. CBF was measured over the parietal cortex by laser doppler flowmetry and expressed in relative units (perfusion units, PU). Five min after 20 mg/kg of pentobarbital were given, the increase in CBF elicited from the FN was markedly reduced (right-middle panel). Administration of additional pentobarbital (10 mg/kg, i.v., cumulative dose 30 mg/kg) abolished the response (right-lower panel). Notice that after administration of this dose of pentobarbital the cortical electrical activity is still present (left-lower panel).

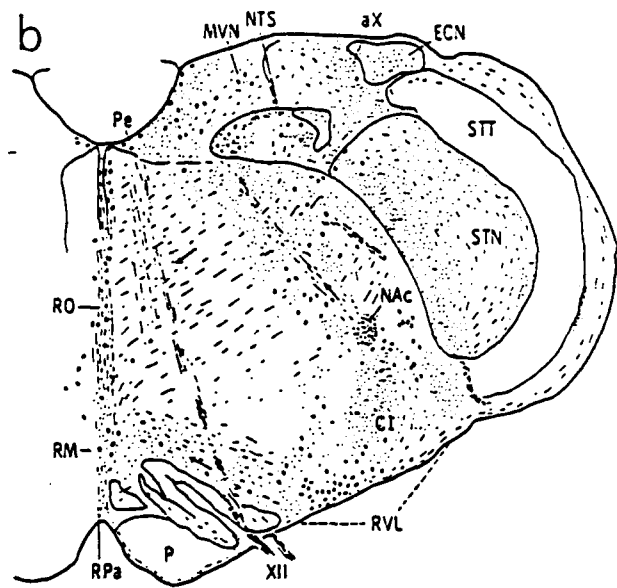
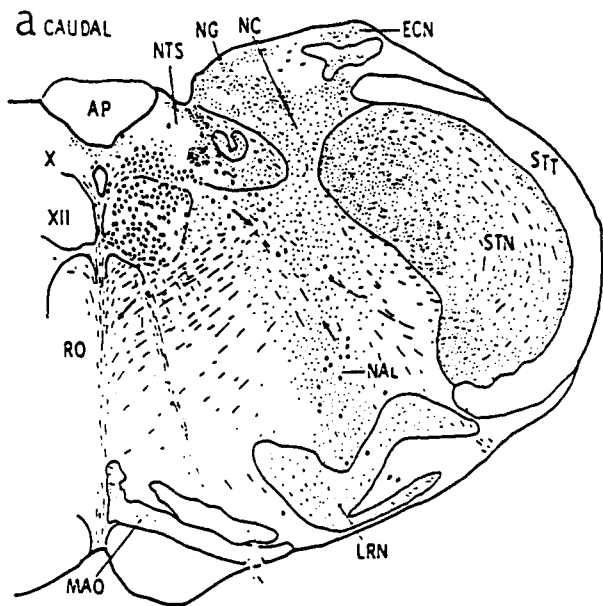


Fig. 13. Camera lucida drawings of transverse sections through the medulla oblongata labeled immunocytochemically for ChAT. (a,b) Perikarya (black dots), axons (lines) and punctate varicosities (finer stippling) are labeled in several autonomic substructures in the rostral and caudal ventrolateral medulla, lateral tegmental field (nuclei reticularis dorsalis and parvocellularis), nucleus tractus solitarius, raphe, pararaphe (extending between the nucleus raphe magnus and the rostral ventrolateral medulla) and periventricular gray. In RVL (b), note the compact and diffuse fields of punctate processes directly underlying the compact division of the nucleus ambiguus or lying further ventrally in the C1 area, respectively. Arrows indicate possible directionality of labeled axon trajectories as traced on serially sectioned tissues.

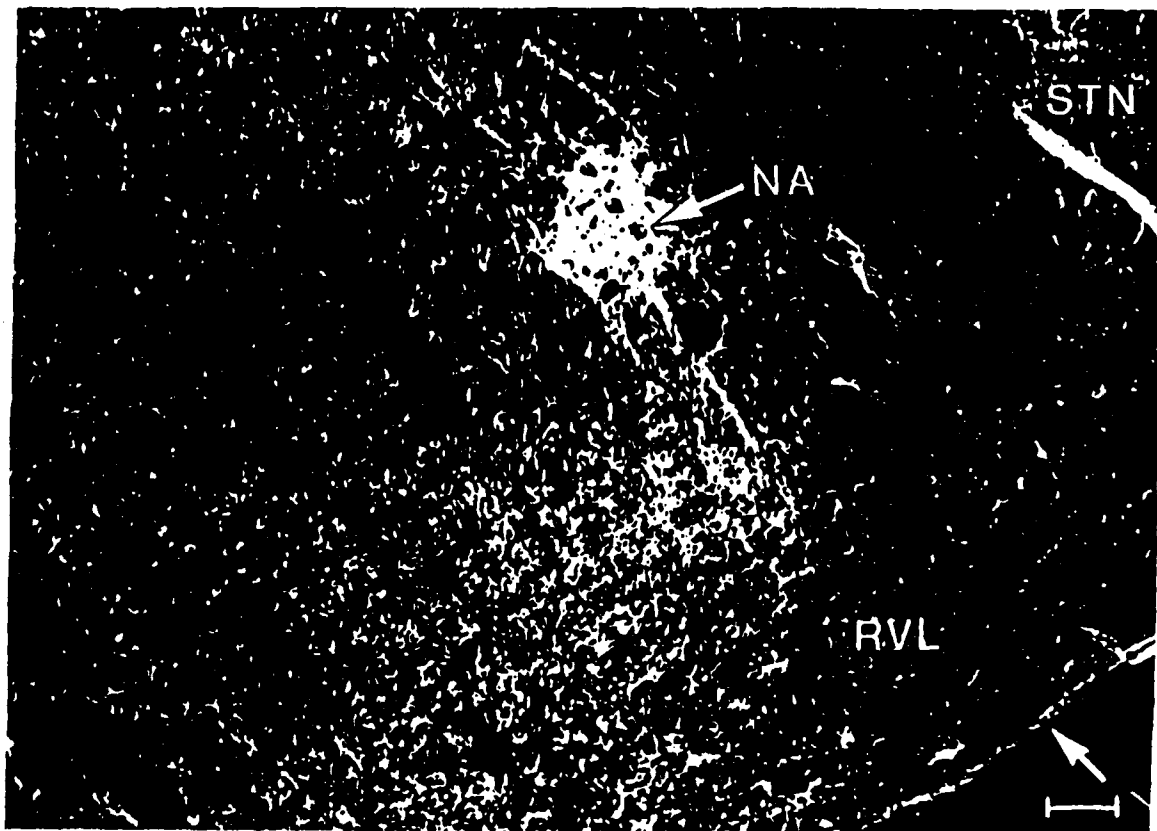


Fig. 14. Darkfield photomicrograph of fine punctate varicosities (and coarser processes) in the rostral ventrolateral reticular nucleus (RVL) underlying the nucleus ambiguus (NA). The presence of terminals in RVL was supported by electron microscopy (Dr. T. Milner, in press) and muscarinic receptor autoradiography (Ernsberger et al., 1988a,b). Coarser processes within RVL are derived (in part?) from cholinergic dendrites of parasympathetic neurons of the NA. These data suggest that afferent projections into the RVL may simultaneously influence sympathoexcitatory premotor neurons and parasympathetic outflow via the efferent limb of the vagus nerve. Bar = 120 μ m.

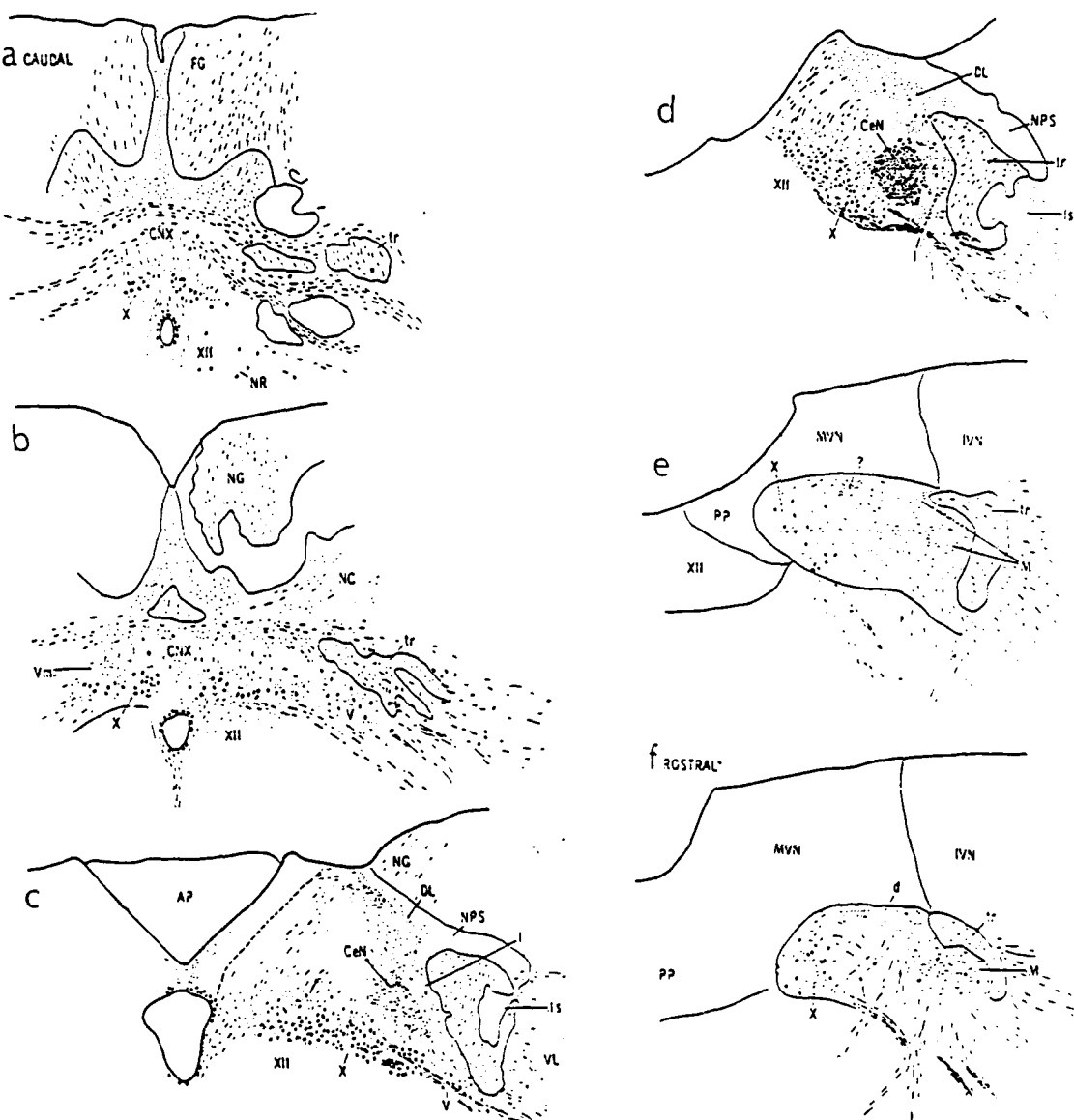


Fig. 15. Camera lucida drawings depicting ChAT-immunoreactivity at commissural (a,b) intermediate (c,d) and rostral (e,f) levels of the nucleus tractus solitarii (NTS). Perikarya (filled circles) were labeled in commissural (a), ventral (b,c), medial and intermediate (d-f) subnuclei. Labeled terminals (fine punctate varicosities) are limited to discrete fields of the NTS within dorsal, intermediate and medial subnuclei. These sites are densely labeled at intermediate (c,d) and rostral (e,f) levels of the nucleus. Also note the following: cholinergic cell bodies surrounding the central canal (a-c), the admixture of cells and processes in the dorsal motor nucleus (X) and the presence of processes passing between the NTS and the underlying tegmentum (their direction is unknown). The origins of cholinergic afferents to the NTS also remain to be determined by double labeling and electrophysiological techniques. On the basis of painstaking analysis of serially sectioned tissues it was our impression that processes in the NTS are derived from both extrinsic and local neurons.

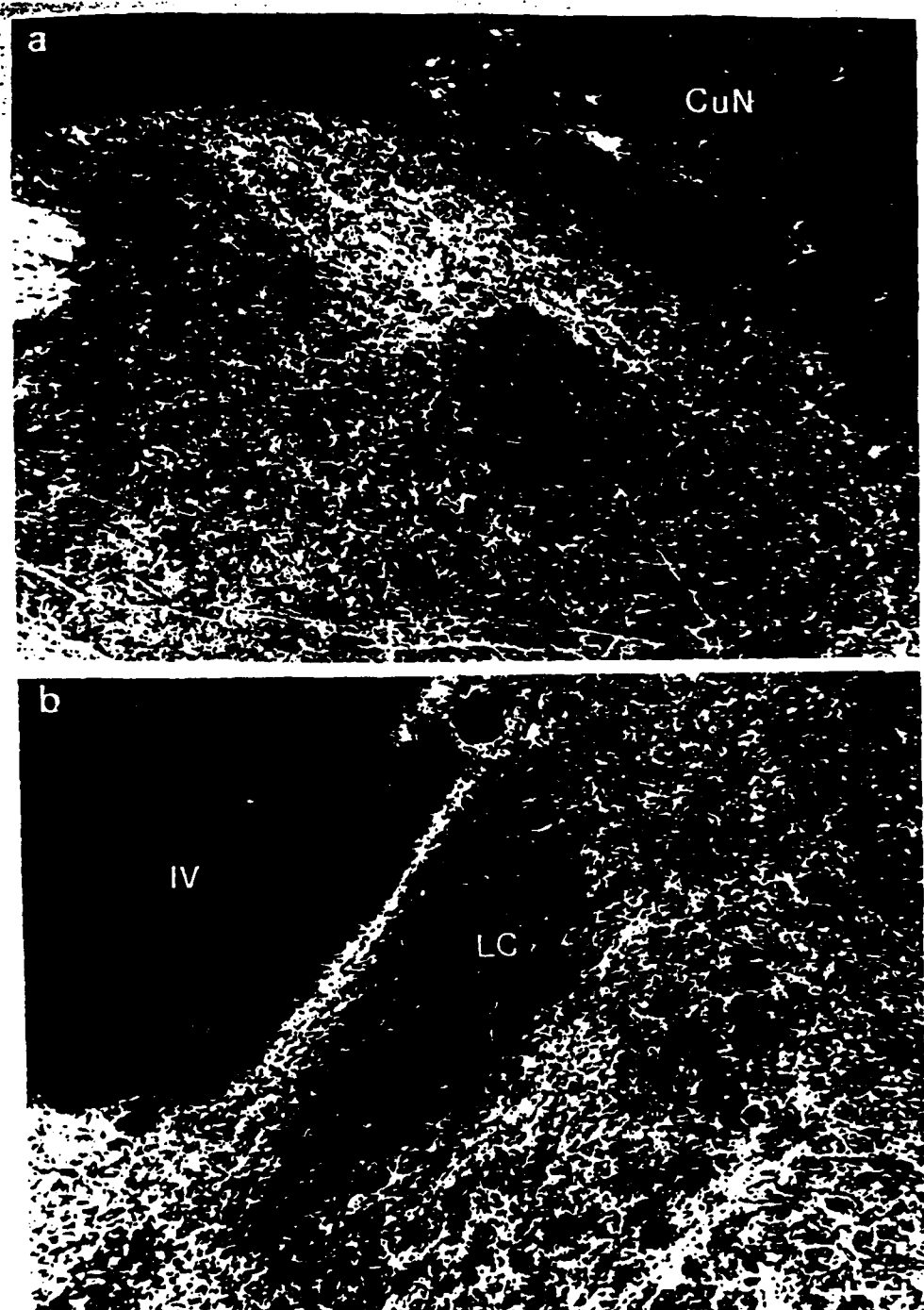


Fig. 16. Darkfield photomicrographs demonstrating clusters of punctate varicosities in the dorsolateral pons. In (a), note the terminal-like cluster in the dorsal-lateral subnucleus of the parabrachial complex (PBC) underlying the cuneiform nucleus (CuN). In (b), note the virtual absence of punctate varicosities in the locus ceruleus (LC) and the presence of terminals surrounding LC in the periventricular gray (medially), the nucleus subceruleus and the mesencephalic trigeminal nucleus, (ventrolaterally) and the medial parabrachial nucleus (dorsolaterally). Bar = 120 μ m.

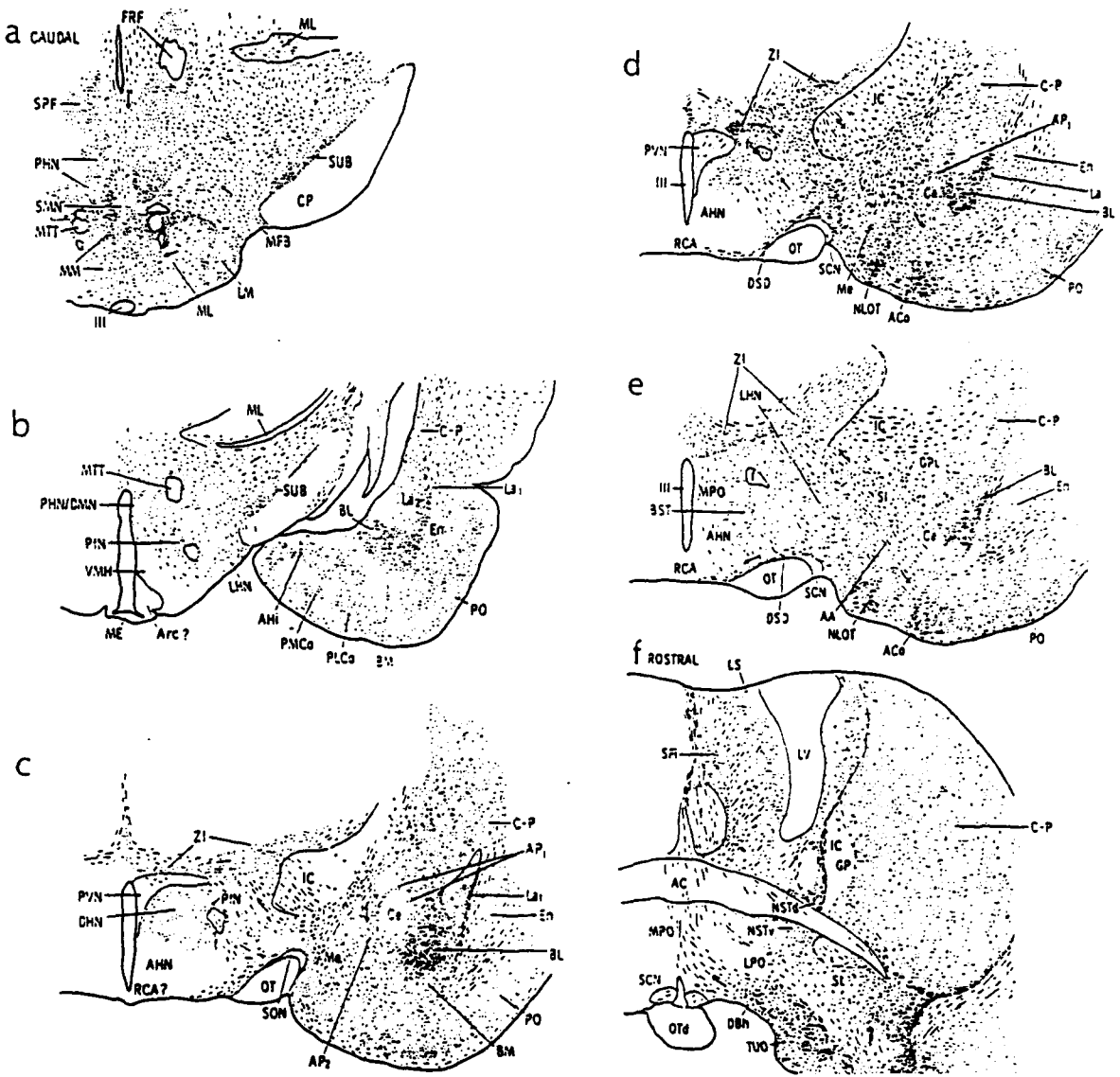


Fig. 17. Camera lucida drawings of ChAT-immunoreactive processes in the forebrain. In the hypothalamus, punctate varicosities (resembling terminal fields) outlined nuclei (or portions thereof) known to play a role in cholinergic regulation of arterial blood pressure and heart rate (e.g. the posterior and mammillary hypothalamic nuclei in drawing a. (a-f) That other forebrain areas may be involved is suggested by putative terminal fields in subparafascicular, dorsal, perifornical and lateral hypothalamic nuclei, the bed nucleus of the stria terminalis and amygdala. Functional specificity of cholinergic systems is reflected by the absence of terminals in several other autonomic control areas including the paraventricular and supraoptic nuclei (c-e), the medial preoptic area (e,f) and a central core region of the central nucleus of the amygdala (c-e) bounded by labeled processes in the pericentral groups AP₁ and AP₂ (as defined by Turner and Zimmer, 1984).

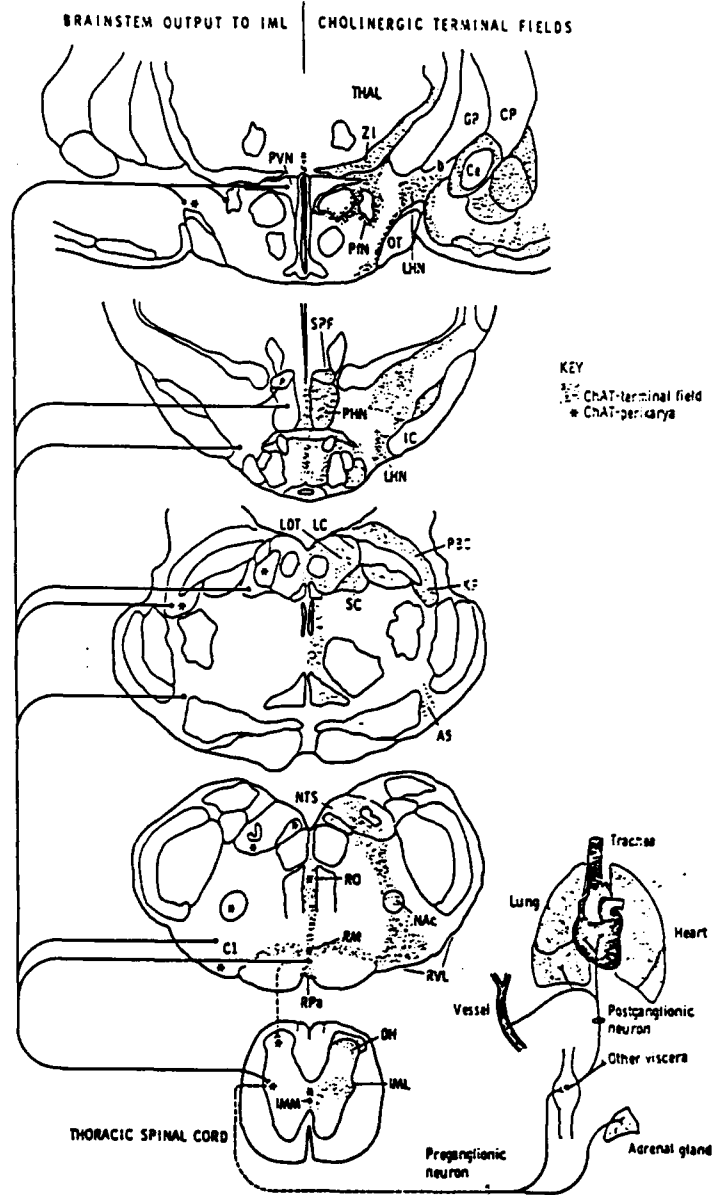


Fig. 18. Schematic diagram summarizing the potential neuroanatomical substrates of cholinergic autonomic regulation. Cholinergic terminal fields (right side) overlap nuclear subgroups which contain catecholamine- and neuropeptide-synthesizing neurons and project directly to the intermediolateral cell column (IML; left side) or cervico-thoracic respiratory lower motor neurons influencing breathing (not illustrated). Anatomical data support the idea that central cholinergic sympathoexcitatory mechanisms influencing arterial blood pressure and heart rate are mediated by bulbospinal fiber systems. In the forebrain, cholinergic terminals overlap several regions (for example, the amygdala) which project to brainstem autonomic nuclei and are thought to mediate preconditioned autonomic and behavioral responsiveness to emotionally arousing stimuli. Perhaps, such fields may contribute to central cholinergic provocation of the arousal/defense response. In this regard, terminals also overlap pre-thalamic and pre-cortical cell groups (for example, in the parabrachial complex and adjacent reticular formation) which are known to influence the sleep-wake cycle. New groups of cholinergic cell bodies (asterisks) were also found in several autonomic nuclei including those which project to the IML or respiratory lower motor neurons (nucleus raphe magnus, nucleus tractus solitarius, retroambigual area and rostral ventrolateral medulla). Double label experiments are in progress to determine whether cholinergic neurons in these cell groups project to the spinal cord.

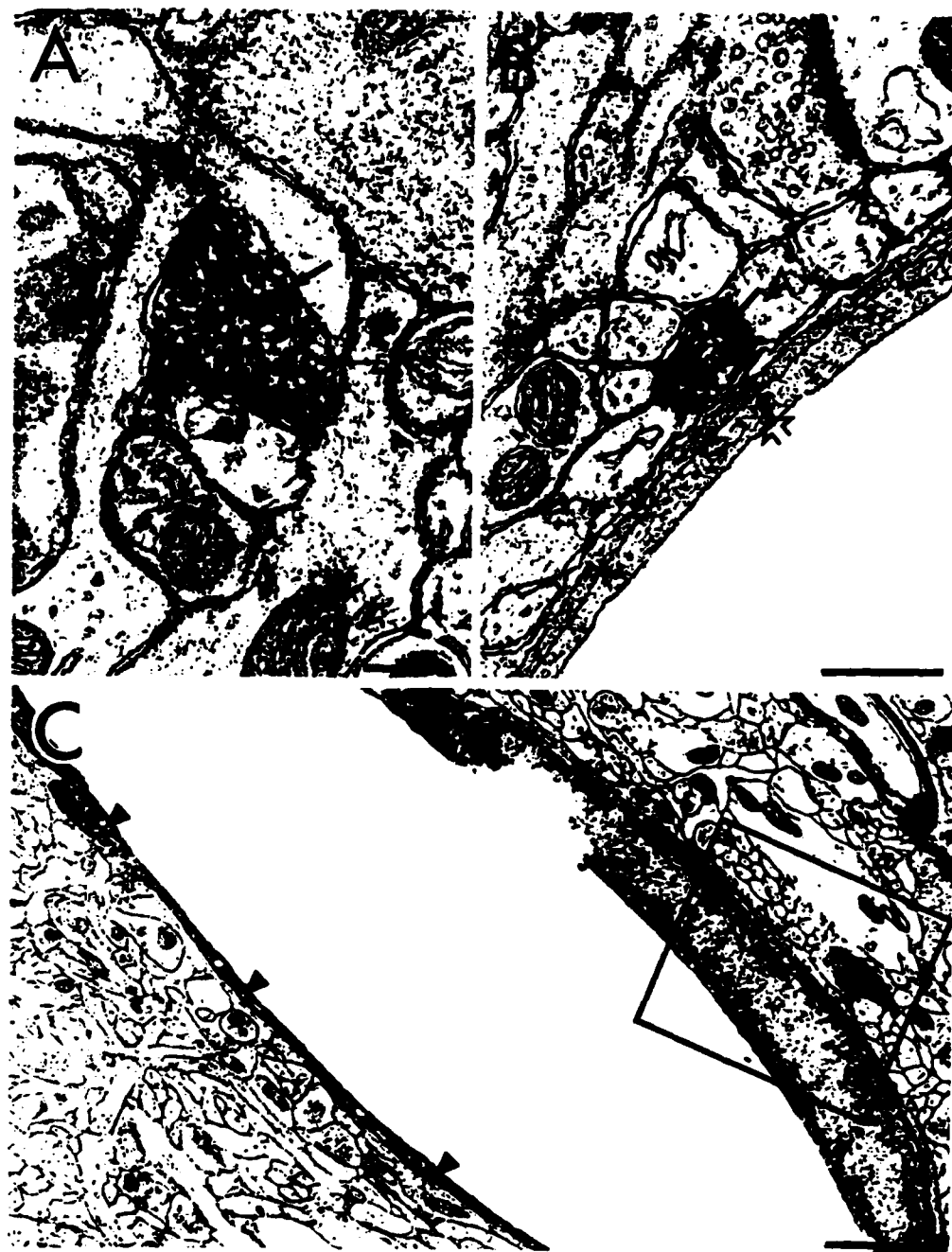


Fig. 19. Ultrastructural localization of ChAT-immunoreactive processes in layer III of the cerebral cortex. **A.** A ChAT-immunoreactive terminal (T) which contains numerous small clear vesicles (scv) and lacks a direct vascular association is shown. **B.** A ChAT-labeled axon (S) is found in close apposition (arrow) to the basal lamina of an unlabeled endothelial cell. The axon and basal lamina are actually separated by a very thin astrocytic lamina. Bar = 0.25 μ m. **C.** An endothelial cell (En) of a small capillary is immunoreactive for ChAT. The boxed area containing a ChAT-containing terminal is enlarged in Fig. 17A. Bar = 0.5 μ m.

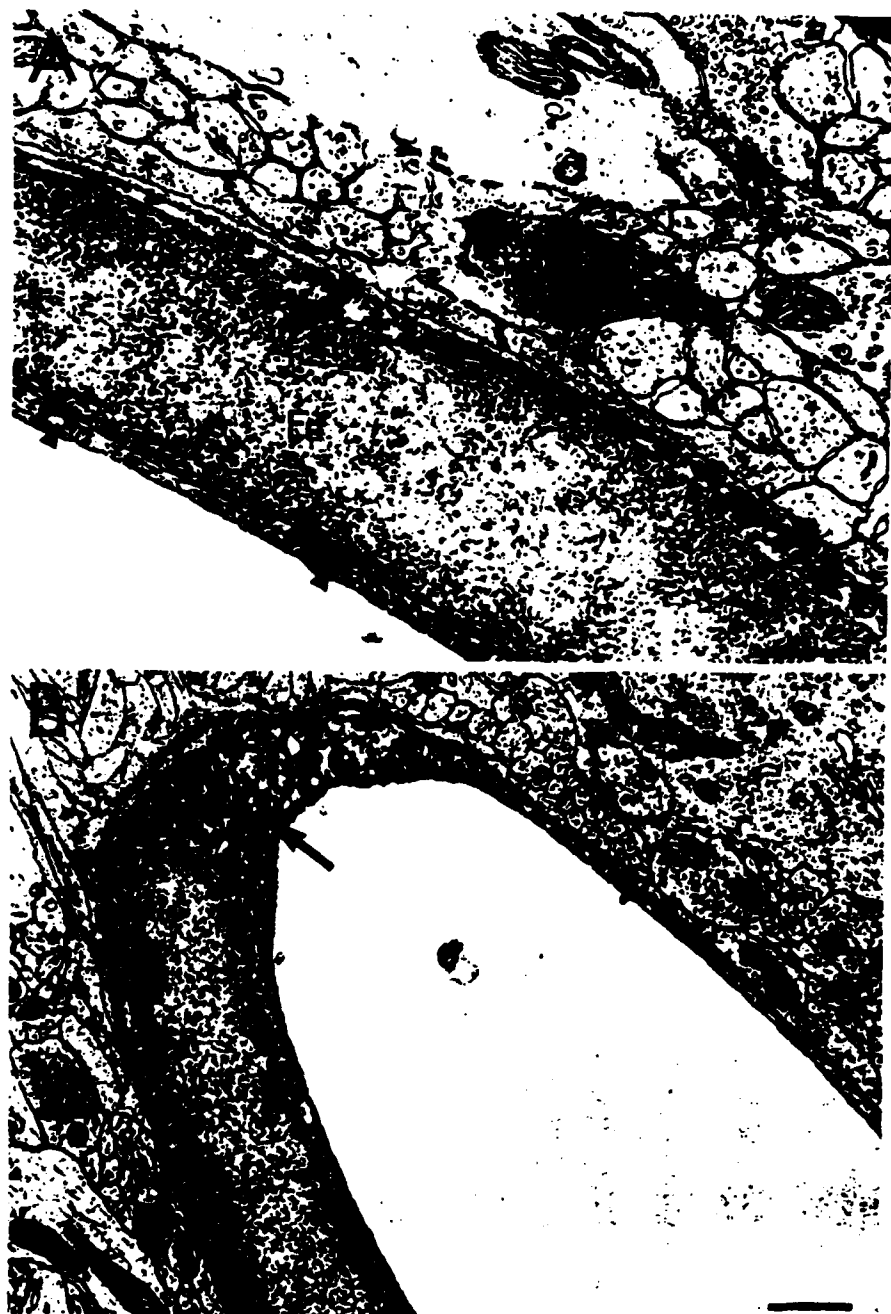


Fig. 20. Ultrastructural localization of a ChAT-immunoreactive axon terminals and endothelial cell from layer III of cerebral cortex. **A.** Higher magnification of the boxed area in Fig. 16C shows that the labeled terminal (T) which contains numerous small clear vesicles (scv) is separated from the basal lamina surrounding ChAT-labeled endothelial cell (arrowheads) by a thin astrocytic process (*). Bar = 0.25 μ m. **B.** A serial section of the endothelial cell (En) in Panel A showing the dense PAP reaction product in the cytoplasm (arrow). Bar = 0.25 μ m.

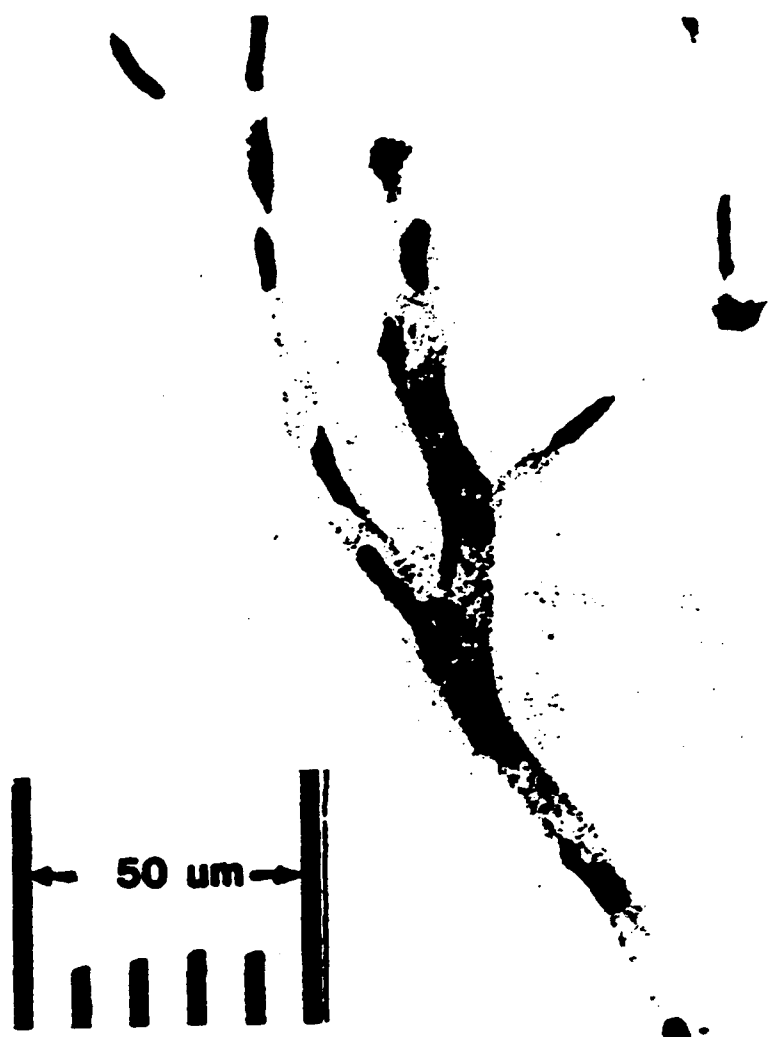


Fig. 21. Light microscopic photomicrograph of microvessels prepared from the cortex and stained with methylene blue.

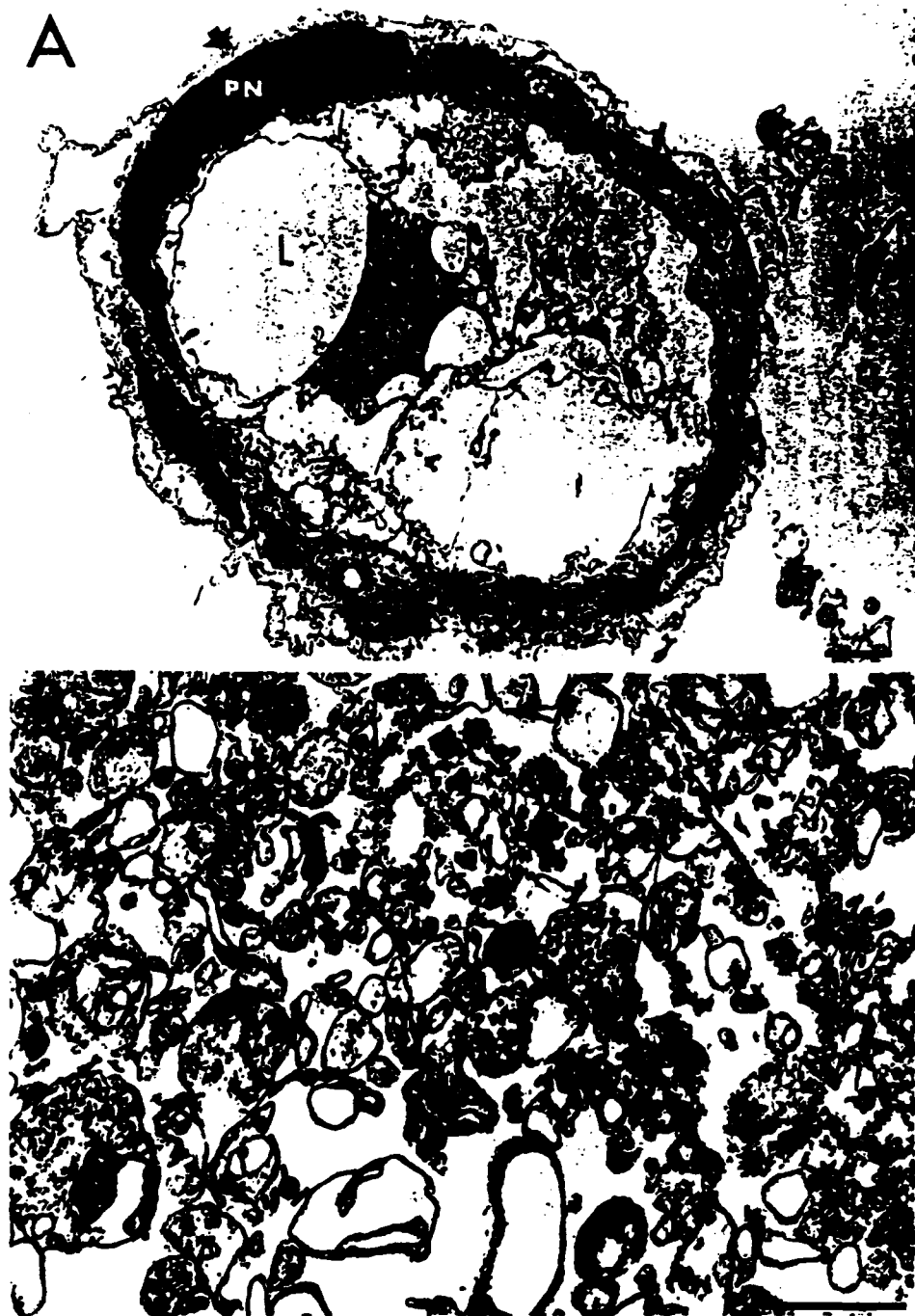


Fig. 22. *A.* An electron photomicrograph of a microvessel isolated from the cerebral cortex which details many of the cellular elements commonly attached to the abluminal side of the basal lamina. The arrow at the upper right indicates the basal lamina which surrounds the lumen (L) of the vessel. The solid arrow at the upper left indicates a pericyte and accompanying pericyte nucleus (PN). The open arrow at the lower left indicates the position of what may be either a pericyte process or smooth muscle cell. The assignment of the nomenclature for the morphological aspects of this photomicrograph is based on the report of Rennels and Nelson (1975). Bar = 1 μ m. *B.* An electron photomicrograph of the synaptosomal (P₂ fraction) preparation of the cerebral cortex. The arrow indicates an axon terminal with an adjoining postsynaptic density. Bar = 0.25 μ m.

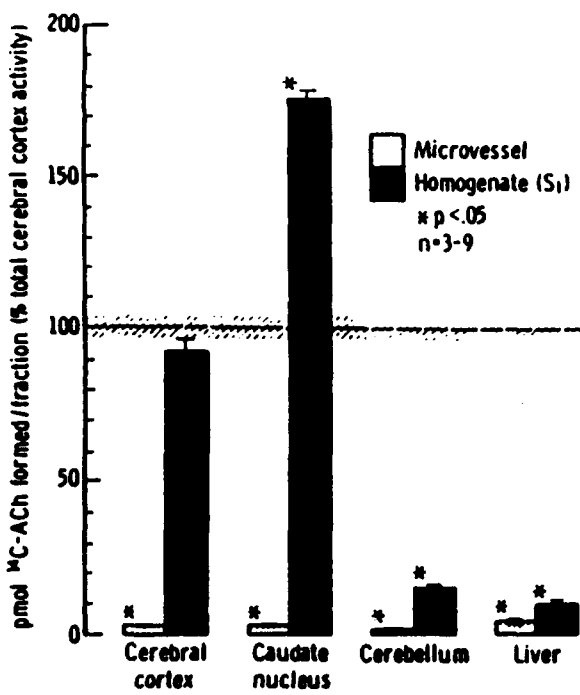
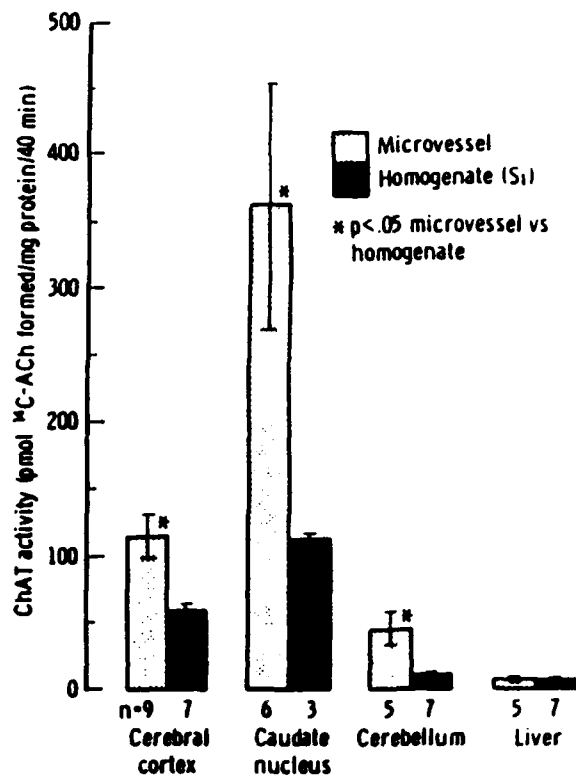
A**B**

Fig. 23. A. ChAT activity measured in different tissues and subcellular fractions when expressed as the absolute amount of [¹⁴C]ACh synthesized relative to the amount synthesized from a 100-mg (wet wt.) section of the cerebral cortex. Total enzyme activity was determined in the whole tissue homogenate after sonication of the tissue using the procedure indicated in the Methods section. Thus, the activity of ChAT in all cellular fractions of the cerebral cortex were assessed in the whole homogenate which served as a point of reference. Values are means \pm SEM; asterisks indicate that the value is significantly different from the cerebral cortex whole homogenate value, $P < 0.05$. **B.** The same data as in A, except now it represents ChAT activity from different tissues and subcellular fractions expressed as a specific activity (i.e., nmol [¹⁴C]ACh formed/mg protein/40 min). Values are means \pm SEM; asterisks indicate that the value is significantly increased above the nerve terminal fraction, $P < 0.05$.

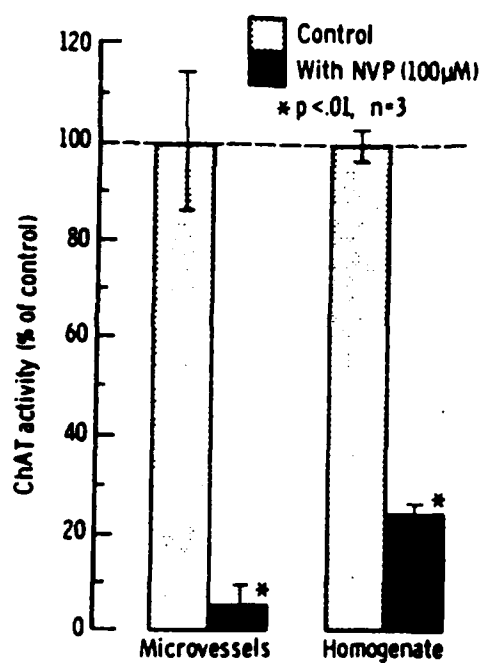


Fig. 24. The effect of the specific inhibitor of ChAT, 4-naphthylvinylpyridine (NVP, 100 μ M), to inhibit the formation of [14 C]ACh in cortical microvessels or nerve terminals. Values are means \pm SEM; asterisks indicate that the value is significantly different from control, $P < 0.01$.

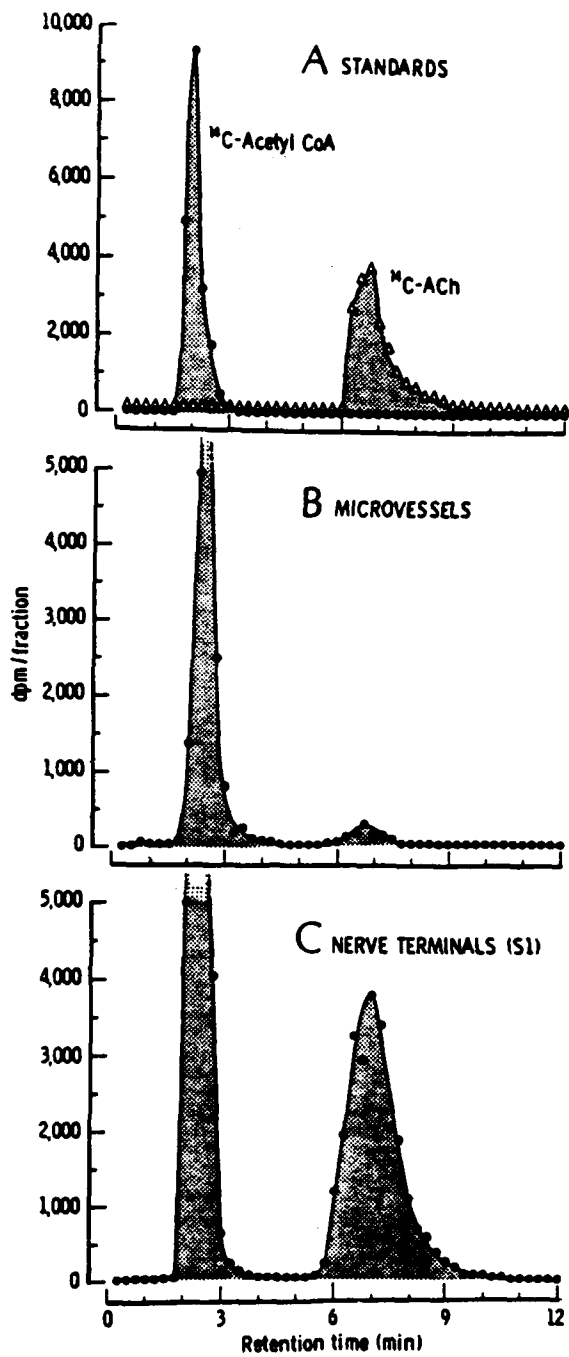


Fig. 25. Representative chromatographs depicting the separation of [¹⁴C]acetyl CoA and [¹⁴C]ACh by the use of HPLC analysis. Peaks were detected by counting 15-s fractions with liquid scintillation spectroscopy. A. Standards containing known quantities of [¹⁴C]acetyl CoA and [¹⁴C]ACh were injected, and the observed retention times are shown. B. the formation of a small quantity of radioactive product produced from cortical microvessels that co-chromatographs with the [¹⁴C]ACh standard is shown. C. As expected, even more product that co-chromatographs with the [¹⁴C]ACh standard is produced by the fraction containing cholinergic nerve terminals (S₁).

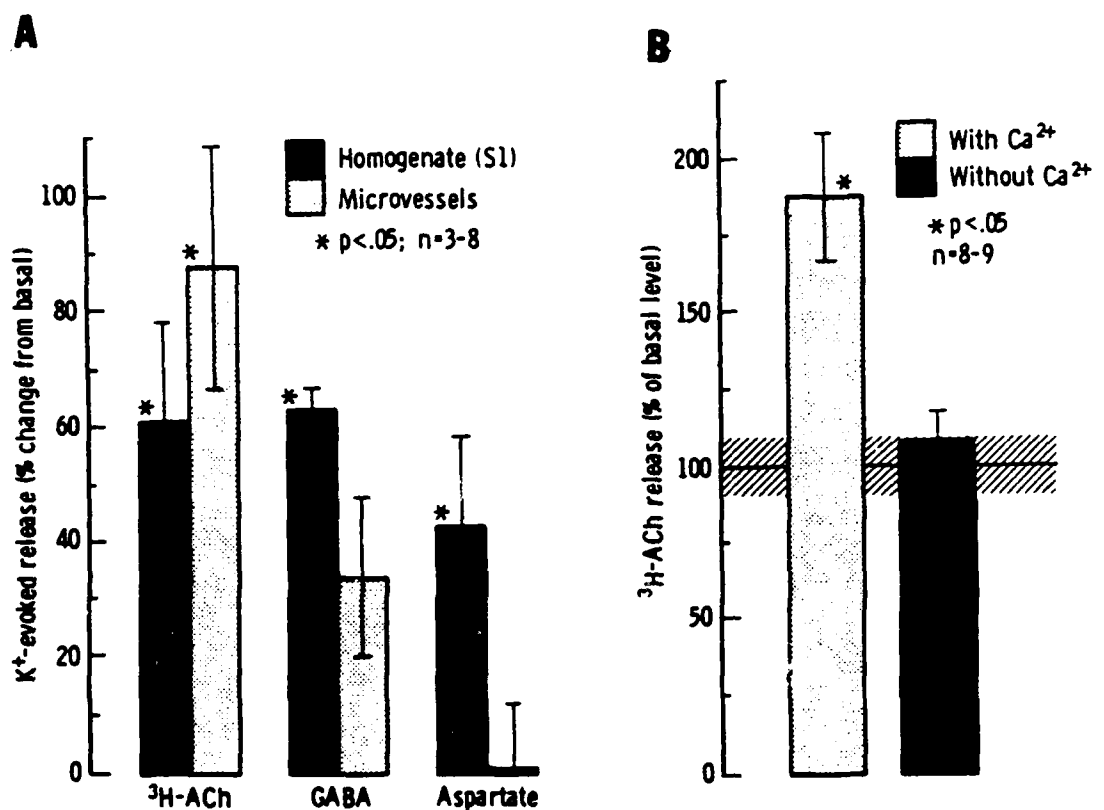


Fig. 26. A. The release of 3H ACh, GABA and Asp evoked by 55 mM K^+ in the presence of 1.2 mM Ca^{2+} , from cerebral cortical microvessels (MV) and nerve terminals (S₁). B. The effect of removing extracellular Ca^{2+} on the release of 3H ACh evoked by 55 mM K^+ from cerebral cortical microvessels. Values are means \pm SEM; asterisks indicate that the value is significantly elevated above the spontaneous release value, $P < 0.05$.

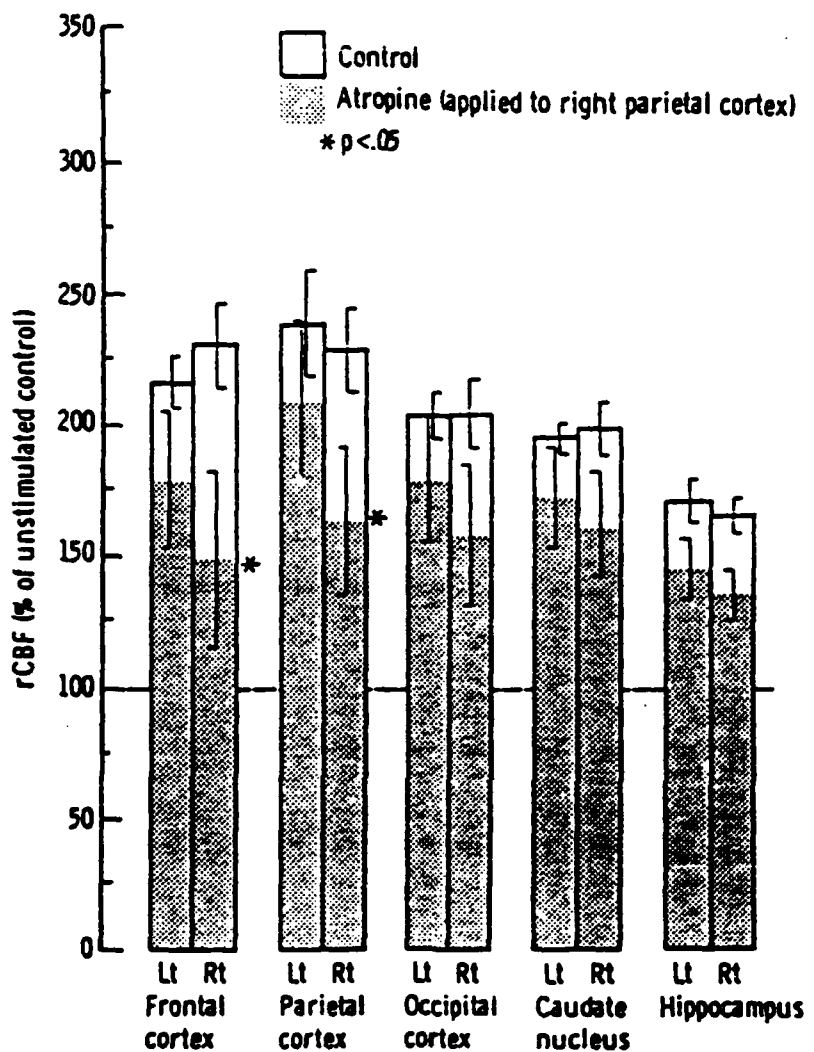


Fig. 27. Effect of atropine sulfate (100 μ M) applied to the right parietal cortex (vehicle to left) on the increases in rCBF elicited by electrical stimulation of the FN. FN stimulation increased rCBF symmetrically (paired t-test, right to left; $P > 0.05$) and significantly (ANOVA, $P < 0.01$, $n = 11$) as compared to unstimulated controls ($n = 6$). Note that atropine applied 20 min prior to rCBF measurement attenuated by 59% the FN-elicited increase in rCBF in the frontoparietal CX region without affecting rCBF in other adjacent areas ($n = 5$, $P < 0.05$). Values are means \pm SEM.

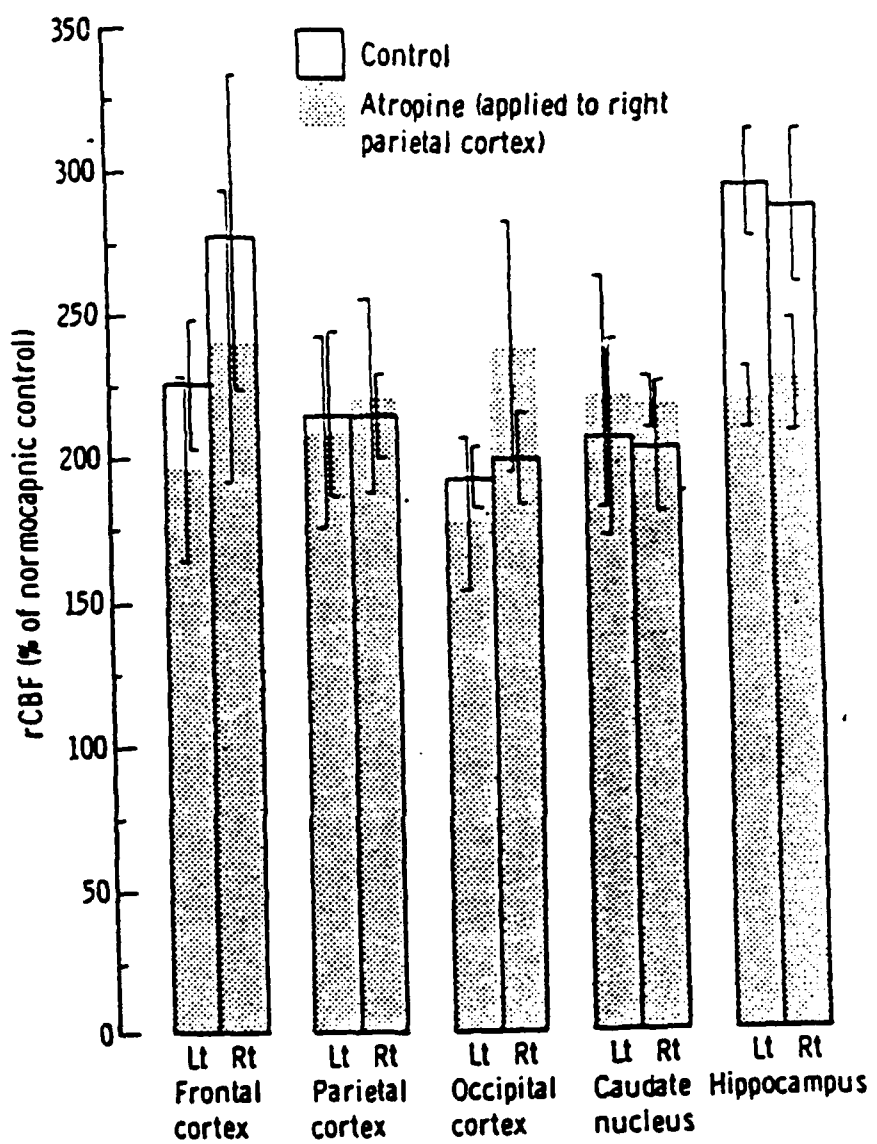


Fig. 28. Effect of atropine sulfate (100 μ M) applied to the right parietal cortex on CO_2 -elicited increases in rCBF. Arterial pCO_2 was elevated with 5% CO_2 inhalation to 59.0 ± 1.4 mm Hg in 5 rats, which increased rCBF to a similar level obtained by FN stimulation. However, atropine applied 20 min prior to rCBF measurement did not significantly affect the cortical cerebrovasodilation produced by hypercarbia ($P > 0.05$). Values are means \pm SEM.

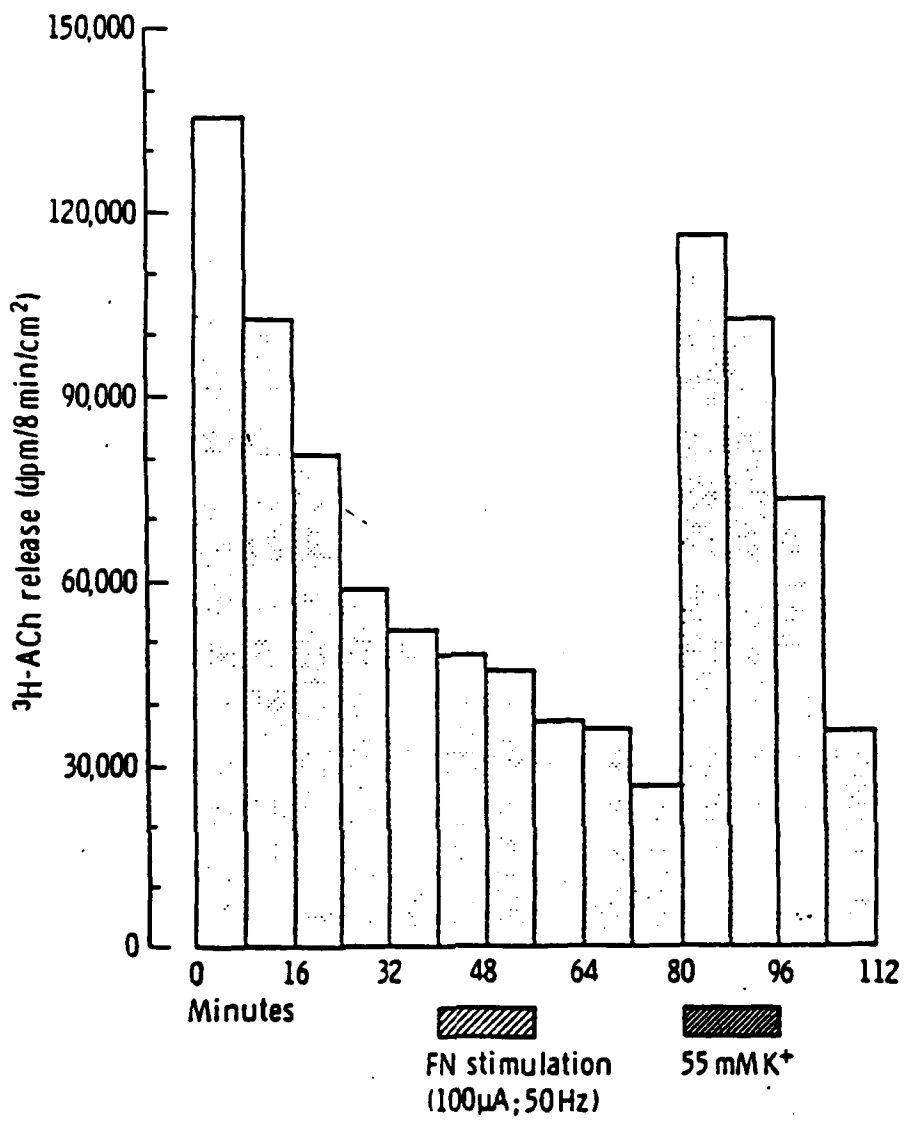


Fig. 29. A representative experiment showing the effect of electrical stimulation of the fastigial nucleus or potassium depolarization on the release of [³H]ACh from the parietal CX of anesthetized, paralyzed and artificially ventilated rats.

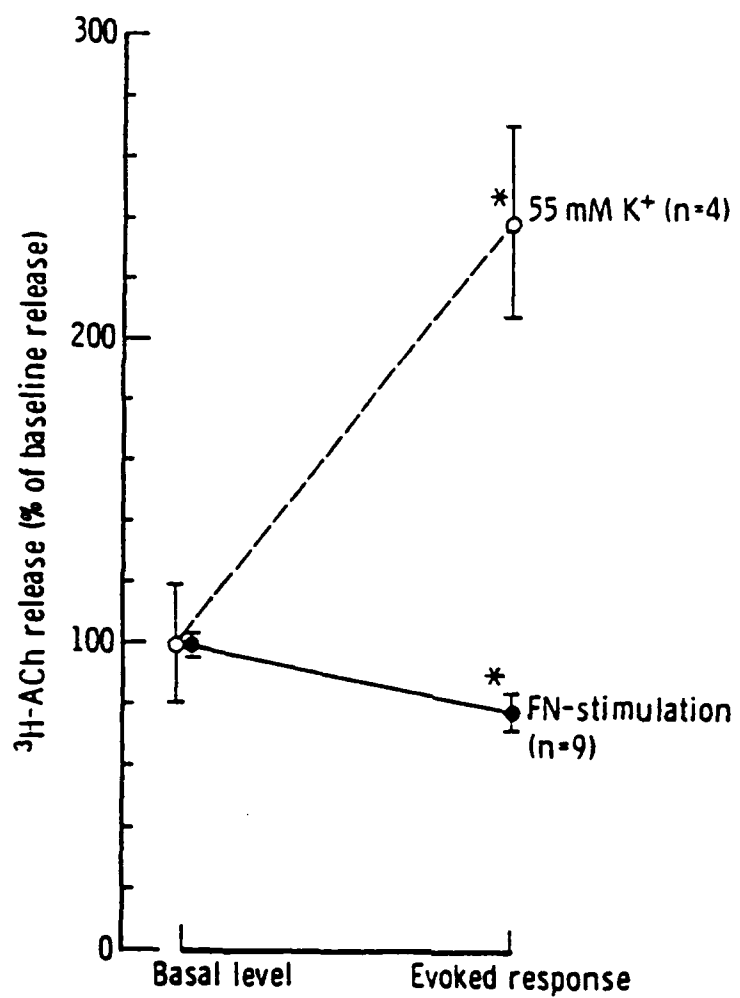


Fig. 30. Grouped data demonstrating the effect of potassium depolarization (55 mM) or electrical stimulation of the FN on the release of [³H]ACh from the parietal CX of anesthetized (chloralose), paralyzed and artificially ventilated rats. Values are means \pm SEM; *, significantly different from basal control values ($P < 0.05$).

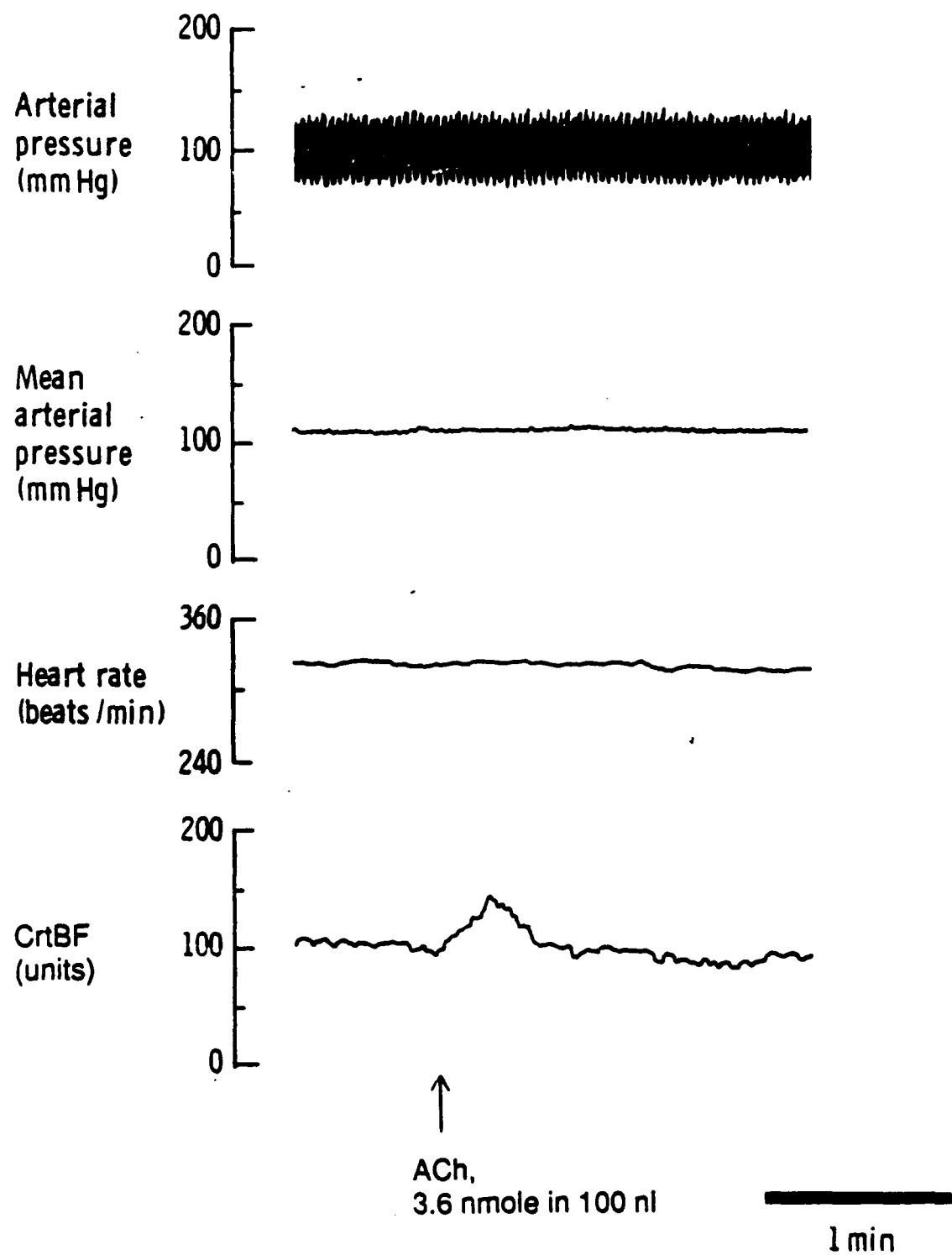


Fig. 31. Cardiovascular and cortical blood flow (CrtBF) responses to acetylcholine (ACh) microinjection into the parietal cortex.

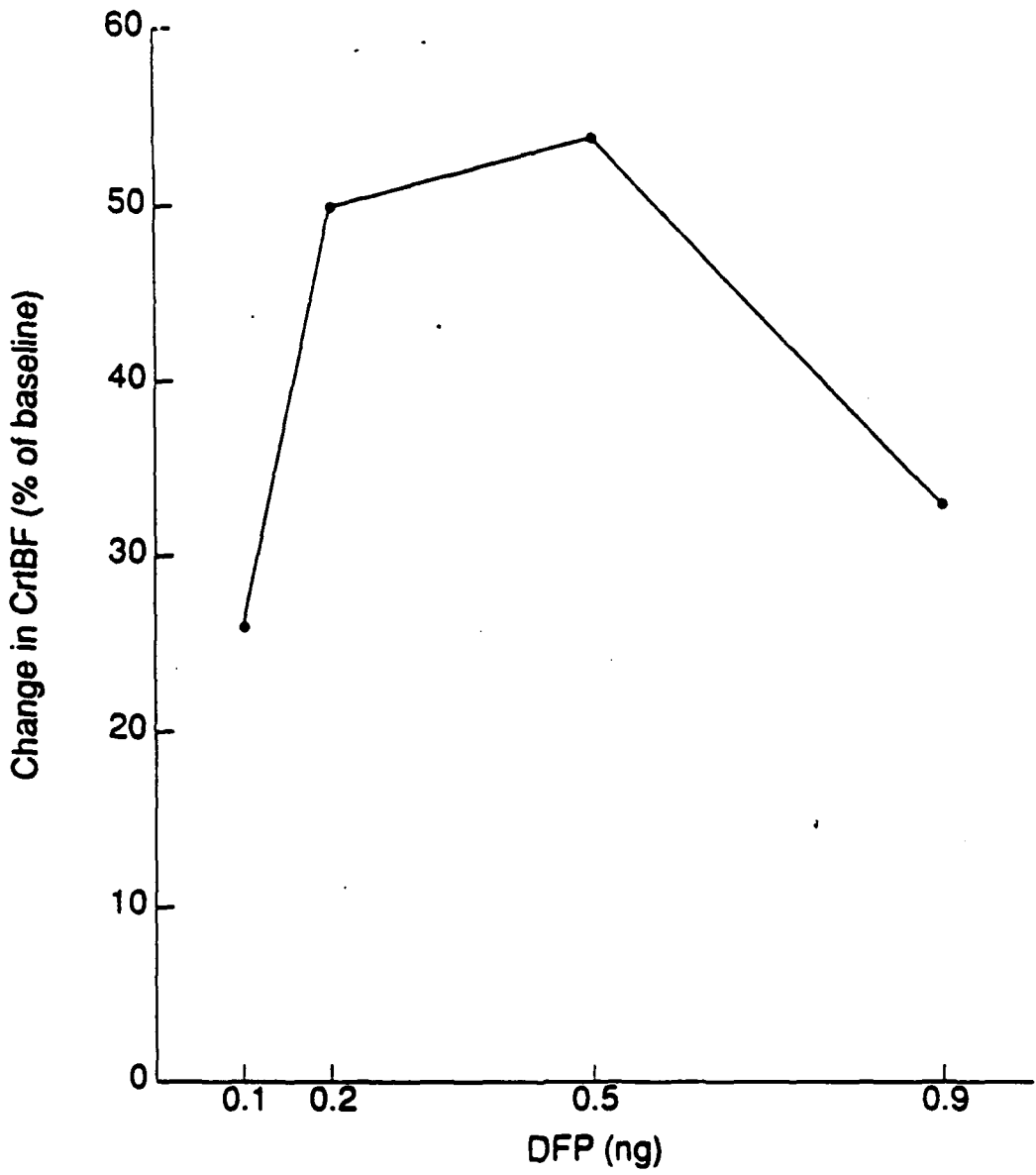


Fig. 32. Change in cortical blood flow (CrtBF) elicited by local microinjection of diisopropyl phosphofluoridate.

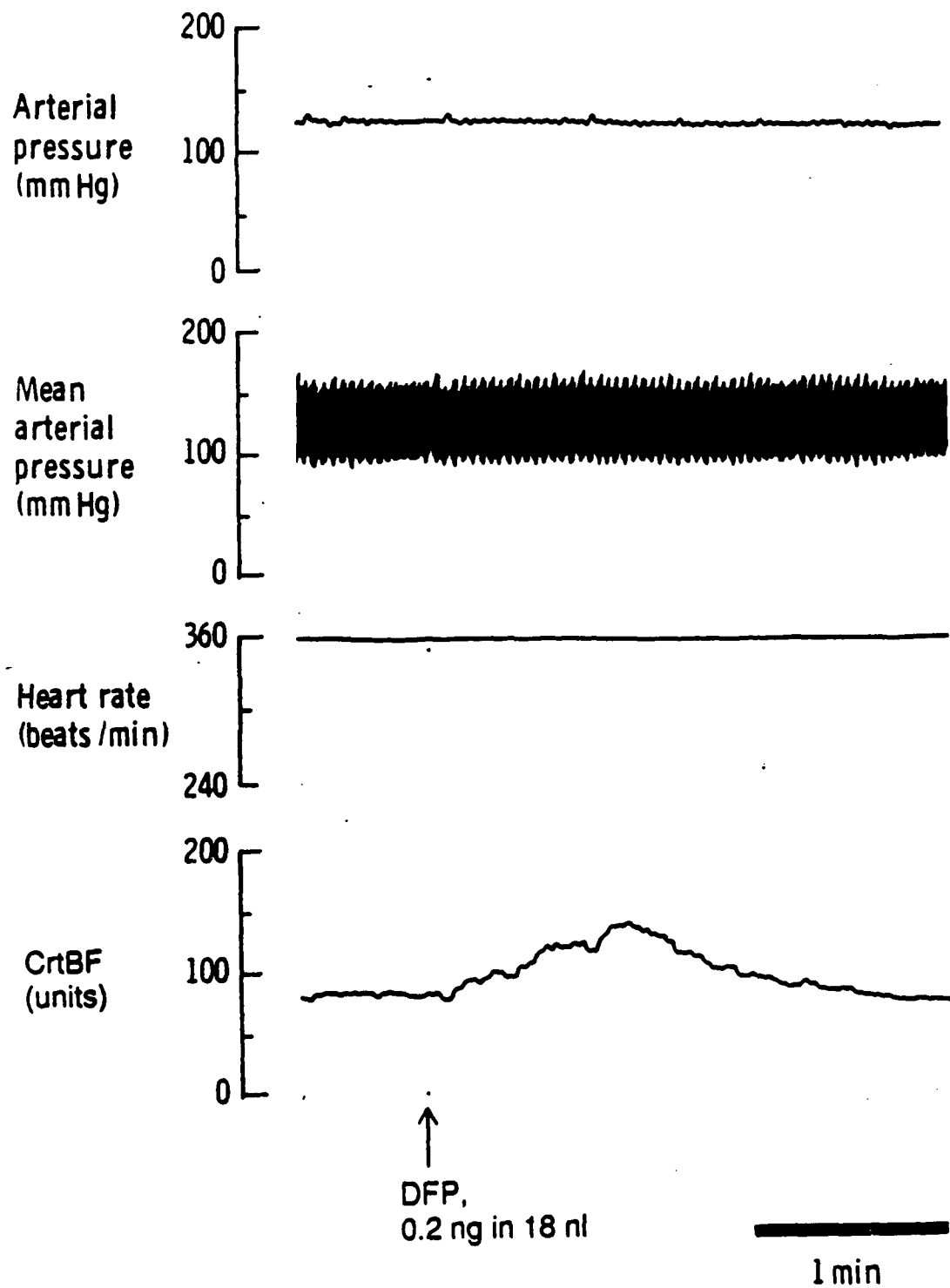


Fig. 33. Cardiovascular and cortical blood flow (CrtBF) responses to diisopropyl phosphofluoridate (DFP) microinjection into the parietal cortex.

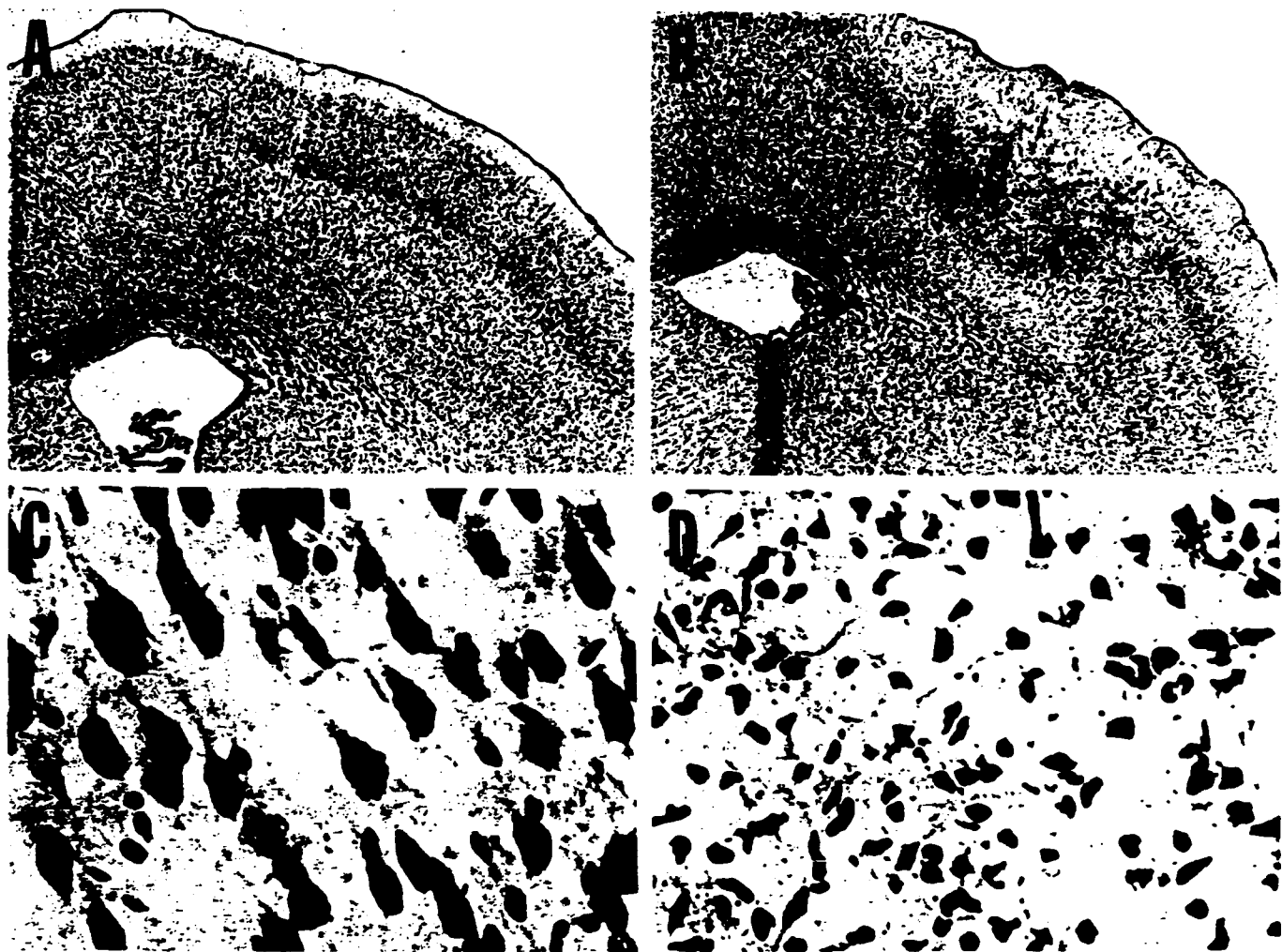


Fig. 34. Photomicrographs illustrating effects of microinjection of excitotoxin ibotenic acid ($10 \mu\text{g}/1\mu\text{l}$) in primary sensory cortex (Sml) of rat. **A.** Low power (x24) view of Sml in sham-lesioned controls. Note typical laminar pattern (Nissl stain). **B.** Sml 5 days after local microinjection of ibotenic acid. Note well-demarcated disruption of laminar pattern and marked increase in cellular density in center of lesion (Nissl stain; magnification as in **A**). **C.** Higher-power view (x450) of Sml in sham-operated controls. Note, among other neurons, medium-size and large pyramidal neurons of lamina 5b (Nissl stain). **D.** Sml, at same level as in **C**, 5 days after local microinjection of ibotenic acid. Note absence of neurons and marked increases in number of nonneuronal cells. These cells do not have morphological characteristics of neurons as they appear on Nissl-stained sections (Nissl stain; magnification in **C**).

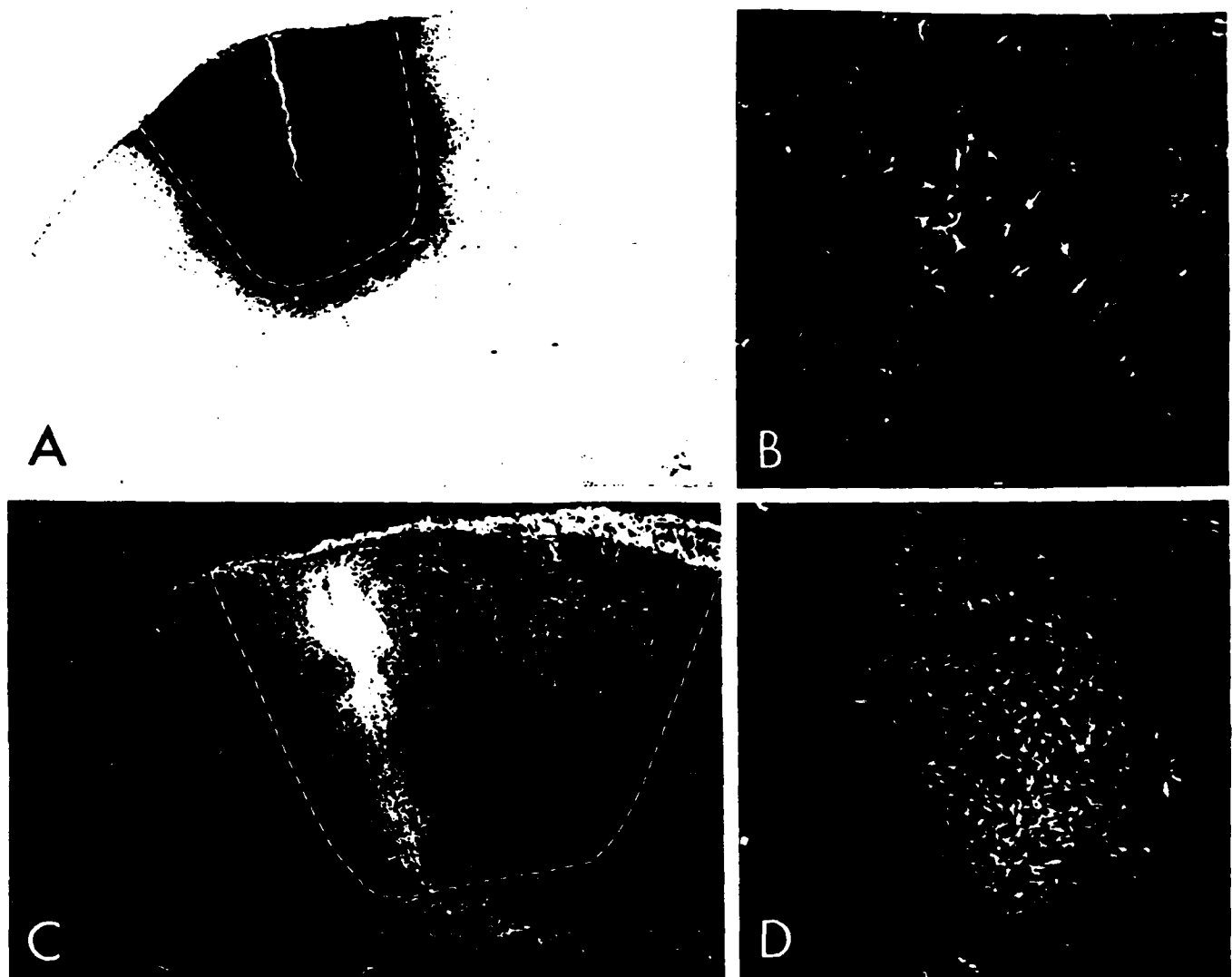


Figure 35. Anterograde and retrograde transport of wheat germ agglutinin conjugated with horseradish peroxidase (WGA-HRP), into and from area of lesion, 5 days after microinjection of ibotenic acid in primary sensory cortex of rat; **A.** microinjection of WGA-HRP (30 nl of 2% solution in H_2O) confined to area of lesion (*broken line*). **B.** Retrograde transport of WGA-HRP from area of lesion (see A for injection site). Note cells densely labeled with reaction product in medial part of globus pallidus, a major source of projections to area of cortex involved by lesion. **C.** Anterograde transport of WGA-HRP into lesion (*broken line*). Tracer was injected into contralateral primary sensory cortex. Note densely labeled fibers traveling into corpus callosum, entering lesions and giving rise to a dense terminal field within dorsolateral part of area of lesion. **D.** Retrograde transport of WGA-HRP from lesion into ventrobasal nucleus of thalamus, another major source of neural input to cortex involved by lesion.

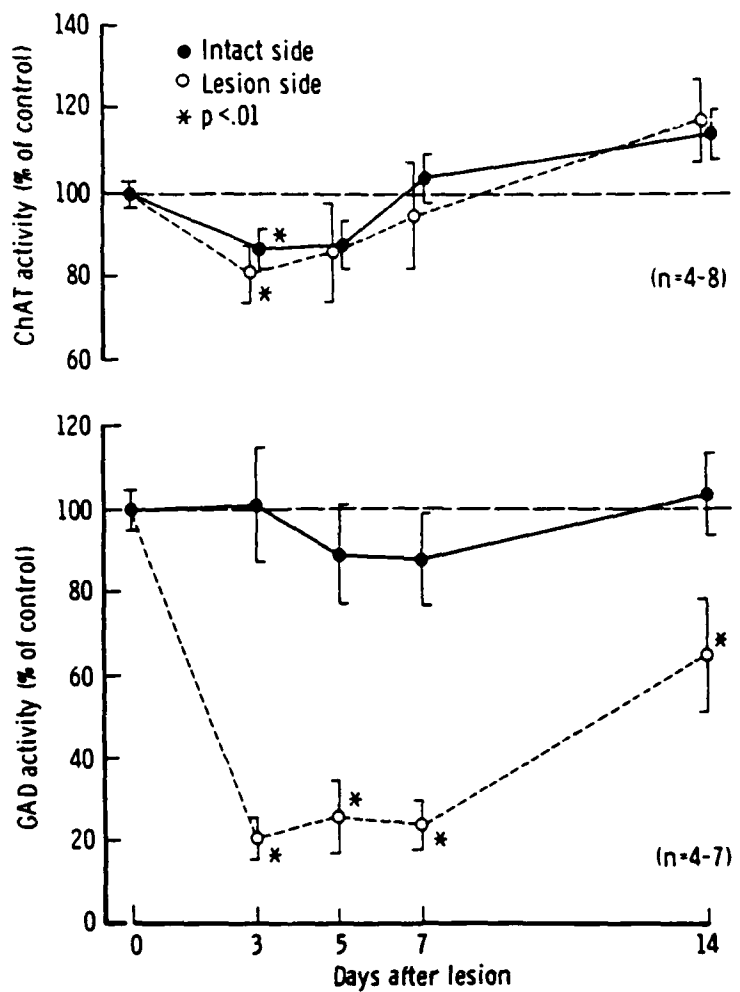


Fig. 36. Time course of activity of choline acetyltransferase (ChAT) (top) and glutamic acid decarboxylase (GAD) (bottom) within lesions of primary sensory cortex produced by excitotoxin ibotenic acid. Values are means \pm SE and are expressed as percent of sham-lesioned controls. *Top:* within lesion (open circles), activity of ChAT, a marker of cholinergic fibers and terminals, declines slightly at day 3 ($P < 0.01$; analysis of variance and Duncan's new multiple range test), but by day 5 values are not different from sham-lesioned controls ($P > 0.05$). In contralateral homotopic cortical area (closed circles) ChAT activity follows a similar time course. *Bottom:* within lesion, GAD activity, a marker of local GABA-ergic neurons, declines dramatically by 3 days after microinjection of ibotenic acid ($P < 0.01$) and remains significantly reduced throughout time period studied.

TABLE 1

Mean Arterial Pressure (MAP), pH and Arterial Blood Gases in Rats Examined

<u>UNOPERATED</u>	<u>VEHICLE</u>	<u>ATROPOINE</u>	<u>UNSTIMULATED</u>		<u>PIN-STIMULATION</u>		<u>HYPERCARBIA</u>	
			<u>VEHICLE</u>	<u>ATROPOINE</u>	<u>VEHICLE</u>	<u>ATROPOINE</u>	<u>ATROPOINE</u>	
MAP (mmHg)	124 ± 11	124 ± 6	136 ± 4	134 ± 2	130 ± 5	130 ± 5	110 ± 6	
pO ₂ (mmHg)	409 ± 14	429 ± 19	431 ± 20	427 ± 10	409 ± 21	409 ± 21	408 ± 30	
pCO ₂ (mmHg)	34.8 ± 0.5	35.7 ± 0.5	34.9 ± 1.0	36.5 ± 0.5	36.6 ± 0.9	36.6 ± 0.9	39.0 ± 1.4*	
pH	7.42 ± 0.02	7.41 ± 0.02	7.41 ± 0.01	7.32 ± 0.02*	7.32 ± 0.01*	7.32 ± 0.01*	7.24 ± 0.01*	
N	6	6	4	11	5	5	5	

Values represent means ± S.E.M.; animals are anesthetized, paralyzed and artificially ventilated with 100% O₂;

* p < 0.05, significantly different from unoperated control.

TABLE 2

pH, pCO₂ and pO₂ of Buffer Solutions Applied to the Parietal Cortex of Rats with and without PN-stimulation or with Hypercarbia.

	UNSTIMULATED			PN-STIMULATION			HYPERCARBIA					
	VEHICLE		ATROPINE		VEHICLE		ATROPINE		ATROPINE			
	R	L	R	L	R	L	R	L	R	L		
pH	7.40 ± 0.05	7.46 ± 0.00	7.39 ± 0.05	7.38 ± 0.05	7.36 ± 0.05	7.35 ± 0.04	7.54 ± 0.05	7.39 ± 0.07	7.63 ± 0.09	7.58 ± 0.09		
pCO ₂ (mmHg)	R	L	32.7 ± 4.2	33.7 ± 3.8	33.9 ± 1.6	33.9 ± 1.5	31.9 ± 1.6	31.8 ± 1.6	25.8 ± 6.0	32.9 ± 5.1	21.8 ± 3.1*	20.5 ± 2.0*
pO ₂ (mmHg)	R	L	428 ± 77	425 ± 78	490 ± 36	508 ± 35	414 ± 49	410 ± 49	394 ± 67	463 ± 77	373 ± 72	384 ± 50
N	6	4	11	11	5	5	5	5	5	5		

(a) Values are means ± S.E.M.; * p < 0.05, significantly different from corresponding vehicle, unstimulated control (ANOVA).

(b) Buffer solutions were bubbled with 95% O₂: 5% CO₂, the above values determined and the solution applied to the parietal cortex. Solutions were continuously bubbled with 95% O₂: 5% CO₂ following application to the cortex.

(c) Atropine sulfate (100 uM) applied to right parietal cortex.

(d) No right-to-left differences with any treatment (p > 0.05; paired t-test).

TABLE 3

Effect of atropine sulfate (0.3 mg/kg i.v.) on the minimal current required to elevate arterial pressure (AP) (threshold current) (mean \pm SEM) and on the elevation in AP and heart rate (HR) produced by stimulation of the fastigial nucleus (FN Stim) in anesthetized rat.

	<u>Before atropine</u>			<u>After atropine</u>		
	<u>Resting</u>	<u>FN Stim[†]</u>	Δ	<u>Resting</u>	<u>FN Stim[†]</u>	Δ
AP (mmHg)	128 \pm 4	206 \pm 7*	78	131 \pm 6	211 \pm 10*	80
HR (bpm)	430 \pm 8	529 \pm 2*	99	505 \pm 6*	539 \pm 7*	34#
Threshold current (μ A)	—	21 \pm 5		—	20 \pm 2	

†FN Stim at 50 Hz and 5x threshold current

*p < 0.001 (paired t-test), from resting

p < 0.005 from corresponding Δ before atropine

n = 5

TABLE 4

Effect of stimulation of the fastigial nucleus (FN) on rCBF (mean \pm S.E.M.) with and without administration of atropine (0.3 mg/kg i.v.)

Region	rCBF (ml/100 g x min)					
	Unstimulated			FN Stimulation		
	Untreated	Atropine	Untreated	% of Cont.	Atropine	% of Cont.
Medulla	80 \pm 4	83 \pm 7	127 \pm 11	159**	92 \pm 3	111
Cerebellum	84 \pm 8	92 \pm 6	110 \pm 5	131*	104 \pm 4	113
Pons	81 \pm 5	85 \pm 7	123 \pm 9	152**	98 \pm 4	115
Inferior colliculus	111 \pm 9	117 \pm 8	135 \pm 9	122	124 \pm 5	106
Superior colliculus	106 \pm 7	104 \pm 9	130 \pm 10	123*	105 \pm 4	101
Hypothalamus	98 \pm 4	98 \pm 10	119 \pm 7	121*	97 \pm 3	99
Thalamus	86 \pm 1	90 \pm 9	141 \pm 15	164**	103 \pm 6	114
Hippocampus	77 \pm 5	79 \pm 7	108 \pm 12	140*	82 \pm 5	104
Caudate nucleus	84 \pm 4	89 \pm 8	127 \pm 16	151**	90 \pm 7	101
Frontal cortex	84 \pm 4	99 \pm 9	207 \pm 42	246**	105 \pm 9	106
Parietal cortex	88 \pm 6	108 \pm 9	182 \pm 32	207**	120 \pm 10	111
Occipital cortex	79 \pm 6	95 \pm 8	127 \pm 20	161*	110 \pm 15	116
Corpus callosum	54 \pm 3	61 \pm 6	82 \pm 9	152*	61 \pm 4	100

*p < 0.05, **p < 0.01, analysis of variance and Newman-Keuls test

*Differences between groups not significant (p > 0.05)

TABLE 5

Enrichment of γ -glutamyltranspeptidase and alkaline phosphatase activities in vascular fractions as compared to nerve terminals (S₁) fractions.

Values are means \pm SEM; n=3.

	γ -Glutamyltranspeptidase (μ mol/mg protein/min)		Alkaline phosphatase (nmol/mg protein/min)	
	Cerebral cortex	Caudate nucleus	Cerebral cortex	Caudate nucleus
Microvessels	3.7 \pm 0.5	17.5 \pm 4.4	85 \pm 25	665 \pm 90
Homogenate (S ₁)	0.6 \pm 0.1	0.6 \pm 0.1	30 \pm 10	30 \pm 5
Ratio	6.2	29.2	2.8	22.2

TABLE 6

Rank ordering of the spontaneous release of putative neurotransmitters from cerebral cortex microvessels or homogenates.

Values are means \pm SEM (pmol/mg protein/5 min). Release was measured in the presence of 5 mM K⁺ and 1.2 mM Ca²⁺.

Microvessels: (n = 5-8)	Glycine 68.3 \pm 5.3	>	Aspartate 10.7 \pm 1.4	>	GABA 3.7 \pm 0.9	>>	ACh 0.29 \pm 0.05
Homogenate (S ₁): (n = 3)	GABA 35.1 \pm 4.6	>	Glycine 22.3 \pm 1.2	>	Aspartate 16.6 \pm 2.9	>>	ACh 1.0 \pm 0.05

LCBF, ml·100 g⁻¹·min⁻¹

	Unstimulated		FN Stimulated			Hypercapnia			
	Sham ^a (n = 6)	Lesioned ^a (n = 7)	Sham (n = 7)	% of Control	Lesioned (n = 6)	% of Control	Lesioned (n = 5)	% of Control ^b	
<i>Cerebral cortex</i>									
Lesion	L	121±6	113±25	239±15	197 ^c	137±9	122 ^c	372±78	330
Contralateral	R	117±5	123±7	239±13	203 ^c	211±11	171 ^c	403±65	327
Frontal	R	123±8	120±4	227±17	184 ^c	217±15	181 ^c	473±44	396
Parietal	L	117±8	112±4	232±20	197 ^c	194±17	173 ^c	465±65	415
R	120±16	114±4	229±8	190 ^c	199±16	174 ^c	386±72	337	
Auditory	L	119±15	112±3	223±14	188 ^c	179±13	160 ^c	369±74	329
R	118±21	111±6	224±19	189 ^c	176±12	159 ^c	348±77	314	
Visual	L	114±13	107±5	210±20	184 ^c	156±14	146 ^c	353±89	331
R	107±10	98±4	187±8	175 ^c	162±14	165 ^c	345±80	352	
	L	105±10	94±5	176±12	167 ^c	148±14	158 ^c	332±87	354
<i>Basal ganglia</i>									
Caudate putamen	R	106±8	98±6	193±11	182 ^c	196±10	200 ^c	441±82	452
Globus pallidus	R	106±8	89±5	178±5	168 ^c	182±10	204 ^c	428±89	480
Amygdala	L	74±5	76±8	117±11	158 ^c	135±8	177 ^c	260±36	340
R	67±8	67±6	111±13	165 ^c	120±7	177 ^c	253±48	365	
Preoptic n. magnocellularis	L	91±6	79±7	125±10	136 ^c	135±9	170 ^c	349±68	440
R	87±6	77±9	128±15	147 ^c	125±10	161 ^c	344±42	446	
	R	108±6	93±5	156±10	145 ^c	145±6	157 ^c	393±57	424
	L	108±4	89±6	163±11	151 ^c	145±9	162 ^c	403±59	452
<i>Thalamus</i>									
Anterior	R	118±10	105±6	244±9	207 ^c	197±12	188 ^c	478±55	457
Reticular	L	113±7	107±5	232±6	205 ^c	193±15	181 ^c	454±63	425
Ventral	R	78±9	77±2	157±7	200 ^c	152±8	197 ^c	361±68	467
L	83±9	77±3	163±7	196 ^c	146±8	190 ^c	364±65	475	
Ventromedial	L	100±5	99±3	196±14	195 ^c	170±8	173 ^c	429±68	435
R	98±6	101±4	198±16	201 ^c	158±7	156 ^c	416±74	410	
Intralaminar	L	113±8	96±6	198±11	176 ^c	189±10	197 ^c	447±64	468
	R	112±9	97±5	212±12	189 ^c	179±9	184 ^c	434±69	446
	L	103±8	98±4	214±10	206 ^c	203±14	208 ^c	468±54	480
<i>Hypothalamus</i>									
	R	93±4	76±5	137±12	147 ^c	143±8	188 ^c	349±49	458
	L	94±5	76±5	137±14	145 ^c	136±7	179 ^c	340±38	446
<i>Hippocampus</i>									
	R	97±6	86±4	190±18	196 ^c	159±9	185 ^c	406±43	470
	L	99±7	89±6	182±14	184 ^c	150±10	169 ^c	407±69	459
<i>Midbrain</i>									
Substantia	R	93±5	85±5	155±18	166 ^c	165±6	194 ^c	375±61	443
Nigra	L	97±7	85±5	156±12	161 ^c	167±8	196 ^c	383±65	451
Superior	R	128±5	127±7	195±10	152 ^c	182±6	144 ^c	500±57	395
Colliculus	L	134±8	122±5	187±12	140 ^c	179±5	147 ^c	489±62	401
Inferior	R	157±14	153±9	196±14	122	176±9	116	469±33	306
Colliculus	L	158±14	147±9	194±15	125	170±8	114	476±61	324
Pontine gray	R	122±7	103±8	194±17	159 ^c	189±10	183 ^c	379±46	367
<i>Cerebellum</i>									
Vermis	R	108±6	110±6	161±20	149 ^c	151±14	138 ^c	465±48	424
Hemisphere	L	100±11	110±8	112±7	112	113±9	104	400±71	365
Dentate	L	103±12	107±8	134±12	129	128±8	120	420±59	392
Nucleus	R	185±8	187±11	247±13	133 ^c	197±15	105 ^c	534±37	286
	L	174±10	183±12	272±26	157 ^c	205±15	112 ^c	545±22	299
<i>Pons medulla</i>									
Parabrachial	R	106±5	101±5	183±14	171 ^c	204±10	203 ^c	421±52	418
Complex	L	102±4	95±6	184±13	181 ^c	198±10	209 ^c	433±54	456
Vestibular	R	190±8	196±11	309±27	162 ^c	214±10	109 ^c	583±7	298
Complex	L	187±4	199±14	320±29	171 ^c	220±11	110 ^c	590±5	296
Nucleus reticularis	R	104±5	95±6	196±13	190 ^c	162±5	171 ^c	433±56	455
Gigantocellularis	L	102±5	94±6	191±12	188 ^c	160±4	170 ^c	428±53	457
Nucleus reticularis	R	101±4	96±6	185±13	183 ^c	164±3	170 ^c	469±46	487
Parvocellularis	L	96±3	95±6	194±16	203 ^c	165±3	175 ^c	441±51	466
<i>Corpus callosum</i>									
	R	53±7	52±4	94±6	177 ^c	107±10	205 ^c	258±53	494
	L	56±7	50±3	98±5	177 ^c	94±10	189 ^c	147±43	295

Values are means ± SE. R, right; L, left. See text for definitions. *R-L differences NS (p>0.05; paired t-test) except frontal cortex (p<0.02) and amygdala (p<0.01). ^aIntact group differences (p>0.05). R-L differences NS (p>0.05; paired t-test) except globus pallidus and parabrachial complex (p<0.05). ^bp<0.01, unstimulated-lesioned group. R-L differences NS (p>0.05; paired t-test). ^cp<0.01; ANOVA and Newman-Keuls test. ^dp<0.05, FN stimulation in intact group (analysis of variance on % control). ^ep<0.05.

TABLE 8

Effect of bilateral craniotomy and ATR (100 μ M) on resting rCBF.

Values are means \pm SEM in ml/100 gmin; animals are anesthetized, paralyzed and artificially ventilated with 100% O₂. ATR was applied only to the right parietal cortex. No significant right-to-left differences were detected (paired t-test, $p > 0.05$); nor were there differences between treatment groups (ANOVA, $p > 0.05$).

<i>Region</i>	<i>Control</i> <i>Unoperated</i>		<i>Parietal craniotomy</i>	
			<i>Vehicle</i>	<i>ATR</i>
Frontal cortex	L	92 \pm 8	93 \pm 12	100 \pm 13
	R	94 \pm 9	79 \pm 7	91 \pm 13
Parietal cortex	L	95 \pm 7	82 \pm 12	83 \pm 7
	R	93 \pm 5	70 \pm 6	85 \pm 9
Occipital cortex	L	87 \pm 8	86 \pm 12	88 \pm 6
	R	89 \pm 7	72 \pm 7	85 \pm 9
Caudate nucleus	L	92 \pm 14	75 \pm 6	84 \pm 7
	R	82 \pm 6	75 \pm 6	85 \pm 10
Hippocampus	L	70 \pm 5	78 \pm 8	72 \pm 3
	R	73 \pm 5	74 \pm 6	78 \pm 7
n		6	6	4

TABLE 9

A comparison of the choline acetyltransferase (ChAT) activity measured by different authors from various fractions isolated from the cerebral cortex.

Author	Species	Fractions Containing ChAT Activity			
		Intraparenchymal Vessels		Synaptosomes	Homogenate
		Size	Activity		
Armeric et al., 1986 (present study)	Rat	68% < 10um 32% 10-40um	2850	2150	1475
Santos-Benito and Gonzales, 1985 (J. Neurochem. <u>45</u> :633)	Rat	95% < 10um	55	1435	1005
Goldstein et al., 1975 (J. Neurochem. <u>25</u> :715)	Rat	95% < 10um	14	--	560
Estrada et al., 1983 (Brain Res. <u>266</u> :261)	Bovine	85% < 10um	190	--	1118

Values are mean pmol ^{14}C -ACh formed/mg protein/min.

LIST OF PERSONNEL RECEIVING CONTRACT SUPPORT
(Partial Support)

Professional

Stephen Arneric, Ph.D.
Sergio Cravo, Ph.D.
Rachel Giuliano, Ph.D.
Costantino Iadecola, M.D.
Donald J. Reis, M.D.
Lewis Tucker, Ph.D.
Mark Underwood, Ph.D.*

Technician

Janie Callaway
Lynette Char
Phillip McCauley

*graduate degree received

BIBLIOGRAPHY OF PUBLICATIONS
SUPPORTED BY CONTRACT

Iadecola, C., Underwood, M.D., and Reis, D.J.: Muscarinic cholinergic receptors mediate the cerebrovasodilation elicited by stimulation of the cerebellar fastigial nucleus in rat. *Brain Res.* 368: 375-379, 1986.

Arneric, S.P., Iadecola, C., Honig, M.A., Underwood, M.D., and Reis, D.J.: Local cholinergic mechanisms mediate the cortical vasodilation elicited by electrical stimulation of the fastigial nucleus. *Acta Physiol. Scand.* 127 (Suppl. 552), 70-73, 1986.

Arneric, S.P., Iadecola, C., Underwood, M.D., and Reis, D.J.: Local cholinergic mechanisms participate in the increase in cortical cerebral blood flow elicited by electrical stimulation of the fastigial nucleus in rat. *Brain Res.* 411: 212-225, 1987.

Iadecola, C., Arneric, S.P., Baker, H.D., Tucker, L.W., and Reis, D.J.: Role of local neurons in the cerebrocortical vasodilation elicited from cerebellum. *Am. J. Physiol.* 252: R1082-R1091, 1987.

Arneric, S.P., Honig, M.A., Milner, T.A., Greco, S., Iadecola, C. and Reis, D.J.: Neuronal and endothelial sites of acetylcholine synthesis and release associated with microvessels in rat cerebral cortex: ultrastructural and neurochemical studies. *Brain Res.* 454: 11-30, 1988.

Iadecola, C., Arneric, S. and Reis, D.J.: Local and remote microvascular changes in excitotoxin-induced focal brain lesions. *Brain Res.* 501: 188-193, 1989.

Reis, D.J. and Iadecola, C.: Central Neurogenic Regulation of Cerebral Blood Flow. In: *Neurotransmission and Cerebrovascular Function*, Vol. II, J. Seylaz and R. Sercombe (Eds.), Elsevier, Amsterdam, 1989, pp. 369-390.

Chida, K., Iadecola, C. and Reis, D.J.: Lesions of rostral ventrolateral medulla abolish some cardio- and cerebrovascular components of the cerebellar fastigial pressor and depressor responses. *Brain Res.*, 1989 (in press).

Iadecola, C., Springston, M.E. and Reis, D.J.: Dissociation by chloralose of the cardiovascular and cerebrovascular responses evoked from the cerebellar fastigial nucleus. *J. Cereb. Blood Flow Metab.*, 1989 (in press).

Ruggiero, D.A., Giuliano, R., Anwar, M., Stornetta, R. and Reis, D.J.: Anatomical substrates of cholinergic-autonomic regulation in the rat. *J. Comp. Neurol.*, 1989 (in press).

Iadecola, C. and Reis, D.J.: Cerebral blood flow monitored by laser-doppler flowmetry during cerebellar stimulation. *Am. J. Physiol.*, submitted 9/21/89.

DISTRIBUTION LIST

1 copy	Commander US Army Medical Research and Development Command ATTN: SGRD-RMI-S Fort Detrick, Frederick, Maryland 21701-5012
5 copies	Commander US Army Medical Research and Development Command ATTN: SGRD-PLE Fort Detrick, Frederick, Maryland 21701-5012
2 copies	Defense Technical Information Center (DTIC) ATTN: DTIC-DDAC Cameron Station Alexandria, VA 22304-6145
1 copy	Dean School of Medicine Uniformed Services University of the Health Sciences 4301 Jones Bridge Road Bethesda, MD 20814-4799
1 copy	Commandant Academy of Health Sciences, US Army ATTN: AHS-CDM Fort Sam Houston, TX 78234-6100